Endosomal escape of RNA therapeutics

Du Rietz, Hampus

2024

Document Version:
Publisher's PDF, also known as Version of record

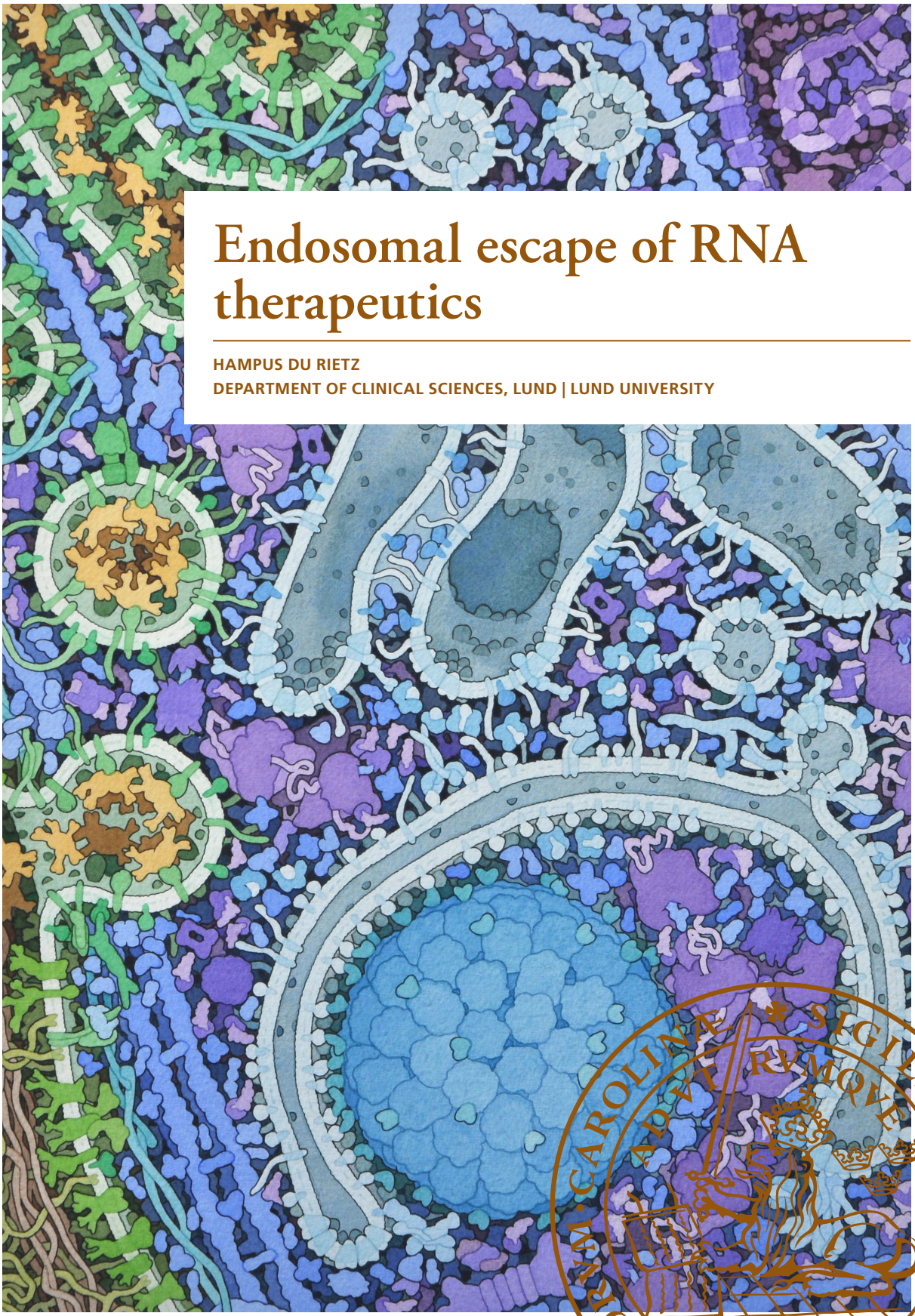

Endosomal escape of RNA therapeutics

HAMPUS DU RIETZ
DEPARTMENT OF CLINICAL SCIENCES, LUND | LUND UNIVERSITY

Endosomal escape of RNA therapeutics

Endosomal escape of RNA therapeutics

Hampus Du Rietz

LUND
UNIVERSITY

DOCTORAL DISSERTATION

Doctoral dissertation for the degree of Doctor of Philosophy (PhD) at the Faculty of Medicine at Lund University to be publicly defended on Friday 14th of June 2024 at 13.00 in Belfragesalen, BMC D15, Klinikgatan 32, Lund Sweden.

Faculty opponent
Prof. Steven F. Dowdy
Department of Cellular and Molecular Medicine
UCSD School of Medicine, La Jolla, California, USA

Organization: LUND UNIVERSITY, Faculty of Medicine, Department of Clinical Sciences Lund, Oncology

Document name: Doctoral dissertation **Date of issue:** 2024-06-14

Author(s): Hampus Du Rietz **Sponsoring organization:**

Title and subtitle: Endosomal escape of RNA therapeutics

Abstract:

RNA therapeutics is a new class of targeted therapies that has entered the clinic in the last decade. Lipid nanoparticles (LNPs) and conjugation to N acetylgalactosamine have proven to be efficient strategies to deliver RNA payload to the liver. Successful delivery of sensitive RNA molecules to other target tissues or tumors remains one of the key challenges with the development of new RNA-based treatments. Extrahepatic delivery is still poor, limiting the therapeutic efficacy. One of the central hurdles to delivery is the intracellular accumulation of RNA therapeutics and delivery vehicles in endocytic vesicles following uptake, without an effective way to exit into the cytoplasm and engage with the therapeutic targets. Knowledge of this rate-limiting process have remained poor, hampering rational efforts to overcome it.

This thesis has aimed to devise and leverage techniques to study the endosomal escape of small interfering RNA (siRNA) and messenger RNA (mRNA) from endosomal compartments into the cytosol — to advance the understanding of the escape process, the interactions between RNA delivery vehicles and endosomes that potentially trigger membrane disruption, and the dose-response relationship between the small amount of siRNA molecules released and the biological response.

The sensitive membrane-damage sensor Galectin-9 was used to probe individual release events, showing that endosomal escape of both siRNA and mRNA formulated in LNPs is very inefficient. Only a fraction of LNPs triggered endosomal damage, only a minority of damage events led to productive release of RNA payload, and most of the payload remained trapped in the damaged endosomes. The endosomal release of lipid-modified siRNA was enhanced by simultaneous treatment with membrane-damaging small molecule drugs, that promoted efficient escape of siRNA payload on a single-vesicle level. In addition, a microscopy-based approach was developed to quantify the number of siRNA molecules delivered to the cytosol while also monitoring the resulting knockdown of a reporter gene. From experimental data combined with mathematical modelling, the cytosolic IC50 of two siRNA sequences with a known difference in potency was determined to be ~970 and ~6,700 molecules, respectively. Finally, a novel dual-labeled LNP was developed, composed of fluorescently labeled ionizable lipid (BODIPY-MC3) and RNA. Dual-labeled LNPs were used to visualize the interaction between ionizable lipid from the LNP and the endosomal membrane, resulting in damage to the lipid bilayer.

This thesis presents detailed investigations of the endosomal escape of RNA therapeutics, providing new insights into the cellular and biophysical barriers limiting payload release and how they could potentially be overcome. The work is of high relevance for ongoing efforts to develop new RNA-based therapies with rational strategies.

Key words: RNA therapeutics, Endosomal escape, Membrane damage

Classification system and/or index terms (if any) Supplementary bibliographical information

Language: English **ISSN and key title**: 1652-8220

ISBN: 978-91-8021-583-1

Recipient's notes **Number of pages:** 157

Signature: **Date:** 2024-05-06

Endosomal escape of RNA therapeutics

Hampus Du Rietz

LUND
UNIVERSITY

Coverphoto by David S. Goodsell and Daniel Klionsky. Adapted and distributed under CC-BY-4.0.
doi: 10.2210/rcsb_pdb/goodsell-gallery-012

The formation of an autophagosome is shown, with Golgi at top left, a mitochondrion at top right, and the autophagosome at bottom center.

Faculty of Medicine

Department of Clinical Sciences, Lund

ISBN 978-91-8021-583-1

ISSN 1652-8220

Printed in Sweden by Media-Tryck, Lund University

Lund 2024

Media-Tryck is a Nordic Swan Ecolabel certified provider of printed material. Read more about our environmental work at www.mediatryck.lu.se

MADE IN SWEDEN

“Education isn't something you can finish.”
– Isaac Asimov

Table of Contents

Abstract

RNA therapeutics is a new class of targeted therapies that has entered the clinic in the last decade. Lipid nanoparticles (LNPs) and conjugation to *N*-acetylgalactosamine have proven to be efficient strategies to deliver RNA payload to the liver. Successful delivery of sensitive RNA molecules to other target tissues or tumors remains one of the key challenges with the development of new RNA-based treatments. Extrahepatic delivery is still poor, limiting the therapeutic efficacy. One of the central hurdles to delivery is the intracellular accumulation of RNA therapeutics and delivery vehicles in endocytic vesicles following uptake, without an effective way to exit into the cytoplasm and engage with the therapeutic targets. Knowledge of this rate-limiting process have remained poor, hampering rational efforts to overcome it.

This thesis has aimed to devise and leverage techniques to study the endosomal escape of small interfering RNA (siRNA) and messenger RNA (mRNA) from endosomal compartments into the cytosol — to advance the understanding of the escape process, the interactions between RNA delivery vehicles and endosomes that potentially trigger membrane disruption, and the dose-response relationship between the small amount of siRNA molecules released and the biological response.

The sensitive membrane-damage sensor Galectin-9 was used to probe individual release events, showing that endosomal escape of both siRNA and mRNA formulated in LNPs is very inefficient. Only a fraction of LNPs triggered endosomal damage, only a minority of damage events led to productive release of RNA payload, and most of the payload remained trapped in the damaged endosomes. The endosomal release of lipid-modified siRNA was enhanced by simultaneous treatment with membrane-damaging small molecule drugs, that promoted efficient escape of siRNA payload on a single-vesicle level. In addition, a microscopy-based approach was developed to quantify the number of siRNA molecules delivered to the cytosol while also monitoring the resulting knockdown of a reporter gene. From experimental data combined with mathematical modelling, the cytosolic IC50 of two siRNA sequences with a known difference in potency was determined to be ~970 and ~6,700 molecules, respectively. Finally, a novel dual-labeled LNP was developed, composed of fluorescently labeled ionizable lipid (BODIPY-MC3) and RNA. Dual-labeled LNPs were used to visualize the interaction between ionizable lipid from the LNP and the endosomal membrane, resulting in damage to the lipid bilayer.

This thesis presents detailed investigations of the endosomal escape of RNA therapeutics, providing new insights into the cellular and biophysical barriers limiting payload release and how they could potentially be overcome. The work is of high relevance for ongoing efforts to develop new RNA-based therapies with rational strategies.

Populärvetenskaplig sammanfattning

Läkemedel baserade på molekyler av den naturliga nukleinsyran RNA utgör en ny grupp av målriktade terapier som har nått klinisk användning under det senaste årtiondet. Leverans av RNA-läkemedel med hjälp av lipidbaserade nanopartiklar (LNP) eller att kombinera RNA med specifika bärarmolekyler har visat sig vara effektiva strategier för att nå målceller i levern. Däremot är leveransen till andra vävnaderna och cancerceller i tumörer fortfarande väldigt ineffektiv, vilket är den största utmaningarna med att utveckla nya RNA-baserade behandlingar. Ett av de mest centrala hindren för effektiv leverans har visat sig vara ackumulering av RNA-molekyler inne i målcellerna, där de förvaras i små membranomslutna blåsor, så kallade endosomer, utan att på ett framgångsrikt sätt kunna nå vidare in i cellen och få möjlighet att utöva sina läkemedelseffekter. Kunskapen kring denna flaskhals i leveransprocessen är fortfarande mycket begränsad, vilket hindrar rationella ansträngningar att försöka övervinna den.

Avhandlingsarbetet som presenteras här har syftat till att framarbeta tekniker för att studera frisättningen av RNA-läkemedel från endosomer inne i cellen, för att kunna belysa aspekter av hur denna del av leversanskedjan fungerar och beskriva sambandet mellan mängden RNA-molekyler som frigörs och läkemedelseffekten.

En sensor för skadade endosomer, Galectin-9, kunde användas för att studera frisättningen av små interfererande RNA (siRNA) och budbärar-RNA (mRNA), som förpackats i lipidnanopartiklar. Frisättningen var mycket ineffektiv — endast en bråkdel av partiklarna utlöste en skada hos endosomerna, och bara en minoritet av skadorna gav frisättning av RNA. Samtidig behandling med membranskadande små molekyler kunde förbättra den endosomala frisättningen av siRNA som kopplats direkt till bärarmolekylen kolesterol. Vidare utvecklades en ny LNP, med två fluorescerande komponenter (RNA och lipid). Lipidnanopartikeln gjorde det möjligt att undersöka interaktionen mellan partikelns lipider och endosomernas lipidmembran, vilket kunde kopplas till uppkomsten av membranskador. Slutligen utarbetades en mikroskopibaserad metod för att mäta antalet siRNA-molekyler som frisattes inne i enskilda celler, och vid samma tillfälle utvärdera den biologiska effekten som detta medförde. Utifrån experimentella data och matematisk modellering visades att det antal siRNA-molekyler som behövde frisättas för att uppnå halva maximala biologiska effekten var ~970 respektive ~6 700 molekyler för två siRNA-sekvenser med olika effektivitet.

Den här avhandlingen presenterar detaljerade studier av den endosomala frisättningen av flera olika RNA-molekyler som utgör grunden för nya målriktade behandlingar, och ger nya insikter kring barriären som endosomernas membran utgör och hur den potentiellt skulle kunna övervinnas. Fynden har hög relevans för det pågående arbetet med att utifrån rationella strategier utveckla nya RNA-baserade terapier.

List of Papers

I. Du Rietz H, Hedlund H, Wilhelmson S, Nordenfelt P, Wittrup A. Imaging small molecule-induced endosomal escape of siRNA. *Nat Commun*. 2020 Apr 14;11(1):1809. https://doi.org/10.1038/s41467-020-15300-1

II. Hedlund H, Du Rietz H, Johansson JM, Eriksson HC, Zedan W, Huang L, Wallin J, Wittrup A. Single-cell quantification and dose-response of cytosolic siRNA delivery. *Nat Commun*. 2023 Feb 25;14(1):1075. https://doi.org/10.1038/s41467-023-36752-1

III. Johansson JM*, Du Rietz H*, Hedlund H*, Eriksson HC, Oude Blenke E, Pote A, Harun S, Nordenfelt P, Lindfors L, Wittrup A. Cellular and biophysical barriers to lipid nanoparticle mediated delivery of RNA to the cytosol.
*Equal contribution
(*Manuscript*)

IV. Du Rietz H, Johansson JM, Hedlund H, Cerezo-Magaña M, Wilhelmson-Andén, S, Wittrup A. Endosomal release of lipid-modified siRNA is decoupled from canonical membrane damage response.
(*Manuscript*)

Abbreviations

2′-F	2′-Fluoro
2′-OMe	2′-*O*-Methyl
ABE	adenine base editor
AF647	AlexaFluor 647
Ago	Argonaute
ApoE	apolipoprotein E
ASGPR	asialoglycoprotein receptor
ASO	antisense oligonucleotide
CAR	chimeric antigen receptor
CBE	cytosine base editor
Chol-siRNA	cholesterol-conjugated siRNA
CI	clathrin independent
CNS	central nervous system
CPP	cell-penetrating peptide
CQ	chloroquine
CRD	carbohydrate recognition domain
d1-EGFP	destabilized enhanced green fluorescent protein
DNA	deoxyribonucleic acid
DSB	double-strand break
dsRNA	double-stranded RNA
EE	early endosome
EEA1	early endosome antigen 1
EGFP	enhanced green fluorescent protein
EMA	European Medicines Agency
ER	endoplasmic reticulum
ESCRT	endosomal sorting complexes required for transport
FDA	U.S. Food and Drug Administration
FRET	Förster resonance energy transfer
Gal-9	Galectin-9
GalNAc	N-acetylgalactosamine
HDR	homology-directed repair

IC50	half-maximum inhibitory concentration
iL	ionizable lipid
IVL	intraluminal vesicle
LAMP1	lysosome-associated membrane protein 1
LE	late endosome
LMP	lysosomal membrane permeabilization
LNP	lipid nanoparticle
LSCM	laser-scanning confocal microscopy
miRNA	microRNA
mRNA	messenger RNA
MVB	multi-vesicular body
NHEJ	non-homologous end joining
PS	phosphorothioate
RE	recycling endosome
RISC	RNA-induced silencing complex
RNA	ribonucleic acid
RT-qPCR	reverse-transcription quantitative polymerase chain reaction
SIM	structured illumination microscopy
SIR	siramesine
siRNA	small interfering RNA
SSO	splice-switching oligonucleotide
ssRNA	single-stranded RNA
TGN	*trans*-Golgi network
TLR	Toll-like receptor
TME	tumor microenvironment
YFP	yellow fluorescent protein

Introduction

Cancer and targeted therapies

Cancers develop through stepwise transition of normal cells and tissues via pathways of tumorigenesis, malignant progression, and adaptive response to treatment. Gene mutation, genomic instability and tissue inflammation are important and early hallmarks of tumorigenesis, that in combination with other mechanisms promote aberrant and accelerated cell proliferation, changes in tissue architecture and potentially dissemination of malignant cells to distant sites and organs[1,2].

As a result of substantial efforts in cancer and tumor biology research, that have progressively advanced treatment options in clinical oncology — in combination with introduction of screening programs and improved detection, diagnosis, surgery and chemoradiotherapy regimens — the curation and survival rates for many cancers have improved considerably in the last decades. As an example, overall cancer survival rates have approximately doubled since the 1970s in several high-income countries including Sweden, where the 5-year survival rate for cancers of the thyroid, breast, prostate, testis and melanoma is now approximately 90% or more [3–5]. Still, there is dire need of new oncological treatment options to further increase the chances of cure and survival for many cancers where improvements have been modest, including cancers of the pancreas, lung, liver, bile duct, and esophagus[5,6].

In addition, emerging trends with increasing global cancer incidence and prevalence will bring an even greater need of new treatment options in the coming decades. Two important developments driving this change is an increasing incidence of early-onset cancers, and an increasing number and prevalence of late-onset cancers in expanding elderly populations.

Increasing incidence of early-onset cancer

Emerging evidence indicate an increasing incidence of malignancies in various organs — including breast, esophagus, bile duct, gallbladder, head and neck, kidney, liver, bone marrow, pancreas, prostate, stomach and thyroid — in adults <50 years of age in

many parts of the world since the 1990s[7,8]. Cancer in adults <50 years of age are often called 'early-onset', whereas cancers diagnosed >50 years of age are often called 'late-onset'. The extended use of cancer screening programmes has partially contributed to the increased incidence of early-onset cancers, through improved and earlier detection — especially in breast, prostate and thyroid cancer[9]. However, a genuine trend of incidence increase of early-onset cancers is still supported by available data[10].

Differences between early- and late-onset malignancies with respect to epidemiology and clinical, pathological, and molecular characteristics are becoming increasingly recognized[11,12]. Certain early-onset cancer types are more likely to be of an advanced stage with worse survival outcomes than their later-onset counterparts[13–15]. Risk factor exposure in early life and young adulthood are likely to have an etiological role in early-onset cancer development, and the early life 'exposome' — including factors as lifestyle, diet[16], obesity[7], microbiome[17], environmental exposures[18] and reproductive factors[19,20] — has changed considerably in the last 50–70 years. Most cases of early-onset malignancies appear to be sporadic[21]. An increased prevalence of germline genetic variations in hereditary high-penetrance cancer-related genes associated with early onset malignancies, perhaps owing to advances in medical treatment and survival, could in theory contribute to the observed phenomenon. As of now, however, no evidence exists to support this kind of a genetic cause, and most likely another few decades would be required for this progression to be detectable[9].

Increasing cancer in the elderly

The proportion of the world's population over 60 years of age will nearly double between 2015 and 2050 (from 12% to 22%), and the number of people aged 80 years or older is expected to triple[22]. Increasing age is an important non-modifiable risk factor for cancer[23]. Approximately 90% of all cancers are diagnosed in persons 50 years of age or older[24–26]. As a consequence of expanding and aging global populations — with addition of other environmental and lifestyle factors — the number of people that are diagnosed with cancer is estimated to increase in the coming decades. A recent report from the World Health Organization's International Agency for Research on Cancer estimated a projected 77% global increase in new cancer cases in 2050 compared to 2022[27]. Consequently, the number of cancer deaths worldwide is expected to double. Since overall medical and socioeconomical progress contributes to decrease death from other causes and diseases, the relative impact on mortality from cancer is likely to increase[28].

An increasing number of cancer cases in combination with expanding treatment options and progressively improved survival will considerably expand the number of

elderly people living with cancer and receiving oncological treatment. This will pose tremendous challenges on both national and global levels, as even high-income countries with low-threshold healthcare systems are predicted to struggle with shortage of healthcare professionals like surgeons, radiation oncologists, medical oncologists, pathologists, in addition to limited resources for in-patient and out-patient care and treatment, and escalating costs of anticancer therapeutics[28]. In addition, with available chemotherapeutics, older patients — more likely to have comorbidities, disabilities or geriatric syndromes — have greater risk of experiencing adverse effects and toxicity, leading to hospitalization, treatment discontinuation and greater overall harm than benefit from treatment[29–31].

Need for novel targeted therapies

While the immediate societal goals should be to improve known and modifiable risk factors both in the early- and later-life environment to decrease risk of cancer development, as highlighted above, new and effective treatment options are of great need for the treatment of both early-onset and later-onset cancer.

With some exceptions, curation is typically not feasible when cancer has recurred or metastasized[32]. Even so, palliative oncological treatment — aiming to balance anticancer effects and adverse treatment effects to improve quality of life and extend survival (sometimes for many years) — is generally pursued if comorbidities are limited. Both available curative and palliative treatment options are currently limited by acquired tumor resistance and risk of excessive toxicity. Traditional cytotoxic chemotherapeutics are considered to be less tolerable — especially in the elderly or patients with significant comorbidities — as they target ubiquitous cellular processes necessary for cell proliferation (*e.g.* microtubule function and stability, or DNA structure and replication) that also affects normal tissues and organs[33].

Mutations that are recurrent in cancers are considered to be drivers of the oncogenic phenotype. Cancer cells may depend on these drivers for survival and proliferation, and their inhibition then often leads to cell death[34]. The elucidation of genetic defects that underlie various cancers has uncovered a plethora of possible drug targets and resulted in a large number of approved targeted cancer therapies. Between 2006 and 2020, the U.S. Food and Drug Administration (FDA) authorized 51 targeted drugs for 36 genomic indications for 18 types of cancer, including small molecule inhibitors (tyrosine kinase inhibitors, hormone therapies, CDK4/6 inhibitors, proteasome inhibitors, PARP inhibitors, angiogenesis inhibitors), monoclonal antibodies including immune checkpoint inhibitors, and antibody–drug conjugates[35].

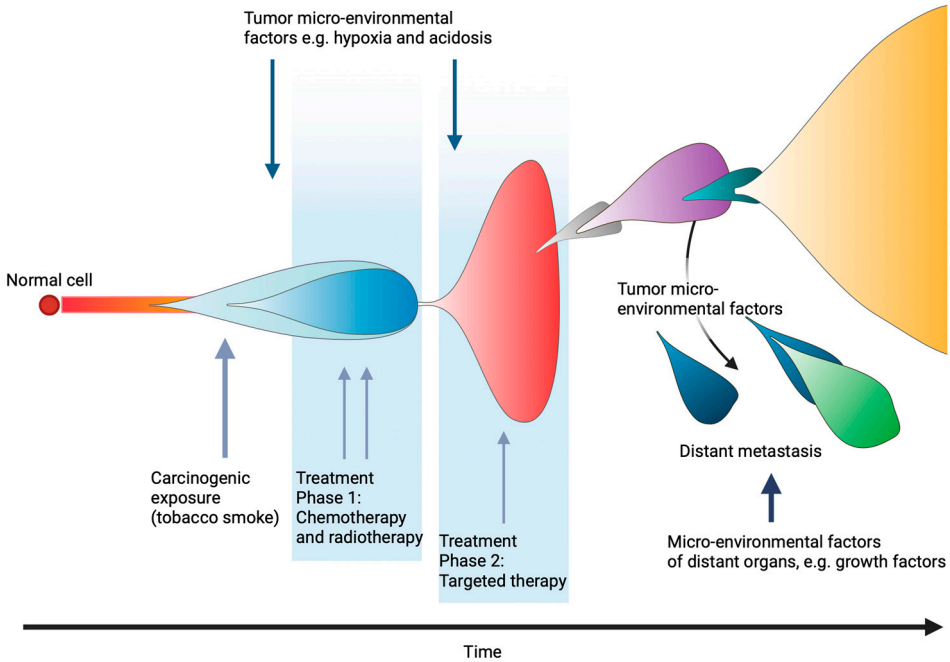

Figure 1. Cancer treatment and tumor environment shape the evolutionary tumor adaptation
Many environmental and genetic factors play a role in cancer initiation and shape the step-by-step evolutionary adaptation of emerging cancer clones (represented by colored bubbles). Clonal proliferation is altered by directly mutagenic factors (grey arrows) and non-mutagenic factors (dark blue arrows). Created with BioRender.com.

Targeted therapies, in general, cause effective antitumoral responses with less toxicity compared to chemotherapies. However, tumors typically acquire resistance to most targeted therapies — especially in advanced cancers and when administered as single agents. In the case of intrinsic resistance, patients fail to respond to therapies from start, due to for example multiple activating mutations in the same pathway, or compensatory upstream signaling. This is exemplified by the lack of objective treatment response with the selective BRAF inhibitor vemurafenib in colorectal cancers with the same V600E mutation as seen in melanoma, where treatment generally have substantial initial clinical response[36,37]. In the case of acquired resistance, the antitumoral response inflicted by the targeting agent is reduced during treatment and is ultimately overcome by resistant cancer cells. Broadly, intrinsic and acquired resistance mechanisms can have genetic or non-genetic origin — *i.e.* resulting from gene mutation or alterations in gene expression.

Genetic resistance can result from 'on-target' mutations that alter the site of the drug target itself — a mechanism that is common with small molecule inhibitors but also affects therapeutic monoclonal antibodies[38–40]. In addition to on-target mutations, treatment resistance can also result from gain-of-function mutations that activate parallel signaling pathways or reactivate the same oncogenic pathway upstream or downstream of the drug target[41]. Non-genetic resistance mechanisms include non-mutational transcriptional changes (*e.g.* target splicing alterations), epigenetic changes and activation of transcriptional programmes (*e.g.* epithelial to mesenchymal transition, EMT), and tumor microenvironment adaptations[42].

With an immediate need for additional treatment options in many cancer settings, the growing challenges facing medical oncology in the coming decades, and the limited success of available targeted therapies, there is a substantial need for novel targeted therapies to help bridge the gap.

RNA therapeutics

RNA interference and microRNA

Discovery of RNA interference

RNA interference was first described in mammalian cells by Tuschl and colleagues in 2001[43]. This finding was a result of decades of cumulative work on endogenous gene regulatory mechanisms and evolving techniques to manipulate protein expression by exogenous oligonucleotides and RNA. Three years earlier, Andrew Fire, Craig Mello and colleagues discovered inheritable silencing of genes in *C. elegans* by the introduction of double-stranded RNA (dsRNA)[44]. The reduction in gene expression — referred to as RNA interference (RNAi) — could not be replicated with homologous single-stranded RNA (ssRNA). This provided evidence of a different basis of gene regulation than what was mediated by antisense RNAs already known and studied at the time. Indeed, endogenous small non-coding antisense RNAs with sequence complementarity to known targets had already been identified and were proposed to inhibit mRNA translation into protein[45,46]. As it turned out, this class of non-coding regulatory RNAs — now known as microRNAs (miRNA) — rely on the same RNAi machinery as exogenously introduced dsRNA for gene silencing.

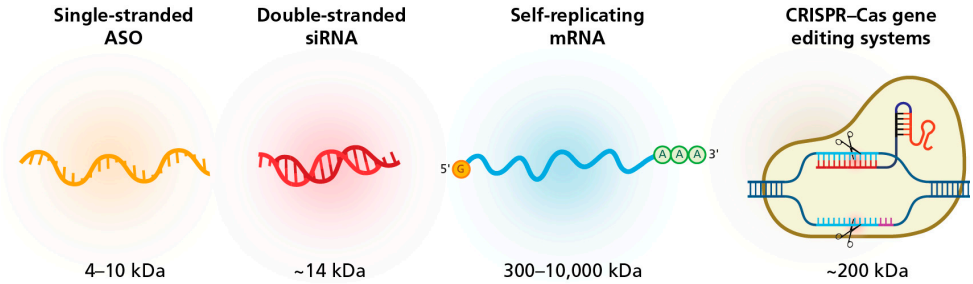

Figure 2. The RNA therapeutics toolkit
The RNA and oligonucleotide toolkit is a versatile collection of therapeutic molecules. ASO – Antisense oligoucleotide; siRNA – small interfering RNA; mRNA – messenger RNA.

The RNA interference machinery

Primary microRNAs (pri-miRNA) are transcribed RNA polymerase II or III and are recognized by DiGeorge Syndrome Critical Region 8 (DGCR8), a nuclear protein named after its association with DiGeorge syndrome[47–49]. DGCR8 forms the Microprocessor complex together with the catalytic enzyme Drosha, having a RNase III domain[50,51]. Transcripts are trimmed by the complex to generate pre-miRNAs — precursor miRNAs that contain ~70 nucleotides (nt) forming a hairpin loop duplex typically containing interspersed mismatched regions and a two-nucleotide 3′ overhang[52]. Pre-miRNAs can be modified through nuclear RNA editing, that can alter *e.g.* downstream cytoplasmic processing or target specificity[53]. A small subset of pre-miRNAs known as mirtrons bypass the Microprocessing complex and are instead spliced directly from introns[54].

Pre-miRNA are exported from the nucleus to the cytoplasm by the nucleocytoplasmic shuttler Exportin-5, that recognize the 3′ nucleotide overhang left by Drosha[55,56]. Here, pre-miRNA are further processed into miRNA–miRNA duplexes of ~22 nt in length by a protein complex containing Dicer, TAR RNA-binding protein (TRBP) and PACT.[57–59] The cleaved duplexes can then associate with members of the Argonaute protein family (Ago) as a part of the precursor RNA-induced silencing complex (pre-RISC)[60]. One of the duplex strands (passenger strand) is removed after binding into pre-RISC, while the active guide strand remains in the mature RISC and act as a template to bind complementary target mRNA sequences via Watson-Crick base pairing, typically at the 3′ untranslated region (UTR)[61]. Binding of the target mRNA repress the initiation of translation[62–64], which is followed by mRNA decay and degradation in several steps and by different pathways[65,66]. RISC can also regulate gene expression by Ago-mediated cleavage of mRNA and subsequent 5′-to-3′ or 3′-to-5′ degradation, as will be discussed for siRNA below[67,68]. However, in mammalian cells,

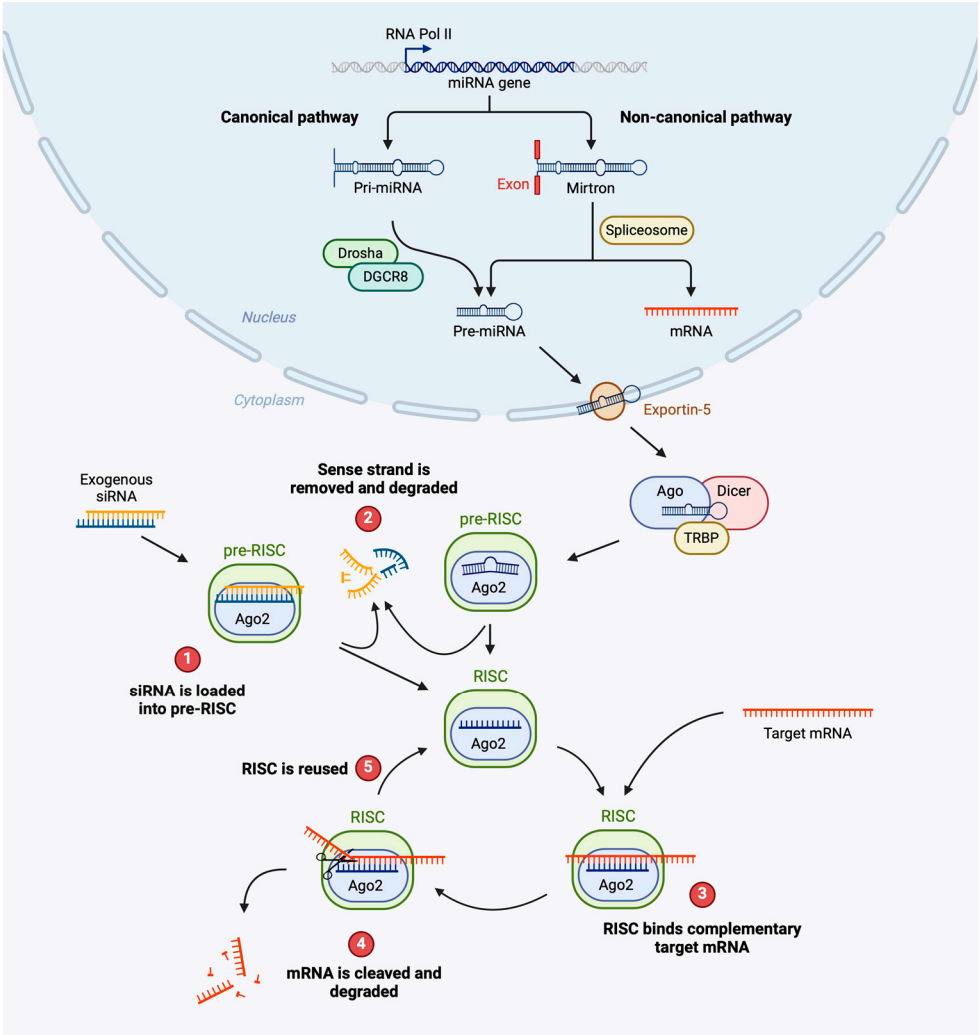

Figure 3. Small interfering RNAs hijack the endogenous microRNA pathway for RNA interference
Cells use RNA interference as a way of post-transcriptional gene expression regulation. Endogenous microRNAs (miRNAs) are transcribed in the nucleus and processed before exported to the cytosol. After Dicer-mediated cleavage they are loaded into the pre-RISC (RNA induced silencing complex). **(1)** Exogenous siRNA that are delivered to the cytosol can be loaded into pre-RISC without processing. **(2)** After formation of the pre-RISC complex, the siRNA can harness the endogenous RNAi mechanisms used by miRNA. The sense strand is removed and degraded, while the antisense strand remains bound to Ago2 in RISC. **(3)** Guided by the antisense strand, RISC can bind target mRNAs in the cytosol that have a complementary sequence. **(4)** The bound mRNA is cleaved by Ago2 and then released from the complex. **(5)** The antisense strand remains loaded into RISC, and the complex can repeat the mRNA binding and degradation process. As the target mRNA is degraded, its translation into protein is inhibited and the gene expression is knocked down as turnover of existing protein continues. Created with BioRender.com.

the sequence complementarity of miRNAs to target mRNAs is typically not high enough to repress mRNA translation through AGO2-dependent cleavage[66].

The field of microRNA biology has expanded enormously in the three decades since the first miRNA was discovered. Ubiquitous roles of miRNAs have not only been uncovered in gene expression regulation that is fundamental for homeostatic cellular processes, but also in the development of many diseases and particularly in cancer. Indeed, functional studies have shown that miRNA dysregulation in many cases is at the core of cancer development and progression, where miRNA act either as tumor suppressors or oncogenes (oncomiRs)[69]. For example, microRNA-21 (miR-21) was one of the first oncomiRs found to be upregulated in a variety of cancers, including breast cancer, colorectal cancer and gliomas. Many of its target genes are associated with key functions in cancer, for example the tumor suppressors *PTEN* (phosphatase and tensin homolog) and *PDCD4* (programmed cell death protein 4)[70].

Consequently, miRNA-focused therapeutics have been pursued to interfere with dysregulated miRNA activity in disease. Therapies in this area can be divided into miRNA mimics and inhibitors of miRNAs (antimiRs). Developed with the aim to replenish lost miRNA expression and function, miRNA mimics are synthetic dsRNA molecules designed to match the corresponding native miRNA sequence. AntimiRs, on the other hand, are single-stranded antisense oligonucleotides (ASOs) designed to bind to and inhibit miRNAs like oncomiRs. AntimiRs can be synthesized with ribose or phosphate backbone modifications, like 2′-*O*-methylation or phosphorothioate bonds (so called antagomiRs), or modified with locked nucleic acids (LNAs), as described in more detail below. Several miRNA therapeutics have reached clinical development and trials. In the context of cancer, examples include mimics of the tumor suppressor miRNAs miR-34 (in advanced melanoma)[71] and miR-16 (in recurrent malignant pleural mesothelioma and non-small cell lung cancer)[72], and an antimiR/antagomiR targeting miR-155 (in cutaneous T cell lymphoma)[73].

siRNA

In addition to the miRNA biogenesis pathway, the RNAi machinery also engages in the processing of longer dsRNAs. Dicer, TRBP and PACT process long dsRNA into shorter dsDNA, typically 20–24 nt in length[74]. The processed fragments — known as small interfering RNAs (siRNA) — have 3′ dinucleotide overhangs, with 3′ OH and 5′ phosphate groups[75,76]. The guide (or antisense) strand, that mediate silencing by incorporating into RISC, is typically designed to have full complementarity to the target mRNA[77]. The thermodynamic properties of the RNA duplex determine which of the two strands that remain loaded in RISC, and which strand that is degraded[78–80].

After binding to the target mRNA, the Argonaute-2 (Ago2) endonuclease cleaves the complimentary sense mRNA at a location 10–12 bases from the 5′ end of the antisense strand binding site[75,76]. Cleavage is typically followed by further degradation of the mRNA and unloading of the fragments from RISC. RISC with the loaded siRNA guide strand is then able to repeat the cycle of target mRNA binding and cleavage[66]. The half-life of mature siRNA–RISC complexes has been estimated to 4–5 days in rodents, during which time it can degrade thousands of target mRNA copies[81,82].

Exogenous inhibitory RNAs can enter the RNAi pathway at different levels to mediate gene silencing. Recombinant RNAs can be designed to mimic pri-miRNA (exogenous miRNA) or pre-miRNA (typically referred to as small hairpin RNA, shRNA)[83]. The most common approach is to utilize 21–22 nt siRNA, mimicking Dicer products and bypassing trimming before RISC loading. In some cases, longer 25–27 nt siRNA that require Dicer processing (Dicer-ready siRNA) can have a higher silencing potency[84,85].

The sequence-specific translation inhibition mediated by RISC makes rational siRNA design possible. Important considerations are the target sequence selection, chemical modifications of the ribose and phosphate backbone, RNA length and nature of the 3′ and 5′ ends.

Target selection and off-target effects

In general, target selection for therapeutic gene silencing (so called knockdown) shares some considerations with conventional drug target selection. In certain aspects, however, siRNA and other RNA or oligonucleotide therapies have additional layers of complexity providing both opportunities and challenges as a new therapeutic modality.

The process of siRNA lead discovery typically starts with *in silico* evaluation of all possible siRNAs against an intended target transcript, to predict specificity and potency. From this, a subset of selected siRNAs can be synthesized and screened in cell culture to evaluate on- and off-target effects. This is followed by *in vivo* pharmacodynamic studies in rodents, identifying a small number of compounds that are advanced into non-human primate studies[86].

The RNAi machinery is expressed in all cell and tissue types, expanding the number of druggable targets to virtually any gene — a substantial improvement compared to the enzymes and receptors that are typically targetable with conventional small molecule drugs[87]. However, all target mRNAs are not equally amenable to RNA interference. First, high mRNA turnover is unfavorable for effective RNAi-mediated gene silencing[88]. Second, work has shown that cellular origin can have an impact on the accessibility of potential mRNA targets to RNAi. This was shown when evaluating knockdown efficiency and comparing the fraction of ApoE mRNA with nuclear or

cytoplasmic in neuronal and glial cells[89]. Intracellular localization of targets mRNA is thus an additional and tissue-dependent aspect that must be considered in target selection.

Sequence-specific off target effects are conferred by partial sequence complementarity of the siRNA with an mRNA other than the intended target, where the gene expression is suppressed by translation repression similar to miRNA activity[90,91]. Early selection and identification of highly potent siRNA sequences is central[86]. In addition to sequence-dependency, the risk of off-target effects is influenced by siRNA concentration and can be reduced by chemical modifications[92].

Most gene products are non-redundant in normal cell biology and physiology, with potential risk of toxicity from efficient, near-total target knockdown. For example, high-level knockdown of PCSK9 — proprotein convertase subtilisin/kexin type 6, an enzyme mediating the degradation of the LDL receptor — is well tolerated, as could be expected considering the rare existence of nonsense mutations in the *PCSK9* gene in some individuals[93]. This mutation results in very low blood cholesterol levels but no other symptoms. In cancer, prioritized targets could likely include receptor-linked kinases in activated signaling pathways (*e.g.* K-Ras or the Ras-Raf-MEK-ERK pathway), oncogenic transcription factors (*e.g.* c-Myc), components important for cell division or DNA repair. Here, it is less clear what the risk of adverse toxicity in normal tissues might be from high and durable knockdown of such targets. On the other hand, current options in oncology treatment include for example 'dirty' small molecule kinase inhibitors, and chemotherapeutics and radiation therapy targeting DNA, DNA repair and cell division — typically with limited sparing of normal tissue — that still have acceptable tolerability. In addition, the extent (depth) and durability of gene knockdown required for therapeutic benefit is an important aspect of target selection, with implications for the clinical doses needed and likely also risk of toxicity. Importantly, with cancer — on the contrary to treatment of for example metabolic disease — considering the lowest level of knockdown achieved across tumor cells is necessary, as disease is more likely to progress no matter the highest level of knockdown if a subset of cells still falls below the threshold for biologically relevant target inhibition.

In the context of target selection and the effects from knockdown in the tissue or organ where the effect is desirable versus normal tissue, targeted delivery of RNA therapeutics is an additional approach to circumvent or limit potential adverse effects[94], as is discussed in more detail below.

Since siRNA act in a DNA/RNA-sequence dependent manner completely different from conventional small molecule drugs, the development of treatment resistance by for example acquired target mutations is likely to behave differently and might be less

common with siRNA than conventional small molecule drugs. In addition, combining two or more siRNA with different target sequences in one gene could provide an opportunity to limit acquired resistance through target mutation. On the same note, combining several siRNA with different target genes could be one strategy to evade acquired resistance development typically observed with for example tyrosine kinase inhibitors (TKIs), where tumor cells upregulate or acquired additional activating mutations in alternative signaling pathways to maintain cell proliferation and tumor growth. On the other hand, as discussed above, potential changes in the site of splicing and primary localization of target mRNAs, or a general inhibition of the RNAi machinery could result in potential loss of efficacy or resistance in cancer cells during tumor evolution, which could be an adaptation to RNAi therapy hard to work around.

Immune stimulation

Systemic administration of synthetic siRNA can activate the innate immune system, with resulting high levels of proinflammatory cytokines including interleukin-6 (IL-6), interferons (INFs) and tumor necrosis factor alpha (TNFα)[95,96]. Innate immune response to siRNA is mediated by pathways that are either dependent or independent on the activation of Toll-like receptors (TLRs).

Three TLRs — TLR3, TLR7 and TLR8 — can be activated by siRNA and predominantly reside in endosomal compartments, where they recognize nucleic acids released from invading viruses and pathogens[97,98]. In addition, TLR3 can be expressed on the cell surface in certain cell types. TLR7 and TLR8 respond to ssRNA, and their activation can be more dependent on the RNA nucleotide sequence, while the dsRNA-sensing TLR3 is less sequence-dependent.[96,99].

Several additional TLR-independent pathways can contribute to innate siRNA-mediated immune activation. Cytoplasmic RNA can be recognized by the dsRNA-binding protein kinase (PKR) or retinoic acid inducible gene 1 (RIG-1) protein. RIG1-activation is mediated by uncapped 5′-triphosphate ends on either ssRNA or dsRNA, which induce a type I interferon response through activation of IRF3 and NF-κB[100,101]. PKR is activated by binding long dsRNA, signaling through pathways that at least in part overlap with RIG-1 to activate INF-response[99].

In addition, asymmetric blunt-end siRNA duplexes can also activate RIG-1[85,102]. Chemical modification of RNA (and other oligonucleotides) has greatly reduced the immunostimulatory effects associated with synthetic exogenous RNAs, as is discussed below.

Chemical modifications

The extensive work and advancements in oligonucleotide chemistry have been instrumental in bringing oligonucleotide and RNA therapeutics into the clinic. Chemical modifications of siRNA that mimic or maintain the structure of the A-form duplex helix is critical to ensure efficient loading into Ago2 and RISC[103]. More than 150 naturally occurring chemical RNA modifications have been identified, including 2′-*O*-methylation (2′-OMe) and complex decoration of nucleobase[104]. Modifications at the 2′-*O*-position of the sugar-phosphate are among the best studied in the context of ASOs and siRNAs. Introduction of 2′-OMe-modified nucleotides inhibits TLR7- and TLR8-dependent RNA recognition and immune response[105], and improves chemical and catalytic stability[106]. The 2′-fluoro (2′-F) modification is a close mimic of natural RNA as well as DNA, increasing the resistance to degradation by nucleases[107]. Additional modifications involving the 2′ position are bicyclic sugars that contain a 2′-4′-*O*-methylene bridge (known as locked nucleic acids, LNA) and 2′-methoxyethyl (MOE) modifications[108].

In addition to the 2′ modifications, phosphate backbone modifications have been instrumental in development of siRNA. Phosphorothioate (PS) modifications were first used in ASO chemistry, where the substitution of one oxygen of the phosphate group with a sulphur atom conferred an improved resistance to phosphodiesterases and increased hydrophobicity[106]. PS modifications are tolerated by TRBP when introduced at the ends of each strand, as TRBP binds siRNA in the middle of the molecule[109]. Another approach made possible by the siRNA–TRBP binding is to reduce the 5′ end of the passenger strand in combination with including an additional 6–8 PS modifications on the 3′ end of the guide strand[110,111]. Additional sugar-phosphate modifications include phosphotriate, phosphorodiamidate morpholino (PMO) and peptide nucleic acid (PNA) backbones. PMO and PNA modifications have neutral backbone structure that are very different from the natural suger-phosphate backbone.

More recent developments in oligonucleotide chemistry include the incorporation of additional terminal PS modifications[112], where the stabilization of the 5′ end of both strands protects against the dominant 5′ exonuclease activity present in the endolysosomal compartment[86]. Sequence-dependent optimization of the 2′-F and 2′-OMe modification pattern is another way to reduce the overall 2′-F content while maintaining siRNA activity and improving nuclease stability. Glycol nucleic acids (GNA) and 5′-(E)-vinylphosphonate are additional chemical advancements, the latter showing promising results for certain extrahepatic tissues like the central nervous system (CNS)[113].

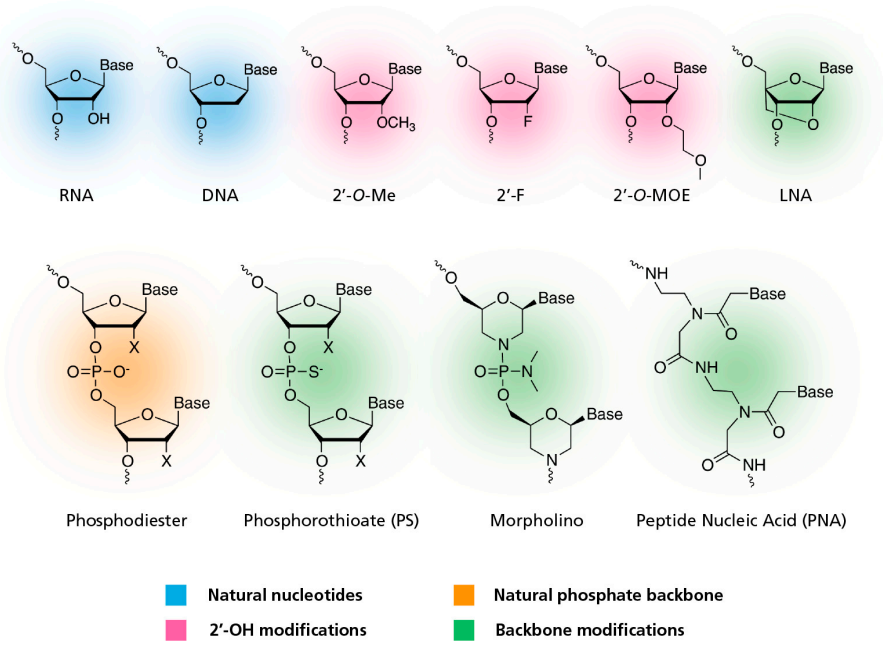

Figure 4. Common oligonucleotide modifications
Modification of nucleotides and phosphate backbone structure of oligonucleotides is important for improved stability, activity and reduced immunogenicity. RNA – ribonucleic acid; DNA – deoxyribonucleic acid; 2′-*O*-Me – 2′-*O*-Methyl; 2′-F – 2′-Fluoro; 2′-*O*-MOE – 2′-*O*-Methoxyethyl; LNA – Locked Nucleic Acid.

A potential safety liability of siRNA therapies is the risk of toxicity originating from unnatural chemical modification of the sugar-phosphate backbone, where 2′-F and PS modifications are the most prevalent. Although concerns have been raised along the way — including late clinical trials of the first GalNAc-siRNA conjugate revusiran — mounting evidence from clinical studies of now approved oligonucleotide therapeutics cannot confirm any adverse toxicity related to the currently used RNA modifications[86].

Clinical use of siRNA therapeutics

At the start of this thesis project, no siRNA therapeutic had yet been approved for clinical use, and only two antisense oligonucleotide drugs had been approved. Since then, siRNA therapeutics have become new and important treatment options in diverse clinical setting.

Patisiran (ONPATTRO) was the first siRNA therapeutic to receive approval for clinical use by FDA and the European Medicines Agency (EMA) in 2018. The drug consists of a chemically modified siRNA directed against transthyretin (TTR), formulated in a

LNP, for the treatment of hereditary transthyretin amyloidosis (hATTR). In Sweden, hATTR is also known as 'Skelleftesjukan' from being particularly prevalent in the region near Skellefteå and Piteå in the north[114]. Patisiran is administrated intravenously with a dosing of one infusion every third week. In the circulation, LNPs interact with serum proteins (in particular apolipoproteins), that promote efficient internalization by the low-density lipoprotein (LDL) receptor on hepatocytes[115]. Through RNAi-mediated knockdown of mutated TTR, protein misfolding and accumulating in tissues is inhibited, preventing the development of polyneuropathy and cardiomyopathy.

The second siRNA therapeutic to reach the market was givosiran (GIVLAARI) in 2019. It incorporates a stabilized (enhanced stabilization chemistry, ESC) siRNA targeting δ-aminolevulinic acid synthase 1 (ALAS1), that have a central role in acute hepatic porphyria (AHP)[116]. Here, hepatic delivery is instead mediated by the conjugation to triantennary *N*-acetylgalactosamine (GalNAc), that bind to the asialoglycoprotein receptor (ASGPR) on hepatocytes for internalization[112]. After RISC loading, givosiran mediates knockdown of ALAS1, reducing the circulation levels of heme intermediates, δ-aminolevulinic acid and porphobilinogens that cause chronic symptoms including neurotoxicity and associated acute porphyria attacks. Givosiran is administrated subcutaneously once a month.

Following the first-in class approval of LNP- and GalNAc-based siRNA therapies, four additional siRNA therapeutics have been approved, all relying on the GalNAc delivery strategy for targeting the liver: Inclisiran (LEQVIO) targets the *PCSK9* gene mentioned above, where knockdown increases recycling of LDL-C receptors to the surface of hepatocytes, mediating enhanced LDL-C binding and reduced LDL plasma levels[117,118]. Two siRNA drugs (lumasiran[119] and nedosiran[120]) have been approved for the treatment of primary hyperoxaluria (PH) — a rare hereditary disease causing accumulation of hepatic glyoxylate — by knockdown of lactate dehydrogenase or glycolate oxidase in the liver. Lastly, vutrisiran is an siRNA drug based on ESC chemistry that targets TTR for treatment of hATTR similar to patisiran, but utilizing the GalNAc-technology for hepatic delivery instead of LNPs[121].

Several additional siRNA therapeutics are currently in late clinical trials. Cemdisiran[122] (GalNAc-conjugate targeting the complement 5 (C5) protein in the liver, in complement mediated disease) and fitusiran[123] (for hemophilia A and B) are both in phase 3 clinical trials. Active phase 2 clinical trials include siRNA treatment of hypertension, non-alcoholic steatohepatitis (NASH), Hepatitis B and D virus infection, alpha-1 antitrypsin liver disease and cerebral amyloid angiopathy[124].

In the early days of RNAi drug development, new anticancer therapies based on siRNA were pursued by many biopharmaceutical companies. Notable early endeavors include

a phase 1, first-in-human trial of two LNP-formulated siRNA targeting vascular endothelial growth factor (VEGF) and kinesin spindle protein (KSP), in the treatment of metastatic liver disease[125]. Although hopes were initially high, efforts were disappointing in early clinical trials and the LNP technology was still plagued by a narrow therapeutic index and inefficient delivery[126]. Setbacks in early clinical development meant that siRNA-based cancer therapies were sidelined, and programs instead shifted focus to benign and genetically validated disease targets expressed in the liver[127]. Now, after largely solving the siRNA chemistry and delivery required for treatment of diseases with hepatic origin, interest in development of anticancer siRNA and other oligonucleotide or RNA therapeutics is again rising.

Anticancer siRNA therapies currently evaluated in early clinical trials include siRNA targeting EphA2 (in advanced solid tumors[128]), K-Ras^{G12D} (in pancreatic ductal carcinoma with *KRAS*^{G12D} mutation[129,130]), HIF2α (in clear renal cell carcinoma[131]), and TGF-β1 and COX-2 (in cutaneous squamous cell carcinoma[132,133]).

Synthetic mRNA

Already in 1990, protein expression was induced *in vivo* in mouse skeletal muscle, after direct injection of mRNA[134]. Similar to siRNA technology, the inherent instability and immunogenicity of mRNA — in addition to the challenge of delivery to target cells — were some of the reasons holding it back from transitioning into the clinic[135]. Therapeutic mRNAs have been investigated in clinical phase 1 and 2 trials as vaccines targeting HIV-1[136], influenza[137], Zika virus[138] and other infectious diseases. The severe acute respiratory syndrome coronavirus 2 (SARS-CoV-2) pandemic accelerated the mRNA therapeutic technology tremendously, with the successful development of two mRNA-based vaccines in record-breaking time, highlighting the potential of mRNA therapies and vaccines[139].

Cancer therapies based on mRNA technology were pursued long before the success of the SARS-CoV-2 vaccines and have been boosted by recent developments. Several strategies exist where protein production from translation of synthetic and/or exogenous mRNA can be leveraged to control tumor progression or trigger and modulate immune response. Briefly, cancer cell proliferation can be inhibited by mRNA-encoded tumor suppressors[140]. Immune response can be triggered by translation of tumor antigens or cytokines, produced by tumor cells or cells in the tumor microenvironment (TME)[141]. Moreover, mRNA-encoded genome editing proteins can disrupt tumor survival genes by targeted gene editing, as is discussed in more detail below. Although ultimately a cell-based therapy, chimeric antigen receptors for T cell engineering (CAR-T cell) is approved (since 2019 in Sweden) for the

treatment of some lymphomas and acute lymphatic leukemia. CAR-T cell therapy is currently investigated for treatment of solid tumors as well, including glioblastoma[142,143]. Here, mRNA-encoded and transiently expressed CARs could offer advantages over strategies where genes are delivered by retroviral or lentiviral gene transfer, that puts the recipient cell at risk for genetic mutation[144].

There are several approaches for improving the stability and translation efficiency while reducing the immunogenicity of therapeutic mRNA, including optimization of the 5′ end cap[145] or 5′ and 3′ UTRs[146], modifications of the open reading frame (ORF) by codon optimization[147], and using natural but modified nucleosides like 5-methyluridine, 5-methylcytidinem, N^6-methyladenosin and pseudouridine (ψ)[148,149]. Modification of the 3′ poly(A) tail[150,151] and exclusion of double-stranded RNA contaminants[152] also improve translation efficiency.

Since mRNA is rapidly degraded by RNases in the bloodstream and cannot be delivered efficiently to target cells in a naked form, various delivery strategies have been used for mRNA delivery. Lipid formulation have typically been the most successful, and the currently approved SARS-CoV-2 mRNA vaccines rely on LNPs based on ionizable lipids[144]. In addition to promoting delivery, these delivery carriers can also have an adjuvant effect that could be beneficial in the vaccine setting[153].

mRNA tumor vaccines

Tumor antigens can be selected to produce specially designed mRNA tumor vaccines, inducing antitumoral T cell or B cell response[154]. Tumor antigens are typically considered tumor-associated self-antigens (TAAs) or tumor-specific antigens (TSAs). TAAs are present in normal tissue but overexpressed in tumor cells, while TSAs represent tumor neoantigens with high tumor specificity and potentially also immunogenicity[155]. Therapeutic cancer vaccines are already used clinically; however, the current treatment options are not based on mRNA technology. One example is Imlygic (Talimogene laherparepvec) — an attenuated and genetically engineered herpes simplex virus type-1 (HSV-1), used for treatment of inoperable, metastasized melanoma[156]. Imlygic is injected into the tumor, where the virus replicates in tumor cells while producing immune stimulatory cytokines (granulocyte-macrophage colony-stimulating factor, GM-CSF) and mediates the release of TAAs or TSAs that promote a systemic antitumoral immune response[157].

Lessons from successful cancer vaccines and numerous preclinical and clinical studies of RNA-based vaccines have demonstrated the feasibility of mRNA vaccines in cancer treatment. In February 2023, FDA granted breakthrough therapy designation to the investigational vaccine mRNA-4157 (V940) in combination with the anti-PD-1

checkpoint inhibitor pembrolizumab, as an adjuvant treatment for patients with high-risk melanoma following surgery[158]. This novel personalized mRNA vaccine consists of a single synthetic mRNA, that is designed and produced based on the mutational signature of the patient's tumor. The mRNA sequence is tailored to encode up to 34 neoantigens, with care also given to the patient's human leukocyte antigen (HLA) type[159]. The mRNA sequence thus provides a unique mutational signature to generate specific T cell response. In the phase 2b clinical trial on which FDA based its decision, the combination of mRNA-4157 (V940) and pembrolizumab showed a 44% decrease in the risk of post-surgical recurrence or death compared to pembrolizumab alone. The anti-PD-1 and tumor neoantigen mRNA combination is now being evaluated in a phase 3 trial[160].

mRNA encoding cytokines and immunomodulatory factors

As mediators of paracrine and autocrine signaling, cytokines are considered to be potent modulators of the TME[161]. Recombinant cytokines have been used for the treatment of some cancers by systemic administration, including IL-2 (renal cell cancer [162]) and INFα2b (adjuvant treatment for resectable melanoma[163]). Typically, systemic administration of recombinant cytokines has shown low treatment efficacy, high safety concerns and was associated with major cost. Using mRNA technology offers several advantages over recombinant cytokines, including rapid and cost-effective production, higher signaling activity and extended half-life using LNP encapsulation both when administered systemically or locally in tumors[144]. The use of LNP formulations also makes it possible to combine mRNA encoding two or more cooperative cytokines in one mixture[164].

One interesting candidate mRNA therapeutic is mRNA-2752 — a 'triplet' mRNA encoding OX40 ligand (OX40L) together with IL-23 and IL-36γ acting as proinflammatory cytokines[165]. Direct injection of the LNP-formulated mRNA into solid tumors causes expression of OX40L on the surface of cells in the tumor niche, as well as cytokine production. OX40L is also known as the tumor necrosis factor ligand superfamily member 4 (TNFSF4), and activation of its cognate receptor expressed on T cells provides a co-stimulatory signal promoting proliferation and survival of activated T cells. Promising results have been reported from an ongoing phase 1 clinical study in patients with advanced solid malignancies, with or without the PD-L1 inhibitor durvalumab as a combination treatment[166]. A previous phase 1/2 clinical trial with a related mRNA candidate — mRNA-2416 — that encoded OX40L alone, was halted prematurely because the efficacy endpoints were not met for either treatment arm[167].

mRNA encoding tumor suppressors

Cancer development and progression is typically associated with lost function of tumor suppressor genes[168]. Thus, restoration of tumor suppressor function is a widely explored strategy for anticancer therapy, via the use of small-molecule inhibitors, protein delivery or DNA-based approaches[169]. Delivery of mRNA encoding the key and in cancer often mutated tumor suppressors p53 (*TP53*)[169] and PTEN[170,171] using various nanoparticle formulations have been studied in several preclinical models with promising results, but positive results from late clinical trials are still lacking[172]. One important difference when considering the delivery of mRNA encoding immune-modulatory or -stimulatory proteins like cytokines or antigens, as compared to mRNA encoding tumor suppressors, is what fraction of cells that needs to be targeted for a significant and durable effect. Production of cytokines and antigens for therapeutic tumor vaccination could very well be highly effective treatments (through the activation of immune response) even if only a fraction of tumor cells (or other cells in the TME depending on the strategy used) are targeted. To achieve restoration of tumor suppressor function, in principle all cancer cells need to be efficiently targeted if the treatment response is to be successful, if not considering immune-mediated secondary effects or strategies with repeated dosing — a significantly more challenging task. Adding to this is the relative inefficiency of particulate carriers like nanoparticles to efficiently penetrate often dense and hypovascularized tumors[173], the few numbers of mRNA molecules carried by each LNP[174–176] and the limited lifetime of delivered mRNA in target cells.

Antisense oligonucleotides

The front gate to the alley of antisense therapeutics was first unlocked in 1978, when it was discovered that Rous sarcoma virus (RSV) translation and proliferation could be inhibited by a 13-mer DNA oligonucleotide in a sequence specific manner[177,178]. In brief, antisense oligonucleotides (ASOs) are single-stranded oligonucleotides designed to pair with complementary regions of an mRNA sequence via Watson-Crick base pairing, to inhibit translation or modify RNA splicing[179]. After binding to its RNA target, ASOs can inhibit protein translation via steric block of the ribosomal machinery[180]. Alternatively, they can recruit RNase H after binding to pre-mRNA or mRNA targets, to silence gene expression. This class of ASOs — known as gapmers — consists of a core DNA sequence flanked by modified RNA mimics (typically LNAs, 2′-F or 2′-OMe modified bases) that provide nuclease resistance[181]. After ASO binding to form RNA–DNA duplexes, RNase H1 of the ubiquitously expressed RNase H

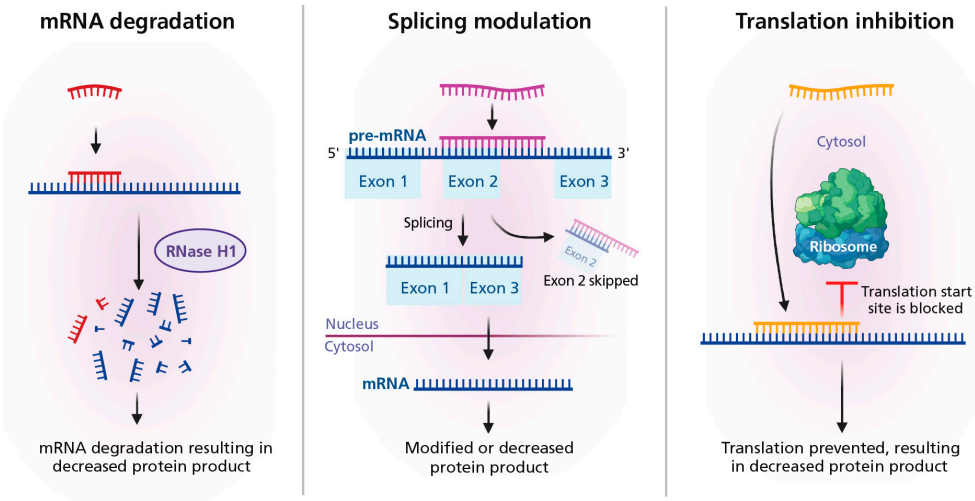

Figure 5. Mechanisms of antisense oligonucleotide target inhibition and modification
Antisense oligonucleotides (ASOs) can downregulate gene expression by RNase H-mediated degradation of mRNA, alter the mRNA sequence or inhibit translation by changing splicing of pre-mRNA into mRNA, or inhibit translation via steric block of the ribosome. Created with BioRender.com.

family hydrolyzes the target RNA strand with subsequent degradation of the fragments[182]. A third category of ASOs function by altering mRNA splicing through for example exon inclusion or exon skipping — so called splice-switching oligonucleotides (SSOs)[183]. Depending on the intended strategy, designing ASOs to hybridize with splice sites, silencer elements or enhancer elements within pre-mRNA transcripts can make it possible to manipulate the splicing machinery to induce exon skipping, change the ratio of splice forms or restore splicing patterns[179]. Additionally, ASOs can mediate target suppression by introducing out-of-frame deletions by modulation splicing, with subsequent nonsense-mediated decay of the transcript and gene silencing[184].

In contrast to the RNAi machinery and siRNA, SSOs act in the nucleus to modulate splicing, and ASOs eliciting RNase H can mediate target degradation either in the nucleus or cytosplasm[106]. Thus, ASO design that influences its subcellular localization after endosomal escape will also affect its potency.

In similarity to siRNA, ASOs can be designed to bind non-coding RNAs and aberrant RNAs that cause disease, expanding targets beyond protein-encoding mRNA.

ASOs have typically been synthesized and administered in the naked form[108]. ASOs with a PS backbone become highly associated to plasma proteins with low affinity following intravenous administration[185]. Plasma protein-binding reduces renal

filtration of naked ASOs and improves tissue uptake, primarily in the liver[186]. Neutrally charged ASOs such as PNAs or PMOs bind weaker to plasma proteins, increasing renal filtration and lowering the dose delivered to target tissues[187].

Following systemic administration, ASOs distributes broadly into most tissues, but in particular the liver, kidney, bone marrow, adipocytes and lymph nodes[188–190]. Despite being readily reachable after intravenous injection, ASO delivery to muscle is inefficient, probably related to the large amount of muscle tissue that needs to be targeted to achieve meaningful effect, and significant muscle-to-muscle variability[179]. Since oligonucleotides do not cross the blood-brain barrier[191], approved ASOs rely on intrathecal administration to reach the CNS. After injection into the cerebrospinal fluid (CSF), ASOs distribute broadly and rapidly in the CNS and are internalized by neurons and glial cells[192,193]

Several cell-surface receptors have been suggested to bind naked and/or plasma protein-associated ASOs — including scavenger receptors[194], integrins[195] and TLRs[99] — to mediate their internalization via endocytosis. ASOs with PS backbones can shuttle continuously between the cytoplasm and nucleus by passive diffusion and active transport[196]. Like other oligonucleotide therapeutics, ASOs need to escape from the endosomes to mediate biological response.

Clinical use of ASOs

Fomivirsen was the first ASO to be approved by FDA in 1998, for the treatment of cytomegalovirus (CMV) retinitis through translation block[197]. It was followed by mipomirsen (Kynamro) for familial hypercholesterolemia in 2013, although mipomirsen was rejected by EMA in 2012 and again in 2013[106]. After a couple of years, the introduction of new ASOs into the clinic picked up speed, as the SSO nusinersen (Spinraza) was approved in 2016 for the treatment of spinal muscular dystrophy (SMA), highlighting the potential of oligonucleotide-based CNS therapies[198]. Also in 2016, the first SSO for the treatment of Duchenne muscular dystrophie (DMD) was approved by the FDA. To date, in total four SSOs that induce skipping of exon 51 (eteplirsen), exon 53 (golodirsen and viltolarsen) or exon 45 (casimersen) for treatment of DMD have been approved by FDA[199]. However, no SSOs for treatment of DMD have been authorized by EMA, ruling that the evidence put forward for the authorization of eteplirsen were not satisfactory for showing the medicine was effective, why it was refused in 2018[200]. In June 2020, viltolarsen was granted orphan designation by EMA[201], and clinical trials are ongoing[202,203].

Eplontersen — a GalNAc-conjugated ASO targeting TTR in the liver[121] — was approved by FDA late in 2023 for the treatment hereditary transthyretin-mediated

amyloidosis, marking the first approval of a GalNAc-conjugated ASO and the first medicine for the treatment of TTR-related polyneuropathy that can be self-administered via an auto-injector[204].

Very recently (February 2024), the Committee for Medicinal Products for Human Use of EMA recommending granting of a marketing authorization (under exceptional circumstances) for tofersen (Qalsody) for the treatment of a type of amyotrophic lateral sclerosis (ALS) caused by a defective superoxide dismutase 1 (SOD1) protein[205]. Approved by FDA in 2023, tofersen is administered intrathecally and binds to the mRNA of the encoding SOD1, leading to its breakdown via RNase H. Mutations in the *SOD1* gene account for ~2% of all ALS cases, and more than 180 different *SOD1* mutations have been reported[199].

Lastly, ASO therapeutics are also pursued for individualized 'n-of-1' treatments, where the antisense sequence is custom-tailored to treat (more-or-less) unique pathological variants. This was first shown by the development of Milasen by Timothy Yu and colleagues: a SSO for the treatment of Batten's disease in a single patient — Mila[206]. Since then, several additional patients have been treated with individualized ASOs, raising important technical, legal and ethical questions about drug development, authorization, safety and cost[207].

RNA-based genome editing systems

The discovery of the clustered regulatory interspaced short palindromic repeats (CRISPR)–Cas genome editing systems have launched a new era in gene therapy[208–210]. As of today, four classes of genome editing agents derived from CRISPR–Cas are available — nucleases, base editors, transposases/recombinases and prime editors. In addition to targeted alterations in genomic DNA sequences, CRISPR applications can also be used for RNA editing[211], transcriptional regulation[212], epigenetic modifications[213] and nucleic acid detection[214]. Genome editing technologies and applications are advancing rapidly, and this is largely a topic that is outside the scope of this thesis. However, since genome editing approaches typically deploy RNA as part of the targeting technology, or rely on delivery of parts of the ribonucleoprotein complex as mRNA, they represent invaluable tools in the RNA therapeutics toolkit. Additionally, it shares many delivery challenges with other oligonucleotide drugs.

CRISPR-Cas nucleases

Naturally occurring bacterial and archaeal CRISPR–Cas immune systems have been classified in groups and subtypes, depending on the number of proteins involved in nucleic acid cleavage and the type of Cas protein[215]. Most Cas9 and Cas12 variants

possess RNA-guided DNA endonuclease activity, making them highly relevant for DNA editing. CRISPR–Cas activity require that a short sequence — protospacer adjacent motif (PAM) — exists near the target DNA site[216]. Most Cas9 applications use a single guide RNA (sgRNA) to confer target sequence recognition[208]. Recognition of target sites begins with binding of the Cas9–guide RNA ribonucleoprotein complex to the PAM sequence, followed by formation of an RNA●DNA heteroduplex between the sgRNA and target DNA strand[217]. After high complementarity RNA●DNA binding, Cas9 undergoes conformational changes that activate its nuclease domains[218], followed by hydrolysis of the phosphodiester backbone of DNA to create predominantly blunt-end double strand breaks (DSB)[208]. Following the generation of DSBs, DNA is repaired by either nonhomologous end-joining (NHEJ) or homology directed repair (HDR)[219]. NHEJ repair mechanisms (of which there are several versions) yields uncontrolled but predictable DNA insertions or deletions (indels), typically disrupting gene function[220]. HDR is a competing repair pathway, that is less efficient and occurs primarily in dividing cells[221]. It requires the presence of a donor DNA template to install targeted mutations or to knock in larger DNA sequences[222].

Base editors

Current base editors contain a catalytically impaired CRISPR–Cas nuclease that is unable to generate DSBs, fused to a single-stranded DNA deaminase[223]. In some cases, the ribonucleoprotein complex also contains proteins that manipulate DNA repair pathways. Using a guide RNA targeting the desired DNA sequence, base editors precisely install targeted point mutations without generating DSBs and the need of donor DNA templates or HDR. Two main classes of base editors are available, namely adenine bas editors (ABEs), catalyzing the conversion of A●T base pairs to G●C base pairs; and cytosine base editors (CBEs), catalyzing C●G-to-T●A conversions[224]. In this way, ABEs and CBEs together mediates all four possible transition mutations.

Prime editors

Prime editors represent a recent genome editing technology, that extents the type of point mutations from the transition mutations achievable with base editors, to include all six possible base pair conversions (12 possible point mutations)[225]. In addition, prime editors enable small deletions and small insertion in a targeted and precise way. Prime editors are fusion proteins between partly inactivated Cas9 domains (Cas9 nickase, where the HNH nuclease domain is inactivated) and engineered reverse transcriptase domains. The prime editing fusion protein is targeted to the editing site by a prime editing guide RNA (pegRNA). The pegRNA is engineered so that it specifies the target site and encodes the desired edit[226].

Transposes and recombinases

Even though Cas-promoted HDR can insert desirable genetic sequences at a specific genomic site, these strategies are limited to actively dividing cells, substantially limiting their usefulness for many applications[226]. Recently, natural CRISPR-associated transposases and engineered transposase systems with fused Cas-domains have been reported[227,228], that are able to integrate genomic cargos at DNA sites without HDR-dependency. In addition, studies have also shown that engineered Cas-fused recombinases can modify substrates or delete target DNA *in vitro*, but so far with low efficiency and highly restricted target sequences[229]. In summary, CRISPR-targeted transposases and recombinases represent recent and exciting opportunities in genome editing, that could achieve precise arrangements of large DNA sequences.

Clinical use of RNA-based genome editing systems

In late 2023, the UK Medicines & Healthcare Products Agency approved the first CRISPR-Cas9 gene editing therapy followed shortly by FDA[230] and EMA. The therapeutic — Casgevy — is a cell-based gene therapy for the treatment of sickle cell disease with serious symptoms. After isolation of $CD34^+$ hematopoietic stem cells from patients, CRISPR components are introduced *ex vivo* as a ribonucleoprotein complex by electroporation. Casgevy acts not by restoring normal adult hemoglobin — a tetrameric protein consisting of two α-globin and two β globin chains, $\alpha 2\beta 2$, where the β-globin gene harbors the disease-causing mutation. Instead, Cas9 mediates disruption of *BCL11A*, a gene encoding a repressor that acts directly on the fetal γ-globin gene promotor[231]. Derepression of the γ-globin gene leads to formation of fetal hemoglobin, consisting of two α-globin and two γ-globin chains ($\alpha 2\gamma 2$). Sufficient levels of circulating fetal hemoglobin ameliorates the effects of the mutated β-globin chain, reducing risk of serious disease episodes (vaso-occlusive crisis)[232].

Base editors have been used in clinical trials to generate universal CAR-T cells from healthy donor T cells, that were transduced with lentivirus to express a CAR with specificity for CD7 — a surface receptor protein expressed by cells in T cell acute lymphoblastic leukemia (ALL). Base editing was then used to inactivate three separate genes, encoding CD52, CD7 and the β chain of αβ T cell receptor. The safety of the edited cells was investigated in a phase 1 study, in three children with recurrent ALL[233].

Delivery of CRISPR-Cas9 systems for safe *in vivo* genome editing is a substantially more difficult prospect than *ex vivo* editing and subsequent transplantation of immune cells. Currently investigated in a first-in-human phase 1b open-label trial, the base editing therapy VERVE-101 uses mRNA encoding an adenine base editor and a guide RNA targeting *PCSK9*, packaged in a LNP and delivered as a one-time intravenous infusion. After internalization by hepatocytes in the liver, the mRNA and gRNA

payload escapes to the cytosol where the mRNA is translated into functional ABEs that disrupt the *PCSK9* splice donor site by A●T to G●C base pair conversion. The base editing inactivates the *PCSK9* gene and lowers plasma LDL-C levels by increased expression of LDL receptors on the hepatocyte cell surface[234]. Interim results from the study were presented at the American Heart Association's Scientific Sessions in November 2023[235].

CRISPR-based technologies have gained substantial attention within cancer research as well, both as invaluable research tools but also methods or strategies for cancer treatments. As exemplified above, several phase I clinical trials are currently ongoing, where *ex vivo* CRISPR engineering of allogenic or autologous T cells is investigated to either disrupt immunosuppressive genes (*e.g.* PD-1), or to integrate CAR elements into T cell receptor genes[236]. However, although preclinical and translational strategies are being explored, direct targeting of tumors with CRISPR-Cas systems *in vivo* is a considerably harder task and not currently on the clinical horizon.

The billion-year-old barrier

Some two billion years ago, emerging eukaryotic cells evolved the ability to interact with the surrounding environment not only externally, but also after internalization of components from the outside to the inside of cells[237]. Strict and well-regulated separation of internal cellular processes and material derived from the exterior world required a fundamental barrier, composed of specialized lipid membranes and the intricate network of diverse compartments they form.

Structure and composition of endomembranes

The elaborate endomembrane system is one of the most significant traits that distinguish eukaryotic from prokaryotic cells. The various compartments it encompasses exists in all major eukaryotic groups, indicating that the endomembrane system was present in the last eukaryote common ancestor, and that its origin could be linked to the origin of eukaryotes themselves[238].

Theories for the origin of the endomembrane system have often derived it from plasma membrane invaginations, where the lumen of endosomes and the endoplasmic reticulum (ER) are topologically homologous to the external environment. Alternative theories have proposed that as the proteobacterial ancestor of eukaryotic mitochondria became an endosymbiont in its archaeal host, it was still able to produce outer

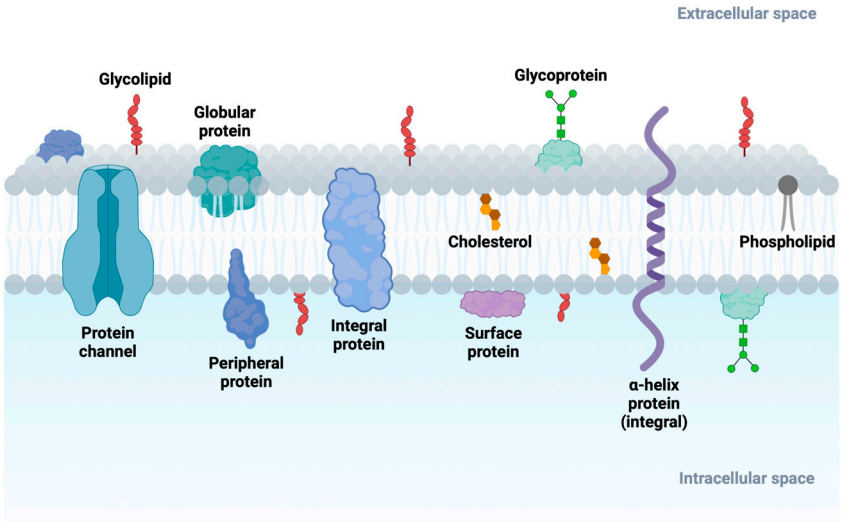

Figure 6. The lipid bilayer composition
Cellular membranes are complex lipid bilayer structures composed of different phospholipids, sphingolipids and cholesterol. The lipid species, the ratio between them and their localization to the inner and/or outer membrane leaftlet or nanodomains is important for membrane structure, fluidity and function, and varies between subcellular compartments and over time. The lipid bilayer is also housing a vast number of different proteins and carbohydrate structures with many and diverse functions. Created with BioRender.com.

membrane vesicles — vesicles that are budded and secreted outward — that provided the initial seed of the eukaryotic endomembrane system[239].

Whatever its evolutionary origin, compartmentalization provides eukaryotic cells with functionally specialized aqueous spaces that are separate from the cytosol. In addition, many vital biochemical processes take place on membrane surfaces, including for example lipid metabolism and oxidative phosphorylation, and the endomembrane system expands the total membrane area available for such processes vastly compared to the plasma membrane alone. Organelle membranes — including membranes of the endolysosomal system — have a lipid bilayer with specific composition that is impermeable to most hydrophilic molecules and macromolecules. Instead, membranes contain various transport proteins that are responsible for the transfer of metabolites between the luminal and cytosolic side of the bilayer. In addition, organelles have mechanisms for importing, incorporating and maintaining specific membrane proteins and component that confers its identity and specialized functions[240].

The major lipid constituents of cellular bilayer membranes are classified into glycerophospholipids (GPL), sphingolipids and sterols. In mammals, sterols are mainly represented by cholesterol. GPLs have a polar head group and two hydrophobic hydrocarbon tails, that are usually fatty acids of different lengths where one chain typically contains one or more *cis*-double bonds. Lipids in cellular membranes are amphiphatic, meaning they have a hydrophilic (polar) end and a hydrophobic (non-polar) end, that in combination with the molecule shape cause them to spontaneously form bilayer structures in aqueous environments. The same properties that drive formation of the lipid bilayer also provides self-healing properties, as a small disruption in the bilayer cause rearrangement of surrounding lipids to eliminate the interaction between the free membrane edge and neighboring water molecules[241].

The fluidity of lipid bilayers is crucial to membrane functions. Membrane fluidity depends on its fine-tuned composition, determined by both chemical diversity (various structures of lipids) and compositional diversity (ratio of different lipids). The alkyl chain length and number of *cis*-double bonds (*i.e.* level of saturation) of phospholipids influence their packing and thus membrane fluidity and temperature-dependent properties. Incorporation of cholesterol into the bilayer enhances its permeability-barrier properties, as the orientation and interaction of cholesterol with hydrocarbon chains within the bilayer makes the membrane less deformable and decreases its permeability to small water-soluble molecules. Complex compositional diversity of lipid membranes is seen over scales ranging from species, tissues, cells, organelles and even membrane leaflets (inner and outer halves of the bilayer) and membrane subdomains[242].

The endolysosomal system

The endolysosomal system is a highly dynamic and complex cellular network of membrane-enclosed intracellular compartments that handle trafficking, sorting and degradation of material internalized from the exterior environment via endocytosis. At several levels throughout this network, there is interplay and connections with other trafficking routes (*e.g.* with origin from the Golgi complex or ER) and interactions with specialized compartments like peroxisomes. The endocytic pathway is elusive, as the large number of entities collectively forming the compartments that it entails are scattered and undergo continuous but asynchronous fusion, fission, transformation and maturation at subcellular sites that typically are not very predictable[243].

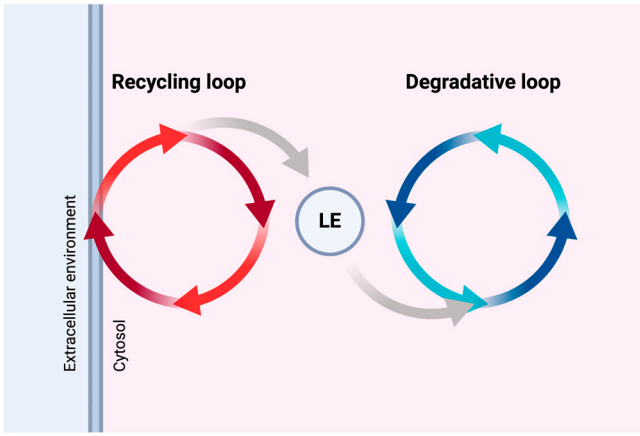

Figure 7. Schematic representation of the endocytic pathway
At its core, the endocytic pathway consists of a endocytosis–recycling loop and a degradative loop, that are connected via a feeder pathway where late endosomes (LE) is the key mediator. Created with BioRender.com.

The endocytic pathway in a nutshell

In a reductionistic representation, the core processes of the endocytic pathway can be described with just a few elements:

- An endocytosis–recycling circuit shuttles components between the plasma membrane and early endocytic compartments. A typical mammalian cell cycles the equivalent of 50–180% of the surface area of the plasma membrane every hour through various kinds of endocytosis[244]. Only a small fraction of all internalized material and fluid is directed toward the degradative system, while the majority is recycled back to the plasma membrane.
- A degradative system, centered around lysosomes, is responsible for digestion of endocytosed macromolecules.
- A feeder pathway connects the endocytosis–recycling circuit and the degradative system, where late endosomes (LE) are the mediator. The feeder pathway relies on stringent sorting and selection of membrane components and associated luminal cargoes that become destined for the degradative system. Bulk fluid and solutes that enters the endocytic/recycling loop are typically not specifically sorted, and thus spread throughout the endolysosomal compartments in a way that is dictated by overall fluid flux[243].

Endocytosis

Endocytosis is the key cellular internalization process that transport a wide range of cargo molecules from the cell exterior and plasma membrane to small (60–120 nm) intracellular vesicles. Several important endocytic pathways have been described in eukaryotic cells, where clathrin-dependent endocytosis is typically the most abundant[245]. In addition to clathrin, over 50 other proteins are involved in the formation of clathrin coated vesicles[246]. Although still completely understood, several endocytic adaptor proteins (AP2, FCHO1/2) and scaffold proteins (EPS15, EPS15R) and other co-factors form endocytic sites on the plasma membrane in a cooperative manner, where they bind to cytosolic regions of different transmembrane cargo molecules to recruit them to the site of the plasma membrane that will produce the endocytic vesicle[247]. Transmembrane proteins that bind external cargoes — *i.e.* receptor–ligand pairs — can be recruited into endocytic sites in a manner that is dependent or independent on ligand binding (receptor-mediated or constitutive endocytosis, respectively)[248]. Receptor interaction with adaptor proteins is mediated by short linear sequence motifs or modifications such as phosphorylation or ubiquitylation[249]. After recruitment of cargo to the endocytic site, the membrane is shaped into an invagination by the clathrin coat, actin filaments and scission proteins. With the help of BAR proteins, dynamin GTPases separate the vesicle from the plasma membrane by constricting the tubular neck of the invagination[250].

In addition to the clathrin-dependent endocytic pathway, several clathrin-independent (CI) endocytic processes have been described. Although less abundant and still less characterized, CI pathways mediates cellular uptake of many extracellular receptors, ligands and pathogens[251]. CI endocytosis can be dependent or independent on dynamin GTPase to form the endocytic vesicles. Caveolae-mediated endocytosis is the best characterized dynamin-dependent CI pathway. Caveolar invaginations are marked by the presence of caveolin proteins[252], and form intermediate compartments called caveosomes. RhoA GTPase-regulated endocytosis[253] and fast endophilin-mediated endocytosis (FEME)[254] are another example of CI dynamin-dependent endocytic pathways.

CI pathways that are also dynamin-independent have been described, characterized by the either the Rho family GTPase CDC42 or the Arf family member ARF6 for their regulation. CDC42-regulated endocytosis produces tubular clathrin- and dynamin-independent carriers (CLICs), that after scission form intermediate glycosyl phosphatidylinositol-anchored protein- (GPI-AP) enriched early endosomes (GEECs). This route is typically referred to as the CLIC/GEEC pathway[255].

Interestingly, several cargos of the CI pathways — including GPI-anchored proteins — do not contain known cytoplasmic sorting motifs for recognition and recruitment to endocytic sites.[256]. Alternative molecular events involved in cargo recruitment have now been identified. One such mechanism is the GL-Lect hypothesis, where extracellular clustering of glycosphingolipids and/or glycosylated proteins into nanodomains that bend the plasma membrane is mediated by secreted lectins (*e.g.* Galectin-1/3/4/7–9)[257]. The GL-Lect mechanism appears to have an important role in the stimulation of the CLIC/GEEC pathway[258]. Although less is known about cargo selection in different CI endocytic pathways, a range of protein-based (ubiquitylation, cytoplasmic motifs), lipid-based (clustering of lipid-tethered proteins) and combined lipid–protein mechanisms (*e.g.* flotillin-dependent endocytosis) have been proposed [255,259].

Evidence suggest that the same endocytic cargo can be internalized by different mechanisms in different cell types; that the endocytic pathways can be switched under certain conditions; and that alternative redundant endocytic mechanisms can be used for some cargo molecules — all contributing to the difficulties to attain a large-scale integrated understanding of the CI endocytic pathways and their functional organization[260].

Two specialty cases of cellular internalization deserve a brief discussion. First, phagocytic immune cells can engulf other cells or large particles (>0.5 μm in diameter) via phagocytosis. Foreign objects are recognized by surface receptors, and actin-dependent remodeling of the plasma membrane mediates the ingestion[251]. Second, pinocytosis is also initiated by the actin-regulating machinery, that organize actin to form large cup-like structures (macropinosomes) that bring fluid material into the cell. In this process — where no specific sorting mechanism at the cell surface is operating — receptors located in the plasma membrane forming the macropinosomes are internalized without discrimination, together with solutes or macromolecules present in the extracellular fluid. The fate of internalized components is decided when macropinosomes fuse with various endolysosomal compartments, and components are sorted or diverted for recycling or degradation[261].

Naturally, endocytosis is a key challenge in the delivery of macromolecules to target cells. Additionally, derangement of endocytic processes in cancer affects cellular properties like the plasma membrane surfaceome, receptor and cargo internalization, signaling, nutrient scavenging, cell polarity, and interactions with the immune system — all of which have therapeutic implications[248]. Mechanistic details and strategies for leveraging endocytosis for delivery of therapeutic molecules is largely beyond the scope of this thesis but will be highlighted below when discussing relevant RNA delivery strategies.

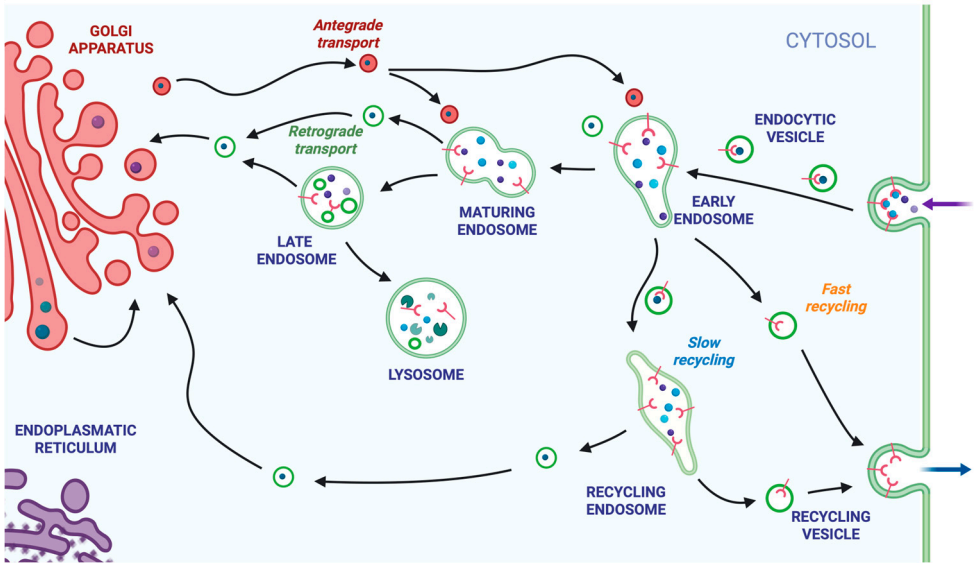

Figure 8. Simplified schematic of the endocytic pathway
Receptor-bound cargo is internalized by endocytosis and routed via endocytic vesicles to early endosomes. Cell surface receptors and internalized molecules can be recycled back to the extracellular environment directly from early endosomes or via specialized recycling endosomes. Internalized cargo and receptors are sorted in early endosomes before endosomal maturation generates late endosoms and multivesiclular bodies. Antegrade trafficking from the *trans*-Golgi network provides material for early, maturing and late endosomes, and molecules can be retrieved from these compartments to the Golgi apparatus via retrograde transport. Late endosomes eventually fuses with acidic lysosomes, containing hydrolases that degrade internalized material. Created with BioRender.com.

Early endosomes and recycling endosomes

Following endocytic uptake, newly formed small endocytic vesicles are thought to fuse and form early endosomes (EEs), that can then receive cargo from vesicles derived from both clathrin-dependent and -independent pathways[255]. EEs are short-lived, typically only accepting incoming vesicles for about 10 min. During this time, some of the incoming cargo will be retained and accumulate over the lifetime of the EE, while lipid membrane and fluid is rapidly recycled away[262]. To support the task of cargo selection and sorting, EEs have a complex structure with tubular and vacuolar domains, and membrane subdomains with different composition and specialized function[263]. Recycling from EE to the plasma membrane can occur by a direct route from EEs (fast recycling), or by an indirect route via specialized recycling endosomes (REs, slow recycling)[264].

Formation of intraluminal vesicles (IVLs) starts already in EEs, where the endosomal sorting complexes require for transport (ESCRT) organizes sorting of ubiquitylated membrane proteins into ILVs formed by membrane invagination and scission [265].

Throughout the endocytic pathway, both antegrade and retrograde traffic between endosomes and the *trans*-Golgi network (TGN) are continuously ongoing processes, responsible for delivery and removal of components from EEs, maturing endosomes, LEs and newly formed lysosomes[266].

Endosomal maturation and late endosomes

Evidence supports at least two ways in which LEs are derived from EEs. First, the Rab GTPase Rab5 present on EE membranes recruit Rab7, after which it is converted to the GDP-bound form and dissociates from the vesicle membrane. The process of Rab5–Rab7 conversion has been observed on the scale of a few minutes[267]. Second, LE can be derived from EE by fission events, where Rab7 is recruited to subdomains of $Rab5^{+}$ EE, followed by separation of the Rab7 domain from the rest of the endosome, that maintains its EE components[268]. It is possible that different mechanisms for LE formation exists for different populations of EE and it could also be influenced by the cargo they contain[243].

Late endosomes also have a role as carriers of components like degradative enzymes (hydrolases) and membrane proteins from the TGN to lysosomes. This influx is required for maintaining the activity and integrity of mature lysosomes[269].

LEs undergo several changes after during their formation, referred to as endosomal maturation. This process involves exchange of membrane components; shift in fusion specificity toward LE, lysosomes and autophagosomes; increased formation of ILVs; relocation toward the perinuclear area; decrease in luminal pH and progressive acquisition of lysosomal components. Inclusion of lysosomal glycoproteins (like lysosome-associated membrane glycoproteins, LAMPs) provide resistance of the limiting membrane of LEs to hydrolases[243].

Lysosomes

Late endosomes formed in the peripheral cytoplasm are moved to the perinuclear area, where they mature, fuse and form larger bodies that undergo both transient fusion events (kiss-and-run) and full fusions with 'prelysosomal' vesicles (hybrid organelles between LEs and lysosomes) and lysosomes[270]. Fusion of LEs with lysosomes delivers macromolecules destined for degradation to the final 'dead-end' station, but also provides many of the components necessary for maintaining lysosomal activity. Several pathways feed material to lysosomes for degradation, contributing to the heterogeneity

of lysosomal compartments and the collection of vacuoles they contain. Functionally mature lysosomes can be defined by four cardinal features: (1) A high degree of acidification, with a pH of 4.5–5.0; (2) high levels of lysosomal hydrolases and (3) lysosomal membrane proteins; (4) the absence of mannose 6-phosphate receptors[271]. Thus, the classical lysosomes with high hydrolase content and high buoyant density typically represent the compartment at a late stage of the degradative process.

In addition to their role as a garbage disposal system within the cell, lysosomes have also been linked to triggering of cell death via lysosomal membrane permeabilization (LMP), coining the term 'suicide bags'[272]. Acidic lysosomes provide the perfect conditions for more than 50 degradative hydrolases. Hydrolytic activity of proteases that are released from lysosomes is counteracted by higher cytosolic pH and the presence of endogenous inhibitors[273]. If the release is substantial, however, cytosolic defense mechanisms can become saturated and result in caspase-dependent or -independent apoptotic, pyroptotic or necrotic types of cell death — collectively defined as lysosome-dependent cell death[274]. Considerable lysosome damage will trigger an autophagic response (lysophagy) to remove the lysosome, whereas limited damage or permeabilization is more likely to trigger repair responses that restore lysosome integrity and function, as is discussed in greater detail below. Although treatments that induce massive LMP have been associated with toxicity and apoptosis since the discovery of lysosome-dependent cell death, findings of lysosome-derived nuclear or cytosolic proteases and their involvement in homeostatic cellular processes suggest that limited, spatially and temporally restricted release of lysosomal hydrolases via LMP may be a regular occurrence that is compatible with cell survival[275–277]. For example, a recent study found that cathepsin B was released from lysosomes positioned near the chromatin metaphase plate to support chromosome segregation in normal mammalian cell division[278].

pH is important for endosome function

Acidification of endosomes is dependent on fusion with LEs and vesicles derived from the TGN, that carry the vacuolar H^+-ATPase (V-ATPase). V-ATPase is a unique class of ATPase, that do not require coupled influx of permeant anions to transport H^+ into the endosomal lumen[279]. To compensate the electrogenic effects of continuous H^+ influx across the endosomal membrane mediated by V-ATPase — that would otherwise result in an increasing positive charge and energetic barrier against maintenance of low pH — vesicular chloride channels that are activated by high H^+ concentration conduct a passive Cl^- ion current compensating the positive charge buildup and permit H^+ influx against a concentration gradient[280]. Additional changes in the ionic environments

have been characterized and are also linked to acidification, including mediators as Na^+ /K^+ ATPase and Ca^{2+}, Na^+ and K^+ ion channels[281].

EEs are only weakly acidic, with a pH typically between 6.1–6.8. Progressive acidification lowers the pH of LE to 4.8–6.0, and lysosomes to pH ~4.5[282]. Acidification of the vesicle lumen throughout the endolysosomal system is required for a multitude of functions, including release of ligands from internalizing receptors (required for receptor recycling); maturation of LEs; optimal function for acidic lysosomal hydrolases, and oxidation reactions[283]. Additionally, intralumenal pH is of key importance for several oligonucleotide or RNA delivery systems, including LNPs using ionizable lipids as discussed below.

Regulators of endosome function

The regulatory systems orchestrating the intricate endolysosomal network and endocytic pathways are extensive and highly complex, why only a very few key aspects of the regulation will be outlined here.

As already introduced, Rab GTPases are master regulators of almost all membrane trafficking processes in eukaryotic cells. This includes the endocytic pathway, where they also serve as important organelle identity marker. Rab GTPases represent the largest family of small GTPases, and more than 60 members that localize to distinct intracellular membranes have been identified in humans[284]. The function of Rab proteins is controlled by switching between two conformational states — a GTP-bound 'on' state and GDP-bound 'off' state. Switching between the states is regulated by sets of guanine-nucleotide exchange factors (GEFs), GTPase-activating proteins (GAPs), GDP dissociation inhibitors (GDIs) and GDP displacement factors (GDFs). The attachment of one or two hydrophobic geranylgeranyl groups confers the reversible association of Rab GTPases with membranes. In the GTP-bound state, Rab GTPases recruit effector proteins that mediate the specialized functions which characterize the compartment the Rab proteins localize to[285].

As mentioned above, the Rab switch with Rab5 to Rab7 conversion is a key step and driver of endosome maturation, and its regulation includes a large number of additional factors and complexes. Depending on the topic of interest, various Rab GTPases receive different level of attention. In the endocytic pathway, apart from the key regulators Rab5 and Rab7, Rab22 mediates bidirectional trafficking between the TGN and early endosomes and Rab9 mediates transport from LE to the TGN. In the recycling pathway, Rab15 is involved in trafficking from EEs to REs, and Rab11 and Rab35 mediate recycling from REs to the plasma membrane[285].

A second class of fundamental regulators of endolysosomal function is membrane tethering complexes, that are a prerequisite for proper fusion of two membrane entities at the right time and place. Briefly, tethering of endocytic vesicles to EEs is mediated by the class C core vacuole/endosome tethering (CORVET) complex. Tethering and fusion of LE with lysosomes is instead dependent on the homotypic fusion and vacuole protein sorting (HOPS) complex[286].

Phosphatidylinositol (PI) conversion is an additional key event in endosomal maturation, where local synthesis or conversion of the membrane lipids phosphatidylinositol-3-phosphate (PtdIns3P) and phosphatidylinositol-3,5-phosphate (PtdIns(3,5)P2) is regulated by specific kinases and phosphatases that allow tight control of compartmentalization through the downstream recruitment of a number of effector proteins with PI-binding domains (*e.g* FYVE, PX, PH, GRAM)[287]. PtdIns3P is primarily found on the cytosolic leaflet of EE membranes, and its synthesis is initiated via Rab5 dependent mechanisms[288]. PtdIns(3,5)P2 is important later in the degradative pathway, and its conversions from PtdIns3P is mediated by the kinase PIKfyve, that binds PtdIns3P with its FYVE domain. This links the production of PtdIns(3,5)P2 to membranes rich in PtdIns3P[289]. Additionally, the control of PI metabolism provides a way of crosstalk between Rab GTPases[285].

Endosome motility is a key aspect of their function as an interacting network, and their movement is closely linked to their function and stage of maturation. Movement between the periphery and perinuclear areas of the cell is mediated by both dynein and kinesin motor proteins along microtubules radiating from the microtubule organizing center (MTOC). Kinesins and dynein provide opposing forces that move attached vesicles in opposite directions on microtubules, towards the periphery (microtubule plus end) or MTOC (microtubule minus end) respectively[290,291]. Net movement is toward the MTOC, and LEs and lysosomes typically enrich at the perinuclear region along this axis.

Protein and lipid components regulating or otherwise residing on endosomes are only partially useful as molecular markers of endosome identity, because the majority of these components either follow the endosomes through multiple steps of transformation or is only transiently associated with the specific compartment organelle.

Not only a shuttling network

In addition to the simplistic view of the endolysosomal system as a routing and degradation system for endocytosed material, several additional and fundamental functions have been associated with it over the years. Species of lysosomes fuse with the

plasma membrane to repair it, and damages in the plasma membrane can be mended by endocytosis[292,293]. Various endosomal compartments also release nondegradable or other material to the cell exterior by exocytosis via recycling endosomes or lysosomes[294,295]. Invagination of the endosomal membrane leads to the formation of intraluminal vesicles (ILVs) in later endosomal compartments known as multivesicular bodies (MVBs), and ILVs that are released to the environment via fusion of MVBs with the plasma membrane is the source of exosomes[296]. Not surprising considering the topological homology of the endolysosomal luminal space to the cell exterior, endosomes have numerous functions in fighting infections. In addition to providing a physical barrier restricting access to the inside of the cell, presence of pathogens can activate immune response via intralumenal receptors like Toll-like receptors (TLRs)[297]. Endosomes are also the site of antigenic peptide generation and binding to major histocompatibility complex class II (MHC-II) molecules[298]. Lysosomes also have an important function as signaling hubs[299]. As an example, the selective metabolic responses mediated by mechanistical target of rapamycin complex 1 (mTORC1) is dependent on its physical recruitment to the lysosomal membrane[300].

Get in, get out – The delivery problem and endosomal escape bottleneck

Extracellular barriers

The challenge of achieving biologically meaningful delivery of macromolecules like RNA to the right tissue and have them execute their specific therapeutic task inside the recipient cells is substantial. Several approaches can be used to administer therapeutic RNA, including intravenous infusion, subcutaneous or intramuscular injection, intrathecal injection, topical administration and direct injection in the target tissue (*e.g.* intratumoral injection). The preferred route of administration is dependent on the formulation and delivery strategy used for the specific RNA molecules, and the properties of the target tissue[87].

RNA constructs and formulation that are administered systemically need to avoid renal filtration and excretion. Nanoparticles have a size that is above the limit of renal filtration. Conjugates of siRNA and carrier molecules typically face larger difficulties, but can be aided by for example binding to circulating lipoprotein particles or albumin[301].

Nuclease stability and immune recognition is two additional challenges encountered both in the circulation, extracellular tissues and intracellular compartments, as discussed above. In addition to chemical modification of RNA molecules, formulation in nanoparticles typically confer nuclease resistance and hide RNA from immune

surveillance mechanisms. Nanoparticles or other delivery molecules typically need to maintain their integrity and stability until reaching the target tissue and being internalized by cells, and the carriers themselves can initiate immune response independent of the RNA payload[302].

Extravasation and/or tissue penetration is another key challenge. The fenestrated endothelium of the liver and spleen promotes extravasation and accumulation of nanoparticles there after systemic administration. Sequestration of nanoparticles in the liver appears to be independent of many physiochemical properties, like size, shape and composition. Sequestration in the liver promotes clearance of nanoparticles by the reticuloendothelial system (RES) — liver-resident Kupffer cells and liver sinusoidal endothelial cells. Kupffer cells clear nanoparticles from the circulation through several endocytic pathways[303,304].

Subcutaneous administration is dependent on the redistribution of the RNA construct into the circulation before reaching the target tissue. Delivery to the CNS following intravenous or subcutaneous administration is severely hampered by the blood-brain barrier (BBB)[305]. With intrathecal administration, however, the cerebrospinal fluid and the continuous ventricular system of the brain facilitates local distribution of RNA and ASO in the CNS. Tumors are often characterized by disrupted vasculature architecture, that typically are more permissive to extravasation of fluid and macromolecules — a mechanism called enhanced permeation and retention (EPR). At the same time, aggressive tumors are also characterized by high cell proliferation with insufficient blood vessel formation, resulting in hypovascularized, dense and hypoxic tumor regions. These features have contributed to doubt over whether the EPR effect is meaningful in real clinical settings and most human tumors[306], especially since LNPs have largely failed to efficiently deliver cargo to tumors[307]. Naturally, tumor architecture and compactness will also influence tissue distribution of non-particulate RNA constructs, both when administered systemically and locally.

Efficient cellular uptake of the therapeutic molecules is a prerequisite for robust biological effect no matter the route of administration. Ligands targeting cell surface receptors can either be conjugated directly to RNA (siRNA) or be incorporated into engineered nanoparticles. Ignoring potential competing internalization mechanisms (*e.g.* accumulation in the liver by interaction with lipoprotein particles or sequestration and phagocytosis), receptor–ligand binding that mediates endocytosis will confer a mechanism of uptake specific to the cells that express the receptor. Delivery vehicles may, however, distribute and extravasate into the extracellular space in tissues even if cells do not express the specific receptor, with less of the therapeutic molecules

accumulating in the target tissue and increased risk of undesirable effects in non-target tissues due to potential internalization via less specific endocytic pathways.

Intracellular barriers

Substantial progress has been made in the delivery of RNAs to target tissues and cells in the last decades, where many of the developments have improved on the extracellular barriers outlined above. Also when considering intracellular barriers, oligonucleotide chemistry and tuning of delivery systems have provided several important advancements, like limiting immune activation, improving RISC incorporation and activity (with siRNA), or interaction with other cytosolic or nuclear targets, and enhancing endonuclease stability[106]. With the increasing success of deploying strategies to achieve intracellular delivery of these macromolecules, the difficulties of overcoming the endolysosomal barrier and reach the cytosol have become exceedingly clear.

Release of RNA payload from the endosomal system has typically been favorable before RNA is accumulated in lysosomes, where payload is at risk of degradation and maintaining membrane integrity likely is of high importance considering the acidic environment and hydrolases contained in lysosomes. At the other end, the majority of internalized bulk membrane and fluid is efficiently recycled back to the exterior of cells and the plasma membrane if not diverted to non-recycling compartments[243]. This means that there likely is a window-of-opportunity during the endocytic trafficking pathway of any RNA payload where release is more likely to occur and more favorable to promote. Even if that is true in principle, improved stabilization chemistry of siRNA has provided convincing evidence that lysosomes do not necessarily have to be considered non-productive dead-ends in the endocytic route. Instead, the integrity of siRNA accumulating in lysosomes seems to be maintained for an extended period, making lysosomes an intracellular depot for release of siRNA cargo to the cytosol[81].

Naked, non-formulated and non-conjugated RNA lack inherent mechanisms to efficiently cross the endosomal membrane[108]. This inefficiency has been known for a long time and several efforts have been made to quantify or 'guesstimate' the fraction of internalized payload that eventually makes its way into the cytosol, where it can exert therapeutic effects. Delivery vehicles try to address this short-coming in several ways, and strategies to promote endosomal escape of RNA have been extensively investigated. In addition, cells have several systems that respond to membrane-perturbations and damage. Although their role in limiting the release and activity of RNA payload delivered with different carriers have been poorly characterized, it is possible that they reduce cargo release promoted by delivery vehicles, and plausible that their baseline activity maintains membrane integrity and reduces the rate of events where unfacilitated release could occur.

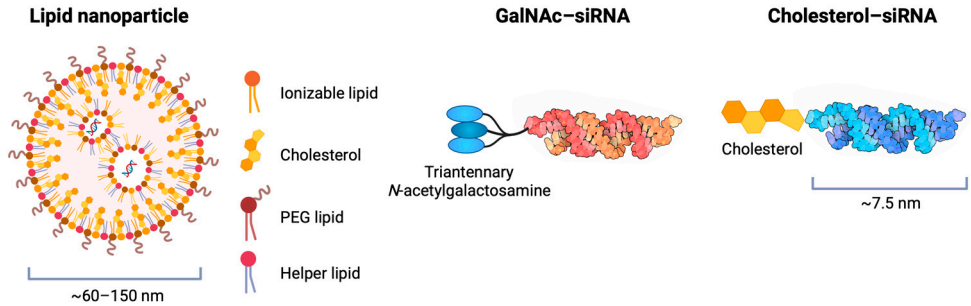

Figure 9. Carriers or modifications are required for efficient RNA delivery to tissues and cells
Many and diverse strategies have been pursued to deliver RNA or oligonucleotide payload to target cells and facilitate uptake across the cell membrane. The most successful delivery vehicles so far have been lipid nanoparticles (LNPs) and conjugation of RNA/ASO to triantennary *N*-acetylgalactosamine. LNPs are often formulated with a mix of ionizable lipids, PEG-lipids, 'helper' phosholipids and cholesterol. Triantennary GalNAc-conjugates have a targeting ligand synthesized from three *N*-acetylgalactosamine chains conjugated to the RNA or ASO payload. GalNAc binds to the asialoglycoprotein receptor expressed by hepatocytes in the liver, promoting internalization of the payload. Lipid-modicifation of siRNA is a third well explored strategy for siRNA delivery, where direct conjugation of cholesterol or similar hydrophobic lipid moieties to siRNA have been used. Created with BioRender.com.

For RNA that is delivered and endocytosed in a particulate formulation, it is conceivable that disassembly of the particle is important for the subsequent escape of free RNA. Some degree of particle disintegration is likely also required to promote membrane disruption. Size of the payload could also be relevant for the release efficiency, as synthetic mRNA is typically considerably larger than siRNA.

The various aspects of the endolysosomal barrier to RNA delivery outlined above have until recently remained largely uncharacterized, contributing to the endosomal escape 'black box'. Efforts to investigate and improve the understanding — on the subcellular, endosomal level — of why and how cytosolic delivery occurs or not, and what rationale strategies could be devised to modulate, assess and improve it is of key importance. Putting the best candidate constructs into the endosomal escape 'black box' and trying to make sense of what eventually comes out of it has, so far, not been successful enough. In part, difficulties have been related to a lack of suitable tools to probe properties of endosomal escape in detail. The current understanding of endosomal escape will be further discussed below for relevant delivery strategies.

RNA delivery strategies

The vast ocean of delivery approaches and vehicles that have been pursued for the intracellular delivery of macromolecular RNA payloads speaks to the difficulties of the

task. Here, special focus will be on RNA delivery strategies used in the papers included in this thesis; namely lipid-conjugation of siRNA and lipid nanoparticle formulation of mRNA or siRNA. Previous work pinpointing various aspects of endosomal escape will then be discussed in more detail.

Lipid nanoparticles

Big molecules in small particles

Non-viral vectors for delivery of genetic material have been pursued to avoid the immunogenicity, inability to repeat dosing, limited packaging capacity and uncontrolled integration of genetic material (with risk of disrupting native gene functions) that have typically been the weaknesses of viral delivery vehicles in clinical settings[304]. Although now a heterogenous group, two classes of biomaterials have mainly been explored in the synthesis of nanoparticles for biomedical applications — lipids and polymers.

Nanoparticles based on cationic polymers are attractive due to their structural diversity and vast chemical space for polymer development. Particle architectures using low molecular weight polyethyleneimine (PEI) have been favored historically for delivery of genetic material, typically transfecting the lungs after systemic administration[308]. Several new classes of cationic polymers with more beneficial or tailored properties have emerged, and their application holds special promise in for example nanoparticle formulation for inhalation or incorporation in hydrogels or other scaffolds[309,310].

Additional particle carriers for delivery of RNA with interesting therapeutic potential, that are not further discussed here, includes extracellular vesicles[311] and engineered virus-like particles[312].

Composition of lipid-nanoparticles

As highlighted in previous sections, formulation of RNA payload into lipid nanoparticles (LNPs) have already proven to be successful in the clinical setting, sparking interest in their use also in extrahepatic delivery. Cationic lipids and ionizable lipids (iLs) are two varieties that have been extensively explored for RNA delivery.

The head group of cationic lipids is positively charged, whereas iLs are protonated at low pH, but will remain neutral at physiological extracellular pH[313]. Cationic lipids have been used to formulate lipid nanoparticles, but was also commercialized as transfection agents where mixing with nucleic acids will produce larger complexes (lipoplexes) via electrostatic interactions. One such transfection agent is Lipofectamine, a combination of 1,2-dioleoyl-*sn*-glycero-3-phosphoethanolamine (DOPE) and

2,3-dioleyloxy-*N*-[2-(speminecarboxamido) ethyl]-*N,N*-dimethyl-1-propanaminium trifluoroacetate (DOSPA)[314].

Ionizable lipids have less interaction with anionic membranes that are encountered in the circulation, due to their neutral charge at physiological pH, improving the biocompatibility of LNPs. As the endosomal pH decreases following uptake, iLs become increasingly protonated and thus positively charged[313]. Many iLs with different properties have been synthesized and used for LNP formulations. Typically, they have been synthesized with a structure that have three sections: an amine head group, a linker group, and hydrophobic tails[87]. The iL 1,2-dilinoleyloxy-*N,N*-dimethyl-3-aminopropane (DLin-DMA) was originally synthesized for siRNA delivery[315]. Optimization of the linker group and hydrophobic tails resulted in 2,2-dilinoleyl-4-dimethylaminoethyl-[1,3]-dioxolane (DLin-KC2-DMA)[316], and further modifications of the amine head group led to (6*Z*,9*Z*,28*Z*,31*Z*)-heptatriaconta-6,9,28,31-tetraen-19-yl 4-(dimethylamino) butanoate, otherwise known as DLin-MC3-DMA or MC3 for short[317]. MC3 is a cornerstone component of patisiran and several additional investigational LNPs[318]. Other well-known iLs are Lipid H (SM-102)[319] and ALC-0315[320] — the iL components of the Moderna mRNA-1273 (Spikevax) and Pfizer–BioNTech BNT162b (Comirnaty) COVID-19 vaccines, respectively[321].

In addition to iL (or cationic lipids), LNPs are typically formulated with three additional lipid components; namely phospholipids, cholesterol and polyethylene glycol- (PEG) functionalized lipids[313].

Phospholipids can be for example phosphatidylethanolamine or phosphatidyl-choline, and functions as helper lipids in particle formulation. The modified phosphatidylcholine 1,2-distearoyl-sn-glycero-3-phosphocholine (DSPC) has saturated tails and a cylindrical geometry that allows it to form a lamellar phase, aiding in stabilizing the structure of the LNP[322].

Cholesterol can improve LNP stability by modulating particle integrity and rigidity, and various cholesterol derivatives with different molecular geometry affect LNP biodistribution[323]. Cholesterol derivatives can also confer a polyhedral shape to LNPs (as opposed to spherical shape) with lipid partitioning and multilamellarity[324].

PEG-lipids help control many properties of LNPs, including particle size, tendency to aggregate and their zeta potential (*i.e* the electrical potential of the particle at the slipping plane — a plane that represents the interface separating mobile fluid around the particle from fluid that remains attached its surface)[321]. PEG-lipids also prevents opsonization and clearance by the RES when in the circulation, thus extending the particle half-life[325]. Additionally, PEG-lipids serve as anchors that can be used to conjugate ligands to the surface of the particle[326].

Lipid nanoparticles are synthesized via coassembly of the lipid and RNA components, typically by rapid solvent mixing. High flow-rate microfluidic mixing is considered the frontrunner for LNP synthesis methods, providing consistency and scalability. It involves rapid combination of organic phases (containing lipid mixture) and aqueous phases (containing nucleic acid payload), yielding LNPs with high homogeneity and at a high encapsulation efficiency. The lipid species used in formulation and their ratio is important in determining LNP size, and to a likely lesser degree the size of the payload and the method of synthesis[327]. Many LNPs have an average size of 60–150 nm, although both smaller and larger particles might have certain beneficial characteristics[328]. Tuning the lipid composition of LNPs is one way that organ selectivity could be improved when developing new extrahepatic delivery vehicles, and substantial efforts are being made to this end[329–331].

LNPs — How do they work?

LNPs interact with plasma apolipoproteins in the circulation, acquiring a protein corona where apolipoprotein E (ApoE) serves a special role for ionizable lipid-based LNPs. ApoE promotes the trafficking of LNPs through the fenestrated endothelium in the liver and binds to LDL receptors on target hepatocytes to trigger receptor-mediated endocytosis[115]. In a broader view, different LNPs can be internalized by several mechanisms, influenced by their composition and specific properties. Clathrin-dependent LDL receptor-mediated endocytosis is the main pathway for LNP uptake in liver hepatocytes, although micropinocytosis and clathrin-independent endocytic routes can mediate uptake of other LNPs in other cells[302].

It has become evident that only a small proportion of all internalized LNP payload is able to escape the endolysosomal compartment and reach the cytoplasm[332–334]. Investigations of the intracellular trafficking of LNPs have shown that ~70% of internalized siRNA is recycled back to the cell exterior from LEs or lysosomes, and this recycling was dependent on vesicle transport between LEs and Golgi or ER, and exosome secretion mediated by Rab8a and Rab27, respectively. Inhibition of Rab11 — controlling recycling from REs — did not affect intracellular LNP retention [332]. Although various LNPs could be routed toward the recycling or degradative circuit in different extent, fast recycling of LNPs would likely limit their therapeutic potential, since the endosomal compartments they reside in during trafficking during recycling are not acidic enough to mediate a high degree of ionization of the iLs.

By using an LNP containing two siRNA with different fluorescent probes, making it possible to monitor the integrity of the particles via Förster resonance energy transfer (FRET), it was found that LNPs disassembled rapidly within the first hour after internalization.[332] Several studies found that release occurs from early endosomal

compartments. A live-cell fluorescence microscopy investigation characterized the releasing vesicles as mainly Rab5$^+$, where most vesicles had lost the early endosome antigen 1 (EEA1) and a minority already acquired Rab7[334]. No release was observed from endosomes with lysosome-associated membrane protein 1 (LAMP1, *i.e.* mature LE and lysosomes), suggesting that release only occurred during a narrow ~10 min window-of-opportunity during the endocytic pathway.

In one study, approximately 70% of LNPs were localized in endosomes marked by either the Rab5 effector Rabankyrin-5, EEA1 or LAMP1 ~6 h after cells were exposed to LNPs, indicating that LNPs could reside in hybrid endosomes having markers of both early and late endosomal compartments[333].

Several studies have used modeling of endocytic trafficking of RNA LNPs — combined with either pharmacological modulation of endocytic trafficking[333], or quantitative information of the amount of RNA payload in various endocytic compartments[335] — to infer correlation between location of payload and downstream biological activity (*i.e.* endosomal escape). The studies implied a role of early endosomal compartments in payload release, specifically APPL1$^+$ EEA1$^+$ and Rab11$^+$ compartments (APPL1 is an effector protein of Rab5). Here, location of mRNA in Rab11$^+$ endosomes had the highest correlation with biological activity, indicating a possible role in release. One of the studies also found that mRNA LNPs (formulated with the three iLs L608, MC3 or ACU5, and used at a moderately high concentration, 1.25 μg mL^{-1}) appeared to accumulate in large EEA1$^+$ endosomes to various extent. High endosomal LNP content was associated with higher endosomal pH in these structures, and the authors predicted that the endosomal escape from such "arrested" endosomes was negligible[335].

Intriguingly, the exact nature of the LNP-induced membrane perturbations allowing for intralumenal RNA payload to escape is still not clear. Protonation of the iLs and their interaction and likely mixing with the endosomal lipid bilayer, transitioning into an inverted hexagonal (H_{II}) lipid phase, is widely considered a key step preceding cargo release[336,337]. However, several biophysical models of membrane–LNP interaction can be considered. For example, it is proposed that mixing of ionizable lipid and RNA with the endosomal membrane could serve as a conduit for RNA translocating to the cytosol without the need of large membrane defects[338]. Alternatively, it is also plausible that release of RNA payload occurs through disruptions ('holes') in the endosomal membrane following its destabilization by iLs when transitioning to the H_{II} phase.

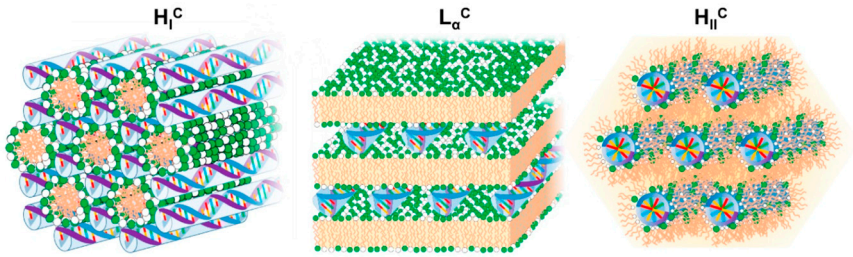

Figure 10. Schematic illustration of common structures in cationic lipid–DNA assemblies
Left: Normal hexagonal phase (H_I), with elongated lipid micelles arranged on a hexagonal lattice and the DNA rods arranged on a honeycomb lattice in the interstices between the lipid micelles. **Center:** Lamellar phase (L_α), with alternating lipid bilayers and DNA monolayers sandwiched between them. **Right:** Inverted hexagonal phase (H_{II}) with lipid-inverted micelles coating the DNA arranged on a hexagonal lattice. Reproduced from Gaspar, Ricardo et al. "Lipid-Nucleic Acid Complexes: Physicochemical Aspects and Prospects for Cancer Treatment." Molecules (Basel, Switzerland) vol. 25,21 5006. 28 Oct. 2020, doi:10.3390/molecules25215006. Distributed under Creative Commons Attribution (CC BY) license (http://creativecommons.org/licenses/by/4.0/).

Tuning the pK_a values of iLs[317,319,339–342] as well as the properties of the lipidic tails[315,343–345] and the ratio of lipid components[323,346–348] influence the efficiency of endosomal escape, but it is currently not known what part of the endosomal escape process that is modulated by such tinkering or how to evaluate individual steps in detail other than measuring downstream results.

The likely most important physicochemical determinant for the property of iLs is their apparent acid dissociation constant (pK_a). In practical terms, the pK_a of a cationic ionizable lipid describes the relationship between H^+ concentration (*i.e.* pH) and the level of lipid ionization. When pH is equal to the pK_a of the iL, at any given time, half of lipids are ionized and half remain neutral. The apparent pK_a is the likely pK_a at the LNP surface, where the interaction with additional LNP constituents influences the properties of the iL[349]. Considering Dlin-MC3-DMA as an example, it contains one ionizable amine group in the lipid head, with an apparent pK_a of 6.44[317]. Thus, half of MC3 molecules will appear protonated (positively charged) at pH 6.44 and half will appear neutrally charged. The iLs that are currently approved for clinical use all have an apparent pK_a between 6–7, so that they remain largely neutral in circulation (pH ~7.5) and become increasingly charged after internalization, as the pH of the endolysosomal compartments decrease[175].

In addition to the pK_a, the molecular shape of the iLs is also of importance, as it has a large effect on the local chemical environment in the LNP due to its influence on lipid packing[350]. Ionizable lipids with large head groups and saturated hydrophobic tails tend

to adopt a cylindrical structure, whereas iLs with small head groups and tails containing unsaturated hydrocarbons tens to adopt a conical structure[87].

Recent work has also investigated the role of LNP structure and core–shell composition, highlighting the complexity and importance of lipid–lipid as well as lipid–RNA interactions in the structure and efficacy of LNPs. For example, surface-active components like PEG-lipids and DSPC are mostly phase separated from iLs and cholesterol that predominantly form the core phase[176]. The internal structure of LNPs can transition into different phases in a pH-dependent manner, where for example bicontinuous cubic and inverse hexagonal internal structures are suggested to facilitate release of the payload[322,351–353].

In a general context, the transition from a fluid lamellar lipid bilayer phase (L_α) to an inverted hexagonal phase (H_{II}) and the properties of membrane structures they form have been studied extensively[354–356]. Lipids with conical shape induce a negative curvature strain on membranes and favor organization into the H_{II} phase, whereas cylindrical lipids favor a lamellar bilayer phase[357]. Mixing of cationic and anionic lipids (derived from LNP iLs and the endosomal bilayer, respectively) also promotes transition into the H_{II} phase[337,358].

Several interesting studies using model endosomal membranes have characterized pH-dependent binding and activity of LNPs with great detail[336,359]. This approach revealed that LNPs undergo stepwise collapse and disintegration after binding to the membrane mimic — on the scale of seconds to minutes — before sudden release of mRNA payload into the acidic environment, that occurred over tens to hundreds of milliseconds. A fraction of mRNA that was released from LNPs remained attached to the membrane mimic, likely because it had formed deprotonation-resistant salt complexes with the MC3 iL[360].

It is evident that disruption of normal endosomal membrane bilayer structure is promoted by the LNP as pH decreases in the endosome. However, even though *in vitro* an *in silico* models of LNP structure and LNP–endosomal membrane interactions are providing more insight into the this process, the exact molecular mechanisms, change of lipid bilayer structure and ultimately disruption or permeabilization that enable egress of RNA into the cytosol is still elusive.

siRNA conjugates

An alternative carrier approach for delivery of primarily siRNA and antisense oligonucleotides (ASOs) is direct conjugation to small carrier molecules with suitable properties, for example receptor ligands[361], lipids[362], peptides[363], aptamers[364],

antibodies[365] or carbohydrates[112]. Oligonucleotide conjugates encompass a substantial variety of customized molecular constructs with diverse and specialized functions. As for lipid-based LNPs, siRNA-conjugates are hindered from engaging cytosolic targets by the endosomal membrane barrier following uptake, with only a minute fraction of the internalized molecules reaching the cytosol.

GalNAc-conjugated siRNA

To date, the most successful examples of conjugated oligonucleotides are based on triantennary *N*-acetylgalactosamine (GalNAc), where both siRNA[116–121] and ASO-based therapeutics[366] are now approved and used clinically to treat diseases by targeting the liver. As already introduced above, efficient internalization of GalNAc-siRNA in hepatocytes is mediated by the cell surface receptor asialoglycoprotein receptor (ASGPR)[112].

The GalNAc–ASGPR delivery pathway has properties that are considered unique for macromolecular drug delivery. The native role of ASGPR in hepatocytes is to bind glycoproteins (missing a terminal sialic acid) in the blood and promote their internalization via clathrin-dependent endocytosis[367]. Intracellularly, the glycoprotein ligand dissociates form the receptor and is trafficked for lysosomal degradation, while ASGPR is recycled to the cell surface already after 10–15 min, where it can repeat the internalization of new ligands[368]. ASGPR is highly abundant on the cell surface of hepatocytes, with $>10^6$ receptors per cell[368]. In theory, this enables internalization of several million siRNA molecules every hour. Similar to endogenous ASGPR ligands, GalNAc-siRNA accumulate in late endosomal and lysosomal compartments within hours after administration *in vivo*[369].

Other known internalizing ligand–receptor systems have considerably lower cell surface receptor abundance (10^4–10^5 receptors per cell), and much slower (~90 min) and less efficient receptor recycling[370]. This means that if all available target receptor would be engaged with ligand-enabled siRNA in the tissue of interest, only ~100,000 molecules would be internalized in a few hours[108]. With GalNAc-siRNA, the large number of molecules taken up by cells is enough to mediate efficient gene silencing, even though only a very limited fraction of all internalized molecules escape the endosomes into the cytosol. With most other known ligand-receptor systems, intracellular accumulation is typically not efficient enough to achieve robust biological activity *in vivo* with such a low spontaneous rate of endosomal release[108].

Lipid-modified siRNA conjugates

Cholesterol and lipids were the first molecules proposed for conjugation to oligonucleotides to improve their cellular delivery and cholesterol is still one of the most

well-studied lipophilic moieties in this context[371]. Constituting 15–30% of cellular membranes[372], cholesterol spontaneously intercalates into lipid membranes when added to cells *in vitro*, driving internalization of the siRNA via endocytosis[373,374]. Following intravenous or subcutaneous administration *in vivo*, cholesterol-conjugated oligonucleotides bind lipoproteins in plasma and incorporate into low-density lipoprotein (LDL) and high-density lipoprotein (HDL) particles[375]. Internalization of cholesterol-conjugates from the circulation can then be achieved by clathrin-dependent receptor-mediated endocytosis by the LDL receptor and scavenger receptor class B member 1 (SR-B1) receptor, recognizing LDL and HDL particles, respectively[376,377]. This mechanism is likely the most important route for internalization after systemic administration[378], whereas several *in vitro* studies have found that uptake was only partially reduced (25–40%) when clathrin-dependent endocytosis was inhibited[374,379]. Indeed, the efficiency of cholesterol-siRNA *in vitro* is substantially reduced when the compound is administered to cells in cell culture medium supplemented with serum, suggesting non-receptor-mediated endocytic pathways are likely to be more important *in vitro*[374]. The relative importance of the different endocytic pathways after local delivery to the CNS is less characterized, although — like plasma — cerebrospinal fluid contains lipoprotein particles responsible for extracellular lipid transport that could likely carry lipophilic siRNA to target cells[380]. Since the brain has the second-highest lipid content of all human tissues (second only to adipose tissue), accounting for ~50% of its dry weight[381], it is conceivable that direct carrier-free distribution and penetration of lipophilic siRNA throughout the brain parenchyma is a significant contributing delivery pathway.

Lipid-conjugation of siRNA prolong cardiovascular circulation and promote extrahepatic target delivery and biological efficacy, both when administrated systemically and locally[375,382–385]. Following subcutaneous injection in mice, cholesterol-siRNA accumulated most effectively in the liver, adrenal glands, spleen and skin at the injection site, but distributed to almost all organs in varying extent[386]. The main factor influencing the biodistribution of lipid-modified conjugates after systemic administration is their lipophilicity, largely influenced by the length of the lipid alkyl chain, that determines the binding of the construct to plasma lipoproteins[375,387]. Lipid-conjugated siRNA with lower lipophilicity — for example conjugates with derivatives of retinoic acid, lithocholic acid or docosahexaenoic acid (DHA) — showed enhanced accumulation in some organs after subcutaneous injection compared to cholesterol-siRNA[386].

Direct conjugation of siRNA to the common ionizable lipid DLin-MC3-DMA improved endosomal escape while maintaining RNAi activity[388]. The tissue distribution *in vivo* was similar to cholesterol-siRNA, likely due to a similar degree of

hydrophobicity. High tissue accumulation, however, resulted in non-specific gene expression changes indicative of toxicity.

So far, no lipid-modified siRNA has been reported to efficiently cross the BBB without additional treatment enhancing extravasation[389]. Instead, local delivery into the CNS niche (*e.g.* intracerebroventricular, intraparenchymal, intrathecal or intratumoral injection) has been explored as a primary administration route, analogous to already approved ASO therapies. Conjugation of siRNA to docosahexaenoic acid (DHA) and docosanoic acid (DCA) have been explored in several *in vivo* studies investigating distribution and target inhibition systemically and in the CNS[390–393]. DHA is the most common polyunsaturated fatty acid in mammalian brains, and administration of high doses DHA-siRNA was well tolerated without triggering neuronal cell death or immune response[390]. Following systemic administration, DCA-conjugates showed improved extrahepatic accumulation compared to cholesterol-conjugates[393]. Phosphocholine (PC)–DCA-conjugated siRNA targeting sFLIT for the treatment of preeclampsia is currently investigated in a phase I clinical trial[394].

Chemically stabilized and lipid-modified siRNAs are also being explored as novel therapeutics in neurodegenerative disease[395]. In this context, hydrophobic siRNAs conjugated to the 2′-*O*-hexadecyl (C16) lipid is being widely investigated both in preclinical and clinical settings. For example, a C16-conjugated siRNA targeting amyloid precursor protein (APP) have shown promising data for the treatment of Alzheimer's disease and cerebral amyloid angiopathy[396]. Interestingly, chemically stabilized divalent siRNAs — that are not combined with any additional carrier molecule — have also demonstrated impressive results in the CNS[397,398].

Cholesterol-conjugation has been used to deliver siRNA to tumors *in vivo* using both systemic and intratumoral administration[301,399,400]. Lipophilic-siRNA conjugates show promise in targeting brain tumors, where efficient tumor accumulation and penetration can be achieved, that with higher doses mediates significant target gene inhibition[401,402]. Interestingly, for many cancers — including glioblastoma — reprogramming of lipid metabolism has become a newly recognized hallmark, linked to cancer development and progression[403–406]. Some characteristics of altered lipid homeostasis include increased *de novo* lipogenesis, increased fatty acid uptake and oxidation (for energy production) and lipid accumulation[407]. This tumor phenotype may provide an opportunity for the use of lipid-modified siRNA for cancer treatment.

Receptor-targeting siRNA conjugates

As mentioned above, many additional kinds of siRNA conjugates have been developed and investigated over the years. Peptide-conjugation of siRNA can provide different

and multiple functions, for example binding to cell surface proteins, glycoproteins or lipids to enable uptake by endocytosis (targeted peptides)[408]; facilitate membrane penetration by various other mechanisms (cell penetrating peptides, CPPs)[409]; and lyse or form pores in membranes[410]. Peptides can be chemically synthesized, offering a high degree of customization and diversity that makes this class of conjugates interesting for extrahepatic RNA delivery[395].

Other interesting receptor-targeting siRNA conjugates includes folic acid conjugates[411]; Centyrin-conjugates[412] targeting for example epidermal growth factor receptor (EGFR), prostate-specific membrane antigen (PSMA), B cell maturation antigen (BCMA) or epithelial cell adhesion molecule (EpCAM); various antibody-siRNA conjugates[413] (*e.g.* anti-transferrin receptor 1–siRNA); and nanobody-siRNA conjugates[414]. Aptamer–siRNA conjugates represent an additional interesting opportunity for targeted siRNA delivery, where siRNA is combined with a synthetic oligoribonucleotide with a complex tertiary structure typically designed to bind cell surface receptors with high affinity[415]. Such aptamer-siRNA chimeras (AsiCs) have been designed to bind to for example PSMA[416] (evaluated in a prostate cancer xenograft model), and EpCAM[417] (evaluated in a triple-negative breast cancer xenograft model) — both examples using siRNA targeting Plk1, a serine/threonine-protein kinase often overexpressed in cancers where it has oncogenic roles in mitosis and cell cycle regulation[418].

Endosomal escape of siRNA-conjugates — Hic Sunt Dracones

Even though intracellular transport, storage or metabolism of many of the molecules or ligands used for siRNA conjugation have been characterized in detail, the intracellular fate of conjugated siRNA — including lipid-modified siRNA and clinically approved GalNAc-siRNA — is still poorly understood. In particular, the spontaneous endosomal escape process is so far, in principle, completely unknown and uncharacterized.

Brown *et al.* showed that metabolic stability of chemically modified siRNA is critical for their potency and activity duration, by improving the survival in highly acidic (and degradative) subcellular compartments. They also demonstrated that functional siRNA could be liberated from late endosomal compartments up to three weeks after GalNAc-siRNA administration *in vivo*, by using a GalNAc-conjugated endolytic peptide. This work provided convincing evidence that highly acidic compartments (lysosomes) serve as an intracellular depot of GalNAc-siRNA from where escape to the cytosol can be induced. It is reasonable to believe that, since accumulation of GalNAc-siRNA is observed primarily in late endosomes and lysosomes, these compartments are also responsible for the slow spontaneous release of payload. Direct observation of this

spontaneous release that would enable characterization of the releasing compartments is, however, still lacking.

Other findings have provided additional clues on how endosomal escape of conjugated siRNA may occur. Clinical data show that GalNAc-siRNA takes 2–3 weeks to achieve a robust knockdown response[117]. As both the delivery to hepatocytes and the RNAi-mediated target downregulation itself once siRNA is finally present in the cytosol is substantially faster than that, the pharmacodynamics suggest a very slow rate of baseline endosomal escape[419].

An *in vitro* CRISPR-Cas9 screen performed in Hep3B cells recently identified several regulators of GalNAc-conjugated siRNA activity[420]. One hit — the Rab GTPase Rab18 — was validated as an important regulator of the cytosolic delivery of siRNA delivered by conjugation to GalNAc, cholesterol, or an anti-ASGPR antibody, but not Lipofectamine (lipoplex) transfection. A substantial improvement in siRNA activity was achieved in Rab18 knockout cells, improving IC50 values more than 20-fold. The mechanistic link to improved endosomal escape remains, however, unclear.

Rab18 has many and diverse functions in intracellular trafficking that could influence siRNA delivery and activity, including roles in lipid droplet (LD) formation, inhibition of COP-I-independent retrograde Golgi–ER trafficking, and regulation of ER structure, secretory granules and peroxisomes. The involvement of Rab18 in the downregulation of retrograde transport from Golgi to ER makes this pathway interesting to consider when trying to identify compartments that release payload into the cytosol. Interestingly, earlier studies suggested that pharmacological inhibition of retrograde transport between EEs and the TGN resulted in improved activity of a ASO and SSO, thus providing (at least in part) conflicting findings[421]. It is, however, not certain that the escape pathway facilitated by Rab18 inhibition (*i.e.* the endosomal compartment mediating release) is the same as is responsible for the majority of payload release when Rab18 activity is unperturbed. Even so, identifying conditions where release of payload is enhanced (other than treatments that directly damage endosomal membranes) will provide better opportunities to investigate endosomal escape of siRNA conjugates, since baseline events are seemingly very rare.

It is conceivable that conjugated siRNA escape from endosomes via short lived, spontaneous small disruptions in the lipid bilayer, that likely occur infrequently but repeatedly over time[419]. One example of when such events could arise is during fusion or fission of various endosomal compartments with homotypic or heterotypic membranes. It is also possible that such events could be more common in endosomes with certain compartment identities, and that localization of siRNA payload there would favor endosomal escape and biological activity. Since lipid-modified conjugates

to various extent interact with endosomal membranes, it is also conceivable that the precise nature of endosomal disruptions and the identity of compartments mediating their release is different from other conjugates like GalNAc-siRNA.

Lysosomes are known to be of major importance for the regulation of cellular cholesterol homeostasis, and contain several membrane integral transporter proteins for cholesterol (*e.g.* NPC1, NPC2, LIMP-2)[422]. Studies have shown that NPC1 is an important regulator of the recycling pathway of LNPs and cationic delivery polymers, and that NPC1 deficiency or inhibition increases intracellular accumulation of LNPs and improves target gene silencing[332,423]. It is not clear if and how homeostatic trafficking, storage and metabolic processes involving cholesterol and other lipids could be linked to spontaneous cytosolic delivery of lipid-modified siRNA.

The transmembrane protein SIDT1 was identified to be involved in uptake of lipid-conjugated siRNA after binding of lipoprotein particles to the cell surface, by mechanisms proposed to be independent of clathrin-mediated endocytosis[375]. Uptake of cholesterol-siRNA and other siRNA conjugates with chemically distinct lipid moieties was impaired after SIDT1 inhibition, leading to the suggestion that the transporter recognized the oligoribonucleotide and not the lipophilic component of the construct. Others have, however, shown that SIDT1 interacts with steroid molecules via a cholesterol-binding domain, and that its subcellular localization depends on the presence or absence of cholesterol in cellular membranes[424]. The SIDT1 homolog SIDT2 have also been implicated in cellular cholesterol transport[424] and was shown to preferentially localize to endolysosomal compartments[425]. Several studies performed in *C. elegans* and *Drosophila* showed that dsRNA or their mimics could be transferred across cellular membranes by the SIDT1/SIDT2 ortholog SID-1, and evidence suggested that it functions as a dsRNA channel[426–428]. It was also shown that overexpression of SIDT1 in mammalian cells enhanced siRNA uptake and gene silencing[429]. More recently, one group have reported that both SIDT1 and SIDT2 transported internalized exogenous dsRNA into the cytoplasm, where it activated immune signaling pathways involved in antiviral response[425,430]. The studies used the immunostimulatory viral dsRNA mimic poly(I:C) — a mismatched dsRNA with one strand being a polymer of inosinic acid and the second strand a polymer if cytidylic acid[431]. Another recent paper, however, reported a role of SIDT2 in the entrapment of ASOs in lysosomes, where it was suggested to limit ASO activity via effects on intracellular localization of lysosomes[432]. Taken together, additional and confirmatory data is still required to elucidate the activity of SID-1 orthologs in mammalian cells — including any true role as functional transmembrane RNA channels or transporters. Indeed, if such an active process mediating endolysosomal-to-cytosolic translocation of RNA was present, it is hard to imagine why practically all naked and conjugated siRNA

and other exogenous RNA constructs synthesized and evaluated would be so inefficient in exploiting this route or provide more convincing direct evidence of its existence.

Pinpointing endosomal escape

As introduced above, a range of methods have been deployed to investigate the intracellular fate of therapeutic oligonucleotides and RNA after internalization — including hints of the endosomal escape process, the fraction of internalized payload that is released to the cytosol and the dose-response relationship between the cytosolic oligonucleotides or RNAs and biological response[433,434]. Some of the key findings and methods deployed with relevance for this thesis is discussed below. To this end, strategies used to take on the endosomal escape investigations will be divided into separate categories depending on their general approach, as (1) direct observation of payload in the cytosol; (2) indirect observation of payload-proxy in the cytosol; (3) release of payload from individual endosomes or particles; (4) detection of possible release events from individual endosomes or particles.

An additional and previously more common strategy to infer information about endosomal escape have been to investigate colocalization — or rather lack thereof — of payload with selected endosomal markers and stainings (typically of LEs and lysosomes). Inference of this kind is, for many reasons, highly uncertain — for example due to difficulties to correctly evaluate (quantify) colocalization, selection of timepoints for evaluation, differences in marker expression or staining specificity, and variations in intracellular trafficking induces by the delivery vehicle or cargo itself or additional treatments used. Moreover, studies of this kind do not provide insight into the endosomal escape process itself.

1. Direct detection of payload in the cytosol

Reports on direct detection and quantification of oligonucleotide or RNA payloads in the cytosol includes a wide range of delivery strategies, *in vitro* and (rarely) *in vivo* models, payloads and detection methods. In addition to detection and quantification *per se*, many have used this metric with additional data to estimate endosomal release efficiency or biological activity (dose-response) in various ways.

An early method reported in 2004 by Overhoff *et al.* described quantitative detection of siRNA in cell extracts based on liquid hybridization of internalized siRNA strands with a probe labeled with a radioactive isotope of phosphorus (phosphorus-32, ^{32}P), followed by electrophoresis and quantitative radiographic detection[435]. The method had a detection limit in the order of 10–100 amol when evaluating siRNA in buffer and 700 amol with siRNA in cellular extracts. Combined with measurements of ICAM-1

protein knockdown, a dose-response relationship between the *total intracellular* amount of a lipoplex-formulated siRNA and target knockdown could be established. This showed that only ~10^4–10^5 intracellular siRNAs were needed to reach half-maximal target inhibition (IC50).

Liu *et al.* used a simple but informative *in vitro* approach to determine the number of cytosolic siRNA molecules required for knockdown of a protein target[436]. Electroporation was used to achieve direct cytoplasmic delivery of either siRNA targeting GFP or fluorescently labeled siRNA. The number of siRNA molecules delivered was determined using flow cytometry and a calibration curve generated by reference beads. When compared to GFP knockdown, this showed that ~10^4 siRNA molecules were required to reach ~50% target knockdown.

Gilleron *et al.* used a combination of quantitative fluorescence imaging and electron microscopy of MC3-based LNPs containing siRNA conjugated to either fluorophores or colloidal gold particles to measure the endosomal release of siRNA to the cytosol [333]. Only approximately 1–2% of intracellular siRNA was located in the cytosol of HeLa cells *in vitro* or in mouse hepatocytes *in vivo* 6 h after LNP administration. The rate of siRNA–gold release to the cytosol followed sigmoidal kinetics, indicating that the release likely occurred at a specific stage in the endocytic route rather than from all compartments with similar efficiency.

Stalder *et al.* used Ago2 immune precipitation to quantify the number of siRNAs loaded into RISC after lipoplex-mediated delivery and related this to the transfected dose and target mRNA knockdown measured by reverse-transcription quantitative polymerase chain reaction (RT-qPCR) [437]. They found that — for several highly potent siRNAs — only 10–110 siRNA-loaded RISC complexes were required to reach IC50.

Rehman *et al.* used fluorescently labeled 17- or 18-mer single-stranded oligonucleotides formulated in lipoplexes (with cationic transfection lipid) or polyplexes (with linear polyethyleneimine, LPEI) to capture release of payload to the cytosol using live-cell fluorescence microscopy[438]. The authors quantified the relative intensity of the oligonucleotide signal in the cytosol and nuclei following its redistribution but did not pursue any downstream analysis making dose-response characterizations possible.

Wittrup *et al.* deployed a high-dynamic range live-cell fluorescence microscopy approach that enabled the detection of release events where lipoplex-formulated siRNA escaped into the cytosol[334]. Using a reference standard to translate siRNA fluorescence intensity to concentration, the cytosolic siRNA concentration was correlated to the knockdown of a destabilized GFP reporter (d1-eGFP) — establishing a cytosolic dose-response relationship. In this study, however, release events of ~2,000 siRNA molecules, that were just at the detection limit, typically resulted in complete target

gene knockdown, making the dose-response characterization less accurate. With siRNA LNPs, however, this approach was not sensitive enough to capture cytosolic release events.

Additional studies have investigated the release of siRNA from LNPs with light microscopy, but often using high LNP doses well above the therapeutic range, raising questions concerning dose-dependent differences in intracellular trafficking and endosomal release mechanisms[439–441]. For example, Basha *et al.* detected cytosolic distribution of siRNA delivered with DLin-KC2-DMA LNPs using 2 μg mL^{-1} siRNA[442].

Patel *et al.* instead used single-molecule fluorescence in-situ hybridization (smFISH) of mRNA delivered with LNPs with various sterol components to detect and quantify cytosolic amounts of mRNA[323]. mRNA molecules that had been released into the cytosol was identified and quantified in fixed samples through object-based image analysis, where an mRNA-electroporated reference sample was used as a fluorescence intensity benchmark to tell apart single (presumed cytosolic) and multiple (non-cytosolic) mRNAs. The efficiency of endosomal escape was estimated by comparing the ratio between the number of cytosolic mRNA molecules and number of detected LNPs inside cells. Although an impressive methodology, achieving quantitative accuracy to reliably detect single cytosolic mRNAs and derive efficiency estimates of endosomal escape events from this approach likely requires further technological advancements.

Maugeri *et al.* investigated the fate of mRNA delivered with LNPs formulated with DLin-MC3-DMA or DLin-DMA[338]. Interestingly, mRNA delivered with LNPs were transferred to and secreted in extracellular vesicles at a 1:1 molar ratio between iL and mRNA. Additionally, it was reported that <1% of total mRNA delivered by LNPs was detected in the cytosol. Detailed information on how this number was derived was, however, not clearly provided.

Several studies have quantified cytosolic amounts of delivered ASOs. Nanoscale secondary ion mass spectrometry (NanoSIMS) was used to investigate uptake and intracellular localization of GalNAc-conjugated ASO, showing that 1–2% of internalized ASOs is released from endosomes in hepatocytes *in vivo*[443].

Van der Bent *et al.* measured the nuclear concentration of an SSO delivered with nanoparticles formulated with cell-penetrating peptides, and correlated this with the effects of altered target mRNA splicing in a model of myotonic dystrophy, using a combination of live-cell fluorescence correlations spectroscopy (FCS) and immunofluorescence microscopy[444]. Similarly, FCS was also used by Buntz *et al.* to calculate the absolute number of LNA-gapmers — delivered naked by microinjection

— that was required for target inhibition, providing another example of an approach to determine the cytosolic dose-response of an oligonucleotide[445]. Adaptations of FCS have also been used to study the incorporation of siRNA into RISC[446].

Very few studies have reported cytosolic measurements of ligand-conjugated siRNAs following endocytic uptake. Investigating the biological basis for extended pharmacological duration of GalNAc-siRNA activity, Brown *et al.* showed that only 0.3% of internalized GalNAc-siRNA was located in the cytoplasm of hepatocytes after *in vivo* administration at any given time[369].

Importantly, as the selection of findings summarized above shows, direct detection and quantification of payload in the cytosol or nucleus after endosomal escape can be used to evaluate the efficiency of release — *i.e.* the amount and/or fraction of total internalized payload released (the latter only if reliable estimates of total intracellular payload amounts can be obtained) — but also establish cytosolic dose-response relationships if it is combined with a read-out of biological effect. In summary, several points of evidence suggest that the fraction of RNA payload released with LNPs is around 1–2%. With ligand-conjugated siRNA, studies have mainly focused on GalNAc-siRNA, indicating a likely release efficiency well below 1% — and maybe even below 0.01%[108].

2. Indirect observation of proxy molecules in the cytosol

Since direct observation of amounts of oligonucleotide or RNA payload in the cytosol that are functionally relevant (*i.e.* typically within the dose-response range) is technically challenging, complimentary methods to evaluate cytosolic (or subsequent nuclear) delivery have been pursued as well. Some of these approaches are also useful for investigations of endosomal damage on its own, for example to evaluate membrane-damaging small molecules or constructs, or to investigate lysosomal membrane permeabilization in various settings.

Permeabilization of lysosomes can be assessed by enzymatic detection of lysosomal hydrolases like β-*N*-acetyl-glycosaminidase (NAG) or cathepsin in cytosolic extracts[447]. Typically, the detection requires permeabilization of the plasma membrane (with a detergent like digitonin) to extract cytosolic contents while at the same time avoiding permeabilization and extraction of the lysosomal fraction during analysis[448]. Immunocytochemical staining of cathepsin B or L can also be used to detect redistribution from vesicular to diffuse cytosolic distribution[449]. Similarly, permeabilization of endosomal membranes can be detected using fluorescently labeled dextran — polysaccharide molecules that can be synthesized with varying lengths and with fluorescent molecules for fluorescence microscopy imaging[450]. Since dextran is

synthesized in different sizes, they can also be used to probe the size of disruptions mediating escape to the cytosol[447]. Dextran is typically considered to be a passive fluid phase passengers of the endolysosomal system after uptake by primarily non-specific pinocytosis. Distribution, recycling and accumulation of dextran inside cells will for that reason be controlled by the net flux of fluid along the endocytic pathway[243]. This is of high relevance when trying to detect its release to the cytosol when targeting different endosomal compartments to trigger escape. Since accumulation of dextran in lysosomes and late endosomes is the primary endpoint in the endocytic route, release of dextran to the cytosol have been mostly evaluated as a read-out for lysosomal membrane permeabilization[448]. Importantly, as with direct detection of RNA payload in the cytosol, small amounts of cytosolic dextran will be hard to detect due to signal-to-noise limitations of standard fluorescence microscopy methods.

More recent methods measure signal that depends on the interaction between exogenous molecules (typically internalized by endocytosis) and protein expression in the cytosol or nucleus. Examples includes split-protein complementation assays[451–453], biotin ligase assays[454], glucocorticoid receptor transcriptional reporter assays[455,456] and assays based on enzyme-specific fluorogenic probes[457]. The chloroalkane penetration assay (CAPA) is another recent assay, where release of internalized chloroalkane-labeled molecules inhibits binding sites on overexpressed cytosolic HaloTags[458]. After staining cells with a chloroalkane-labeled dye (reacting with the remaining HaloTag sites), the total fluorescence is inversely proportional to the amount of the inhibiting chloroalkane-labeled molecule that was delivered to the cytosol.

Importantly, each of the assays above come with various caveats, that are of critical importance when trying to translate detection of a proxy molecule in the cytosol to the endosomal escape of RNA payload. For example, biochemical reactions used for detection are not necessarily linear. Differences in size between proxy molecules and RNA is another important aspect that needs to be accounted for, as is differences in intracellular trafficking. Even if endosomal localization and size is comparable between proxy molecules and RNA payload, efficiency of endosomal escape is likely to vary between the two. Reasons for this could be due to the RNA delivery strategy used, where escape of ligand-conjugated RNA is dependent on their dissociation from the internalizing receptor and might be affected by membrane binding (possibly of importance for lipid-modified siRNA), or disintegration of LNPs to enable translocation of encapsulated RNA payload. Consequently, drawing conclusions on the endosomal escape efficiency of RNA payloads based on the detection of proxy molecules and other indirect assays should be done cautiously. One way to improve on indirect detection assays is to incorporate the proxy molecule in the same delivery vehicle as the RNA payload[459] or direct conjugation of a detectable proxy to the

payload[460]. Even so, some of the concerns above remain unaddressed — *e.g.* differences in LNP disintegration kinetics between RNA and proxy, size differences and possible divergent trafficking routes after LNP dissociation, and non-linear detection and integrity concerns for conjugated constructs.

3. Direct observation of payload release from individual endosomes or particles

Seeing water leaving a bursting balloon is a more convincing observation of its release than later detecting a damp area on the ground. Direct observation of escape of macromolecules from individual endosomes or particles is, however, typically a substantial technical challenge.

Gilleron *at el.* found that vesicular compartments accumulating siRNA LNPs appeared stable over at least 1–2 minutes, and that the number of siRNA-containing compartments did not vary during ~15 min observation[333]. The authors suggested that this implied that siRNA delivered by LNPs at therapeutic doses are not released due to massive bursting of individual endosomes or permeabilization of the endosomal membrane.

Using considerably larger lipoplex-formulated siRNA particles, Wittrup *et al.* were able to detect changes in the fluorescence intensity of individual lipoplex particles or endosomes, perfectly linked in time to detectable cytosolic dispersion of siRNA[334]. Interestingly, the fluorescence intensity of releasing particles typically gradually increased 1–2 min before release and then suddenly dropped. As fluorophores in close proximity are self-quenched, this phenomenon was interpreted as disintegration of the lipoplex and dequenching of the fluorescent molecules. With siRNA LNPs, however, unaided detection of siRNA release from individual endosomes was not feasible due to the large number of LNPs per cell, fast vesicles movement, and signal-to-noise limitations. The authors then identified that a family of cytosolic proteins — galectins — were recruited to the releasing lipoplexes and also many endosomes containing siRNA LNPs. When evaluating only endosomes showing recruitment of galectin after LNP incubation, the appearance of Galectin-8 coincided with a sudden decrease in siRNA fluorescence from individual endosomes, indicative of endosomal escape. The fluorescence intensity of releasing endosomes decreased ~50%, suggesting that on average half of the endosomal siRNA payload was released. This finding identified galectins as responders to membrane damage events where lipoplex and LNP-formulated siRNA could escape to from endosomes, and that burst-like release of siRNA was a readily detectable endosomal escape pathway promoted by LNPs.

More recent work by Paramasivam *et al.* used multicolor single-molecule localization microscopy (SMLM) to investigate the fate of mRNA LNPs in endosomes[335].

Visualization of fluorescently labeled mRNA in relation to transferrin and epidermal growth factor (EGF) in EEs was achieved with nanometer resolution in fixed cells using immunocytochemical staining, where incomplete colocalization of the detected fluorophores was interpreted as likely endosomal escape. However, without temporal or quantitative information — or the use of an additional marker of for example membrane perturbation — such characterization is hard to interpret or use for evaluating the efficiency and dynamics of endosomal escape.

Direct observation of payload release from individual endosomes enables unique characterization of the endosomal escape process, in terms of for example release kinetics and apparent release efficiency on a single-vesicle level. It is also possible to address the frequency of potential release events — especially by indirect methods as discussed below. With currently available methods, however, it is typically not feasible to reliable quantify the total amount of payload released to the cytosol over a relevant period by only observing releasing endosomes or the entire pool of vesicular intracellular payload.

4. Indirect detection of possible release events

As already introduced above, now almost a decade ago, galectins emerged as a tool to study the release of RNA and oligonucleotide payloads in diverse settings, and this has now become one of the 'gold-standard' approaches to investigate endosomal escape. Galectin recruitment is, however, only an indirect observation of one step in the release process — the formation of a detectable membrane disruption — and therefore not equivalent with endosomal escape of RNA payload. Although it can be of high value as for example a screening tool, evaluating galectin response on its own might not be sufficient to precisely determine the endosomal escape efficiency if this is not combined with additional information.

Following the publication of Paper I in this thesis, Munson *et al.* reported on a high-throughput imaging assay for quantifying uptake, endosomal escape and functional delivery of mRNA using nanoparticles formulated with a range of ionizable lipids, polymers and PEG-lipids, based on Galectin-9 (Gal-9) as an endosomal escape reporter[461]. The comprehensive investigation highlighted the capabilities of nanoparticle screens utilizing Gal-9, and also evaluated the effect of several small molecule compounds triggering Gal-9 response. Bost *et al.* similarly used Gal-9 to screen a selection of small molecule compounds to identify candidates that caused endolysosomal membrane damage and improved the activity of an SSO[462].

Kilchrist *et al.* used Gal-8 as a marker to show endosome disruption and predict biological activity of siRNA delivered by rationally designed polymer nanoparticles[463].

The authors also provided *in vivo* proof of principle for using Gal-8 to detect endosome disruption in tumor tissue, following systemic nanoparticle administration in an orthotopic breast cancer tumor model in nude mice. Similarly, Herrera *et al.* used Gal-8 as a reporter to investigate endosomal damage promoted by mRNA LNPs with various phytosterols in place of cholesterol[464].

Several other investigations have used detection of galectin response as a marker of endosome damage and/or endosomal escape using a range of different nanoparticle carriers and also cell penetrating peptides (CPP)[452,465–471]. As with most of the papers discussed, however, they do not provide additional insight into the endosomal escape process itself on a mechanistic or single-event level.

In addition to the detection of endosomal damage or possible release events by galectin recruitment, capturing changes in the endosomal localization of other reporters or proxy molecules can be of value. Response can be analyzed *en masse* (evaluating all detectable particles or endosomes simultaneously without event synchronization) if the trigger is efficient enough. Skowyra *et al.* provided two elegant examples of this, where potent membrane-disruptive small molecule treatment caused loss of a cathepsin-sensitive dye (Magic Red) and shifted the response of a ratiometric pH-sensing dextran assay[472]. Here again, it is critical to assess the size difference between the proxy molecules and a payload of interest. Additionally, even if membrane disruption would allow the escape of lysosomal dyes or other reporters with a mechanism comparable to RNA payload, since many of the most used 'lysosomal' dyes are bases that accumulate in acidic compartments by protonation, loss of the H^+ gradient (increase in endosomal pH) by membrane permeabilization could be enough to lose endosomal contents. Similarly, elucidating the releasing potential of damaged compartments by monitoring pH-sensitive probes alone is likewise problematic[473].

Strategies where internalized proxy molecules with comparable size to RNA is evaluated in individual endosomes to detect endosomal escape is conceivable, as is shown in Paper I of this thesis using 10 kDa dextran. As discussed above, however, in addition to molecular size, the delivery vehicle could significantly alter the endosomal escape efficiency compared to a naked and inert proxy molecule like dextran. Additionally, evaluating the potential release of proxy molecules in individual endosomes is in many settings probably as technically challenging as directly observing a payload of interest.

Endolysosomal membrane damage and response

Cellular systems responding to endosomal membrane damage

Cellular strategies to maintain the integrity of endosomal membranes and detect when damage occurs have likely emerged with the formation of the endolysosomal system itself, but also evolved to counteract and respond to invading pathogens. Important features of some of these cellular systems are highlighted below.

Galectins

The galectin protein family encompasses lectins with conserved β-galactoside-binding sites located within their characteristic carbohydrate recognition domains (CRDs)[474]. They are synthesized as cytosolic proteins, but only reach their galactoside ligands after non-classical secretion or when galactosides inside cells are exposed to the cytosol[475]. In addition, galectins interact with several binding partners that do not contain galactosides. Fifteen galectin family members have been described in mammals, out of which twelve are found in humans (Gal-1 -2 -3 -4 -7 -8 -9 -10 -12 -13 -14 and -16. Galectins can be classified according to their conserved structure. For example, Gal-1 -2 and -7 contain one CRD and are classified as 'prototypical', whereas Gal-4 -8 -9 and -12 are tandem-repeat proteins with two CRDs. The chimeric Gal-3 contains one CRD and one unique N-terminal non-CRD region[476].

The galactoside-binding site of galectin CRDs is a conserved sequence motif of ~7 amino acids, that are flanked by different weaker binding motifs giving each galectin CRD sub-type its unique specificity and affinity[477]. The CRDs also contain binding sites for non-carbohydrate ligands in the cytosol and nucleus. Gal-3 contains a similar accessory CRD site that binds to its own N-terminal domain, whereas Gal-1 -2 and -7 all have accessory CRD sites that promote dimerization. Most galectins can crosslink glycoconjugate ligands and promote their aggregation. Binding of ligands to Gal-1 and -3 can promote their dimerization or oligomerization, respectively[478,479]. Additionally, galectins with two CRDs form non-covalent dimers, increasing the valency of galectin complexes that are important for many biological functions[480].

Galectins have been found to interact with a number of cytosolic and nuclear binding ligands, including H-Ras and K-Ras, basal bodies, centrosomes, nucleus mitotic apparatus protein (NuMa), β-catenin and the Wnt signaling pathway, and the apoptosis regulator Bcl2. Gal-3 also interacts with ALG-2-interacting protein X (ALIX), a component in the ESCRT system discussed below[475].

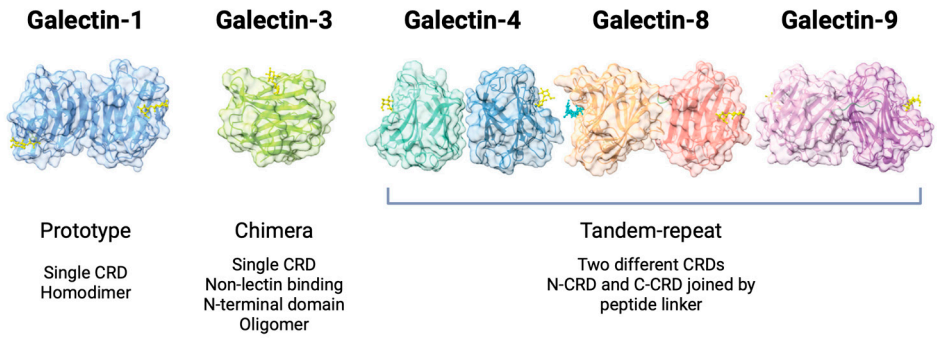

Figure 11. Galectins can be classified according to their conserved structure
Galectins are classified into three groups based on their structural features: 'prototype' galectins (*e.g.* Gal-1) contain one carbohydrate recognition domain (CRD) and formes homodimers; 'tandem repeat-type' galectins (*e.g.* Gal-4, Gal-8 and Gal-9) contain two distinct CRD in tandem, connected by a linker peptide; and the 'chimera-type' Gal-3 that have a special proline- and glycine-rich N-terminal domain fused to the C-terminal CRD. Adopted from Troncoso, María F et al. "The universe of galectin-binding partners and their functions in health and disease." The Journal of biological chemistry vol. 299,12 (2023): 105400. doi:10.1016/j.jbc.2023.105400.

Paz *et al.* reported first evidence of galectins responding to intracellular membrane damage, showing that Gal-3 was recruited to vacuoles containing *Shigella* as they were lysed[481]. It was later shown that Gal-8 was recruited to vacuoles lysed by *Salmonella*[482], and Gal-1, -3, and -9 to adenovirus-containing endosomes[483]. Since then, galectins have been implicated in response to membrane damage induced by various mechanisms in addition to invading pathogens, for example protein aggregates formed in neurodegenerative diseases[484], various small molecule drugs[485], laser-induced photodamage[486] and physical stimuli like silica crystals[472] and osmotic shock[482]. Several galectin family members were also recruited to endosomes releasing lipoplex- or LNP-formulated siRNA[334]. Gal-8 and -9 were strongly recruited to the releasing endosomes, whereas Gal-3 recruitment was weaker and Gal-1 and -4 were barely recruited. This galectin response is triggered as galactoside glycoconjugates on the luminal side of the endosomal membrane bilayer as it is exposed to the cytosol, enabling galectin CRDs to bind them[487].

One functional role of galectin recruitment to damaged vesicles is to promote selective autophagy. This is demonstrated by the interaction of the C-terminal CRD of Gal-8 with NDP52 — a pathogen-specific autophagy receptor — after its N-terminal domain have bound to its glycoconjugate ligand[488]. Gal-3 interacts with another class of selective autophagy receptor, the tripartite motif containing protein TRIM16[489]. Efforts

to elucidate any potential role of galectins in immediate inhibition of endosomal leakage after membrane disruption have, so far, been few and not conclusive[334,490].

As can be expected from the large number of additional both intra- and extracellular galectin-binding factors, galectins are involved in a plethora of cellular and physiological processes — including inflammation, immune response, signaling and cell migration — with implications in diseases like fibrosis, cardiovascular disease and cancer[487]. As discussed above, they can also mediate endocytosis via the CLIC/GLEEC pathway through mechanisms proposed by the GL-Lect hypothesis[257].

The ESCRT machinery

The endosomal sorting complexes required for transport (ESCRT) is an intricate heteromultimeric protein machinery that mediates processes that rely on inverse membrane remodeling or involution. The ESCRT machinery can be subdivided into three subcomplexes that are functionally distinct, ESCRT-I -II and -III. A multitude of cellular processes rely on ESCRT activity. This includes membrane scission, cytokinetic abscission after cell division, neuronal pruning, vesicle budding from plasma membrane, plasma membrane repair, viral replication and budding, nuclear envelope maintenance, endosomal sorting and ILV biogenesis, autophagy, classical-topology membrane shaping, and — importantly — repair of endolysosomal membranes[491].

Several and diverse treatments causing lysosomal membrane damage detected by galectins are now known to also trigger ESCRT recruitment, including various chemical compounds and silica crystals[472,492]. The function of ESCRT-I and the subunit TSG101 at damaged lysosomes is important for later recruitment of ESCRT-III subunits to the site, that are believed to mediate the actual repair. ALIX is also found at lysosomes early after damage, and likely cooperates with TSG101 in recruiting ESCRT-III. In contrast to galectins — that bind galactosides present on the luminal side of the bilayer — ESCRT instead assembles on the cytosolic face in the endosome. The initial recruitment of ESCRT components thus rely on alternative mechanisms, that do not require as large membrane defects as galectin recruitment[472,492]. The initial cues triggering ESCRT assembly on damaged lysosomes are still not well characterized. Efflux of lysosomal Ca^{2+} is likely involved[472,493], as ALIX cooperates with the Ca^{2+}-binding protein ALG-2 and influx of Ca^{2+} into the cytosol via disruptions in the plasma membrane activates ESCRT-mediated repair there. Other studies have, however, indicated that TSG101 appears to have a more important role in the lysosomal context[492,494], and also shown examples of lysosome-associated proteins capable of recruiting ESCRT components[495,496]. Additionally, interactions between Gal-3 and ALIX have been proposed to mediate ESCRT-III recruitment[497]. ESCRT

can also be activated by changes in membrane tension of intracellular organelles, and one hypothesis is that membrane tension relaxation as a consequence of membrane damage could triggering ESCRT recruitment[498].

The exact mechanism whereby ESCRT proteins seal the damaged lysosomal membrane is also still not known. A proposed and plausible explanation is budding of the damaged membrane site into the lumen and subsequent scission that seals the limiting membrane and generates an intraluminal vesicle-like structure containing the disrupted membrane area[499]. However, the lysosomal repair response does not seem to require the same ESCRT subunits as ILV biogenesis, indicating that a different mechanism might be used.

ESCRT and galectin response to lysosomal damage appears to be well coordinated, where ESCRT likely acts as a first level of defense that can sense smaller membrane defects and initiate repair. Recruitment of Gal-3 to such damaged lysosomes appears not to be dependent on TSG101 or ALIX, indicating that galectins can promote removal of the damaged endosomal via autophagy independently if the membrane defect is larger or cannot be resolved by the ESCRT machinery [472,492].

Autophagy

Autophagy is a cellular strategy for continuous rejuvenation of the intracellular organelles, lipids, proteins and carbohydrates under basal conditions, but can also be quickly regulated in response to external or internal stress[500]. During autophagy, a double-membrane structure known as the autophagosome forms around the material to be degraded, followed by fusion of the autophagosome with degradative lysosomes. The turnover of damaged organelles or removal of invading pathogens or protein aggregates is a finely regulated and highly selective process, that requires cargo recognition by the autophagy machinery and adaptor proteins that recruit it. There are several targets of this selective autophagy, including mitochondria (mitophagy), ribosomes (ribophagy), ER (reticulophagy), peroxisomes (pexophagy), pathogens (xenophagy) and protein aggregates (aggrephagy). One of several dozens of proteins forming the autophagy machinery is microtubule-associated protein light chain 3 (MAP-LC3, or more commonly only LC3) — a ubiquitin-like protein involved in the early autophagic response and typically resides on the growing double-membrane structuring (phagophore) that after full closure forms the autophagosome[501].

Lysosomes with substantial membrane defects are removed by selective autophagy, called lysophagy[502,503]. Recognition of the specific cargo is required for selective autophagy. This can be achieved by cargo ubiquitylation by ubiquitin ligases, which promotes their recognition by specifically targeted autophagy receptor proteins. As

mentioned, Gal-8 that bind to damaged endosomes can recruit the autophagy receptor NDP52, and Gal-3 can promote autophagy by its interaction with the E3 ubiquitin ligase TRIM16. Gal-8–NDP52 interaction is thought to be most important in autophagic response to bacterial infection, whereas Gal-3–TRIM16 interaction is seemingly of more importance in promoting lysophagy. Two receptor proteins — p62 and TAX1BP1 — have been reported to regulate lysophagy initiation. In addition to TRIM16, the E3 ubiquitin ligase FBXO27 also promotes lysophagy [501].

Transfection agents are known to induce autophagy[504,505]. LC3 was observed to localize to endosomes within a few minutes after release of lipoplex- or LNP-formulated siRNA[334]. The compartment (autophagosome) with the sequestered endosome and remaining lipoplex decreased in pH 30–50 min later, suggesting fusion with a lysosome. Interestingly, LC3 recruitment after endosome damage from lipoplexes was more dependent on Gal-8 and NDP52 than on Gal-3[334]. Additionally, LNP-induced damage was found to initiate non-canonical autophagy via conjugation of ATG8 to single membranes (CASM), where LC3 recruitment was dependent upon Tectonin beta-propeller repeat containing 1 (TECPR1)[506]. A subset of endosomes showing TECPR1 recruitment were $EEA1^+$, suggesting that this autophagy pathway is not restricted to lysosomes.

Few studies have investigated functional roles of autophagy in RNA delivery, that conceivably could act to reduce the amount of payload released upon endosome damage. One study found no evidence of improved cytosolic release of lipoplex–siRNA after inhibition of Gal-3, Gal-8 or NDP52[334]. This could suggest that the autophagic response is too slow to limit any additional release, that might already be counteracted by other systems responding earlier. On the contrary, knockdown of the autophagy regulating protein ATG5, rendering cells unable to generate autophagosomes, was found to increase lipoplex- and polyplex-mediated DNA delivery ~8-fold[505]. This indicates that multiple pathways might be activated to initiate autophagy or lysophagy in response to membrane damage induced by lipid-based delivery strategies. Additionally, autophagy is also regulated and altered in response to a multitude of stress-inducing conditions and drug treatments, that typically also can have joint effects on endolysosomal trafficking pathways[507], making it hard to pinpoint the functional role of this damage response mechanism for the efficiency of RNA delivery.

Stress granules

Recent studies have described a role of stress granules in the recognition and response to lysosomal membrane damage[508,509]. Stress granules are micron-sized RNA–protein condensates that form in mammalian cells upon translational arrest and subsequent polysome disassembly, which releases exposed RNA into the cytoplasm where it

interacts with a complex network of RNA-binding proteins (RBPs)[510]. Studies have indicated a central role of the proteins G3BP1 and its homologue G3BP2 for RNA-dependent condensate formation[511,512]. It was shown that stress granules can form rapidly at endomembrane damage sites to enable membrane repair through both ESCRT-dependent and -independent pathways[508]. Ca^{2+}-mediated activation of ALIX has been proposed to trigger formation of stress granules at the site of membrane damage[513]. The formed complexes acted as plugs to limit the release of intraluminal contents and to stabilizes ruptured membranes in an *in vitro* model[508]. However, the role of stress-granule formation in blocking the release of larger intralumenal lysosomal molecules *in cellulo* needs to be characterized, as well as the activity and regulation of this system in different tissues and cell types, in order to determine its relevance in the context of endosomal escape of oligonucleotides.

Hints of additional lysosomal membrane repair pathways

Additional cellular systems responding to lysosomal membrane damage and contribute to their repair have been identified recently, that appear to be at least in part independent of ESCRT. This includes Ca^{2+}-activated scrambling and turnover of sphingomyelin on the cytosolic side of the lysosomal membrane[514], directed transfer of cholesterol and phosphatidylserine to lysosomal membranes via damaged-induced ER–lysosomal contact sites[515], and recruitment of Annexins that possibly promote repair via cross-linking functions and membrane curvature modulation[516,517]. The coordination of these systems remains to be elucidated, as well as their link to the ESCRT machinery. Importantly, it is also not known to what extent these responses contribute to limiting the release of larger lysosomal contents — and potentially oligonucleotide payloads — or if they are also operating at earlier endosomal compartment than lysosomes.

Disrupting endolysosomal membranes to enhance RNA delivery

Permeabilization of cellular membranes by for example chemical compounds or other strategies have been researched for decades, with focus on anything from developing laboratory techniques to therapeutic treatment effects. As the endosomal escape bottleneck have emerged as a fundamental barrier against delivery of nucleic acids to target cells, a wide range of strategies have been explored to enhance the release by disrupting the integrity of endosomal membranes. A research area that shares an interest in the permeabilization of primarily lysosomes is the field of lysosome-dependent cell death, as introduced earlier.

Membrane-destabilizing small molecule drugs

Small molecule drugs with membrane-destabilizing properties have been explored extensively in the context of lysosomal membrane permeabilization (LMP) and drug delivery. One of the most prototypical drugs capable of inducing LMP is chloroquine (CQ) — a drug approved for treatment of malaria, but it also has antiviral and anti-inflammatory properties. On the downside, it has a relatively narrow therapeutic index with risk of serious toxicity if overdosed. CQ belongs to a group of lysosomotropic weak bases, that elevate the endosomal/lysosomal pH by entering cells and acid compartment by passive diffusion in their unprotonated form[518]. Once protonated in the acidic environment, the compounds can no longer cross the lipid bilayer due to their charge and tend to accumulate intraluminally in increasing concentration, while also increasing luminal pH. Many intracellular effects of CQ have been reported, but in the context of LMP, the insertion of a hydrophobic motif into the endosomal membrane is believed to be the primary mode of action that disrupts the bilayer at a critical concentration[519]. The ability of chloroquine to enhance delivery of nucleic acids to cells *in vitro* was first reported more than 40 years ago[520].

Chloroquine belongs to a broader group of membrane-destabilizing chemical compounds called cationic amphiphilic drugs (CADs). Hundreds of CADs are known, of which many are approved drugs for treatment of for example allergies and psychiatric disorders[521]. They are characterized by a hydrophobic ring structure and a hydrophilic side chain containing a cationic amine group. The amine group is protonated at low pH, promoting their accumulation in acidic compartments as described above[522]. Association of CADs with the lipid bilayer neutralizes negative membrane charge, which is necessary for several lysosomal lipases residing on the luminal membrane, that are subsequently displaced and degraded in the lysosomal lumen. One lipase that is considered central in the action of CADs is the glycoprotein acid sphingomyelinase (ASMase), that catalyzes the hydrolysis of sphingomyelin to ceramide and phosphorylcholine[521]. The stability of lysosomal membranes has been shown to depend on sphingomyelin–ceramide metabolism, and excessive sphingomyelin in the lysosomal membrane after inhibition of ASMase causes LMP[523,524]. Interestingly, studies have shown that lysosomes of cancer cells often are more vulnerable and prone to LMP from CAD treatment[525]. At least with some compounds and a selection of tumor types, this could provide a wider therapeutic index for triggering lysosomal damage in cancer cells compared to normal tissues.

Many other kinds of chemical compounds also trigger endosomal membrane damage by different mechanisms. One example is the leucine dipeptide L-leucyl-L-leucine *O*-methyl ester (LLOMe), that rapidly accumulates in acidic endosomes where it is polymerized by cathepsin C and increases the bilayer curvature strain until the

membrane is permeabilized[526,527]. Saponins and triterpenes are examples of yet another class of compounds capable of permeabilizing various cellular and endosomal membranes. In this case, however, they are believed to incorporate directly into the bilayer, where their accumulation ultimately creates pores in the membrane[528].

Lysosomes are key hubs for cellular iron homeostasis and storage. Excessive intracellular ferrous (Fe^{2+}) iron and reactive oxygen species (ROS) like hydrogen peroxide (H_2O_2) can form hydroxyl radicals via Fenton reactions, leading to (among other things) lipid peroxidation. Oxidation of unsaturated lipids in the bilayer of endosomes alters membrane fluidity and stability, and extensive lipid peroxidation has been shown to cause endosomal membrane permeabilization[529,530]. Strategies using delivery vehicles that promote lipid peroxidation (*e.g.* iron-containing nanoparticles[531]) or delivery vehicles responding to ROS production intracellularly[532] have been explored in effort to enhance payload delivery.

A typical feature of many lysosomotropic drugs is that they promote lysosomal swelling[533]. This was also described early on for delivery systems based on cationic polymers[534]. The most established explanation for this phenotypic change is the so called 'proton sponge effect', that has been proposed to promote disruption of acidic intracellular compartments like lysosomes[535]. Polyplexes or lysosomotropic small molecules that reach the endolysosomal compartments (via endocytosis or passive diffusion, respectively) buffer H^+ that are provided by the V-ATPase H^+ pump. The buffering capacity of the compounds limit the acidification of the endosomal lumen, maintaining a high V-ATPase activity. The continued transport of H^+ into the endosomes is coupled to the entry of Cl^-, to maintain the intraluminal charge balance. Increased intraluminal ionic concentration promotes water influx to maintain the endosomal osmolarity, causing an osmotic pressure that leads to endosomal swelling and — supposedly — disruption. The relative importance of the proton sponge effect in various cases have been debated ever since it was first proposed, where reports of separate mechanisms of action as well as other inconsistencies have argued against it. The current understanding is that a combination of osmotic pressure, polymer swelling due to charge repulsion upon protonation and membrane destabilization arising from interaction between the charged polymer and lipid bilayer all contribute to membrane disruption[536]. As highlighted above for the selected lysosomotropic small molecule drugs, other mechanisms than intraluminal H^+ buffering and osmotic swelling likely contribute significantly to promoting membrane damage.

Several compound library screening efforts have been carried out, looking for small molecule drugs capable of increasing the biological activity of RNA or ASO payloads delivered by various means[379,537–539] — where some also used galectins as a marker of

endosome damage[461,462]. Additional library screens have focused on identifying compounds that trigger LMP in the context of lysosome-dependent cell death[540,541]. Although many small molecule compounds have been identified that enhance endosomal release and biological activity of RNA and ASO payload *in vitro* — sometimes with surprisingly acceptable toxicity in relation to the number of induced endosomal damages — so far, no candidate have proven to be truly successful *in vivo*. Many reasons likely contribute to this, but a narrow therapeutic index and toxicity are probably the most important limitations[108]. However, strategies where membrane-destabilizing molecules are incorporated into delivery vehicles or directly conjugated to oligonucleotides could potentially be effective in enhancing endosomal escape while also showing improved tolerability[542].

Polymers and peptides to enhance RNA delivery

Strategies using peptides or polymers to trigger endosomal escape of oligonucleotides is an alternative approach to small molecules. One example is the dynamic polyconjugate (DPC) system, that was evaluated in clinical trials to improve the release of siRNA in hepatocytes. It is based on a two-molecule technology, where a cholesterol-siRNA and a membrane-active polymer conjugated to GalNAc is administered in combination[543]. The membrane-active polymer was derived from the pore-forming melittin peptide — the main component of honeybee (*Apis mellifera*) venom[544]. The melittin-conjugate was engineered to have pH-sensitive protecting groups, to limit its activity to acidic intracellular compartments. Although this approach was successful in enhancing endosomal escape and biological activity of siRNA, clinical trials showed toxicity and safety concerns leading to the discontinuation of clinical programs using the melittin-based DPC technology[545].

Peptides promoting escape of oligonucleotides can also be conjugated to the payload itself, or be incorporated into nanoparticle delivery vehicles, to limit non-productive membrane disruption. Many examples of such peptide/protein transduction domains (PTDs) or cell-penetrating peptides (CPPs) exists, including arginine-rich peptides like the TAT-PTD, Penetratin/Antp and 8R[546]; pH sensitive hydrophobic and fusogenic peptides, like derivatives of influenza virus hemagglutinin-2 (HA2)[547] and many others[548]; derivates of the stearyl-TP10 peptide (*e.g.* PepFects, NickFects) and similar peptides that might rely more on the proton sponge effect[409]. Close to 2,000 PTDs/CPPs have been reported[549], but approved therapies are still lacking. Hurdles that remain include issues related to stability, immunogenicity, toxicity, lack of specificity, and limited efficacy in facilitating both intracellular delivery and endosomal escape[409].

Rationale and overall aim

Although there have been considerable advancements in oligonucleotide and RNA chemistry and state-of-the-art delivery strategies in the last decades, intracellular entrapment of internalized therapeutic molecules in endosomes is still one of the major remaining hurdles hampering the potency of this new class of therapeutics. Very little is known in detail about the endosomal release process of siRNA and mRNA — except that it is very inefficient. Contributing to this knowledge gap has been a general lack of appropriate strategies and tools to evaluate endosomal release of oligonucleotide payload and investigate the link between endosomal escape efficiency and biological activity.

To bridge the current knowledge gap, this thesis has aimed to illuminate previously unknown aspects of endosomal escape of RNA therapeutics and the intracellular barriers they need to overcome. The development of new strategies to monitor and probe aspects of endosomal escape is a requirement for properly understanding it. Characterizing the release of payload will enable comparative analysis of the escape process in isolation, for example when comparing different delivery approaches or RNA constructs. Thus, understanding the criteria and processes involved in payload release will also make rational efforts to improve it feasible. Ultimately, overcoming the endosomal release bottleneck is key in order to take RNA therapeutics beyond the liver.

Specific aims

The specific aims of the papers included in this thesis were:

I. To investigate if membrane-destabilizing small molecule drugs could be used to trigger endosomal escape of lipid-conjugated siRNA *in vitro*.

   To establish a microscopy-based approach to visualize and evaluate endosomal escape in live cells.

II. To determine the cytosolic siRNA dose-response between the number of siRNA molecules delivered to the cytosol and knockdown of a reporter gene *in vitro*.

III. To investigate the endosomal escape kinetics of mRNA and siRNA delivered with LNPs *in vitro*.

   To investigate the disintegration of LNPs inside endosomes and the interaction between LNP constituents and the endosomal membrane bilayer.

IV. To study cellular membrane damage-responsive systems during treatment with lipid-conjugated siRNA *in vitro*, in effort to identify the basis for spontaneous endosomal escape.

Methods

Cell culture

Two-dimensional cell culture

The experiments included in the papers of this thesis were performed *in vitro*, primarily in HeLa cells (cervical cancer origin) and to lesser extent MCF7 cells (breast cancer origin). HeLa cells are widely accepted and used as a model cancer cell line to study fundamental biological and cancer-related processes, that have resulted in groundbreaking scientific developments over the years since the cell line was established. Although many fundamental cellular processes are likely to exist in other cell lines or patient tumors, their importance and implications may very well vary from case to case, making it hard to draw general conclusions from very specific observations or exact measurements.

Cells were cultivated in Dulbecco's Modified Eagle Medium (DMEM) (Cytiva HyClone Laboratories, South Logan, UT, USA) supplemented with 10% fetal bovine serum (FBS, Gibco), 100 U mL^{-1} penicillin and 100 mg mL^{-1} streptomycin (Gibco) and 2 mM glutamine (Gibco) at 37 °C and 5% CO_2. For live cell microscopy experiments with cholesterol-siRNA, cells were incubated in OptiMEM during simultaneous incubation with cholesterol-siRNA. For all other cases, imaging medium consisting of FluoroBrite DMEM (Gibco), supplemented with 10% FBS, 2 mM glutamine and 2 mM HEPES (Thermo Fisher Scientific, Waltham, MA, USA) was used. Cell culture medium or imaging medium was supplemented with 1.5 µg mL^{-1} recombinant ApoE (Sigma), prepared according to the manufacturer's protocol, for all LNP experiments. For microscopy experiments, $4–5 \times 10^4$ cells were plated per well in 8-well Lab-Tek II Chamber Slides (Nunc, Rochester, NY, USA) one day before experiments. A Neon Transfection System (Thermo Fisher Scientific) was used for plasmid and siRNA transfection. 5×10^5 cells were used with the 100-µL tips and cell-type specific protocol provided by the manufacturer. Transfected cells were used in experiments between 24 and 48 h after transfection.

Three-dimensional cancer cell spheroids

Growing cells in two-dimensional monolayer cultures poorly recapitulates many properties of tumors and to some extent also cancer cell biology. More complex models may be more successful in reconstituting real-life tumor biology. In **Paper I**, a simple 3D cell culture approach was used, where 5×10^3 HeLa or 1×10^4 MCF7 cells stably expressing fluorescently labeled Gal-9 were seeded in 96-well spheroid microplates (Corning, Kennebunk, ME, USA) in complete DMEM. For the evaluation of Gal-9 foci formation by small molecule drug treatment, the medium was removed from the wells after three days. Complete DMEM supplemented with small molecule drugs was added for 20 h, followed by fixation with 4% paraformaldehyde (PFA) and preparation for fluorescence microscopy. A similar protocol was used for evaluating the effect on d1-EGFP knockdown from small molecule drug treatment in 3D spheroids.

Materials

Galectin-9

In all papers included in this thesis, fluorescently labeled Gal-9 was used as a marker of endosome disruption. HeLa or MC7 cells stably expressing Gal-9 fused to yellow fluorescent protein (YFP) were established by transfection followed by antibiotic selection and the establishment of monoclonal cell populations by single-cell seeding. Other fluorescent fusion proteins of various galectins were used as well, as described in the individual papers.

d1-EGFP reporter system

In **Paper I–IV**, a robust and versatile enhanced green fluorescent protein (EGFP) reporter system for monitoring knockdown response was used. The EGFP protein is destabilized by fusion to a mutated variant of residues 422–461 of mouse ornithine decarboxylase (MODC). MODC contains a protein degradation sequence (PEST sequence) in its C-terminal domain, that targets it for proteasomal degradation. The turnover of the d1-EGFP fusion protein is accelerated considerably compared to wild-type EGFP, resulting in a half-life of ~1 h[550]. This makes the d1-EGFP reporter system well suited to monitor fast changes in protein expression, for example induced by RNAi-mediated target knockdown. Since the d1-EGFP fluorescence intensity of cells can be followed over time, this makes it possible to capture the dynamics of protein expression and knockdown over time and in single cells.

Cholesterol-siRNA

In **Paper I** and **Paper IV**, endosomal release of cholesterol-conjugated siRNA was studied. Several arguments for choosing cholesterol-siRNA in these investigations can be made. It is a well-researched construct among the lipid-modified siRNA conjugates, making it a suitable prototypical lipid-siRNA. In contrast to for example GalNAc, cholesterol-conjugates are not dependent upon a cell-type specific receptor for their internalization, which facilitates their use in several and different *in vitro* cell culture experiment. Lastly, functionally validated cholesterol-siRNA is available commercially (Accell siRNAs provided by Dharmacon Inc., Lafayette, CO, USA).

RNA lipid nanoparticles

In **Paper III**, lipid nanoparticles containing siRNA or mRNA were investigated. LNPs were manufactured and provided by AstraZeneca (Advanced Drug Delivery, Pharmaceutical Sciences, BioPharmaceuticals R&D, AstraZeneca, Gothenburg, Sweden). LNPs were formulated with Dlin-MC3-DMA or BODIPY-MC3 (ionizable lipid), cholesterol, DSPC, and DMPE-PEG2000. LNP formulations were prepared using a NanoAssemblr Benchtop microfluidic mixer (Precision Nanosystems). Lipid solutions were made in pure ethanol at a molar ratio of 50:10:38.5:1.5 for ionizable lipid:DSPC:cholesterol:DMPE-PEG2000. For mRNA formulations, a w:w ratio of lipid to cargo of 10:1 was used, for siRNA containing formulations a N/P ratio of 3 was used. Fluorescently labeled (AlexaFluor647 or Cy5) or unlabeled siRNA targeting EGFP, that was used for LNP formulation, were custom synthesized by Integrated DNA Technologies Inc, Coralville, IA, USA. CleanCap, 5-methoxyuridine- (5moU) modified mRNA encoding EGFP or Cy5-labeled mRNA encoding EGFP was from TriLink BioTechnologies, San Diego, CA, USA.

LNPs were characterized by dynamic light scattering using a Zetasizer Nano ZSP (Malvern Analytical Inc.) RNA concentration and encapsulation efficiency measurements were performed using Quant-iT RiboGreen reagent (Invitrogen). The LNP size (d_z) was typically ~70 nm for siRNA and ~85 nm for mRNA LNPs.

Lipoplex-siRNA formulation

In **Paper II**, the cytosolic dose-response relationship between siRNA targeting EGFP and d1-EGFP knockdown was investigated. Here, cytosolic delivery was achieved by lipoplex-formulation of siRNA, that could be optimized to produce release events where the resulting cytosolic siRNA concentration was within the dose-response interval. Formation of siRNA lipoplexes was performed using a fixed volume of the cationic transfection agent Lipofectamine 2000 and variable siRNA concentrations. siRNA and LF2000 were first diluted in OptiMEM before mixing, and then incubated

for 20 min at room temperature. The ratio of siRNA to LF2000 that was used for lipoplex formation in microscopy experiments ranged from 0.2:4 to 10:4 pmol:µL. Different volumes of the prepared lipoplex-siRNA solution was added to cells in experiments, to vary and optimize the number of lipoplexes that were internalized and the number and timing of the resulting release events.

Fluorescence microscopy

The work presented in this thesis relies heavily on fluorescence microscopy approaches for data acquisition. A selection of aspects and considerations of the microscopy methods used in the papers is discussed below.

High-spatiotemporal resolution microscopy techniques

Fluorescence microscopy is an instrumental technique in biology research, and the possibilities it provides has increased as technological advancements have accelerated. Acquiring microscopy image datasets by monitoring live cells poses extra challenges, and always requires balancing sample health, signal-to-noise ratio, spatial resolution, temporal resolution or acquisition duration, and the field of view. The trade-off between these parameters forms the pyramid of frustration in microscopy.

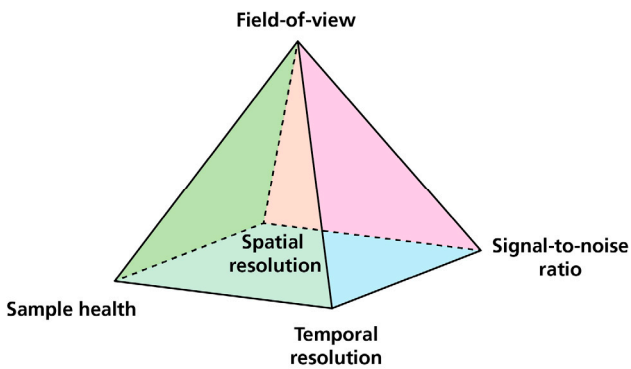

Figure 12. The pyramid of frustration in microscopy
Live-cell microscopy experiments inevitably requires compromise between image resolution (spatial and temporal), size of the sample area that is captured (field-of-view), signal-to-noise ratio and sample health.

Widefield fluorescence microscopy

In **Paper I** and **III**, widefield microscopy was used extensively for acquiring time-lapse image series of live cells. In this case, the sample is excited with non-coherent light from a LED light source. The emitted light is collected and registered on a camera chip. Here, a sensitive sCMOS (scientific complementary metal-oxide semiconductor) camera was used. With triggered hardware control, the image acquisition process is controlled via a hardware circuitry instead of the microscope computer software, accelerating the acquisition speed considerably. To acquire a volumetric dataset, several 2D images are acquired sequentially in the *z*-direction (bottom-to-top of cells) — a so called *z*-stack. Importantly, by combining a LED illumination light source, that can be switched on-off with microsecond speed, and multi-band pass optical filters, it is possible to acquire several channels with different fluorophores in rapid sequences. This is of key importance when evaluating live-cell processes like vesicle trafficking, where the interpretation of the data often relies on the spatial relationship (often colocalization) between markers in different channels. With rapid vesicle movement, a time difference of only a fraction of a second (often even less than 100 ms) will produce artifacts in the image data that can be hard to handle. The widefield microscopy system offers another advantage in that it is typically possible to do live-cell imaging with low phototoxicity, due to the used of gentle non-coherent LED light, efficient detection by sensitive cameras, and registration of all emitted light collected by the objective.

The main disadvantage, however, is that light from the entire 3D volume that is excited is also allowed to reach the camera. Since only a single plane in the 3D volume is in the focal plane of the optical system, the rest of the light registered on the camera is out-of-focus light projected on top of the focal-plane image. This leads to poor image contrast and a 'smeared' appearance. There is, however, tricks to apply in post-processing of the data to improve on this flaw.

Laser scanning confocal microscopy and array detectors

The invention of the confocal microscope provided a clever solution to the problem with out-of-focus light degrading the image quality. By introducing a small pinhole in the light path, between the objective and detector, the out-of-focus light can be blocked from reaching the detector. To use this strategy, the sample is excited by a focused laser beam scanning the sample, and the emitted light have typically been detected with a single-point detector like photomultiplier tubes (PMTs).

As with the widefield technique, volumetric datasets are acquired by capturing 2D images at several *z*-positions. Modern laser-scanning confocal microscopes (LSCM) typically also offers advanced and efficient modes for sequential, near-simultaneous or simultaneous channel acquisition with customizable spectrum bandwidths devoted for

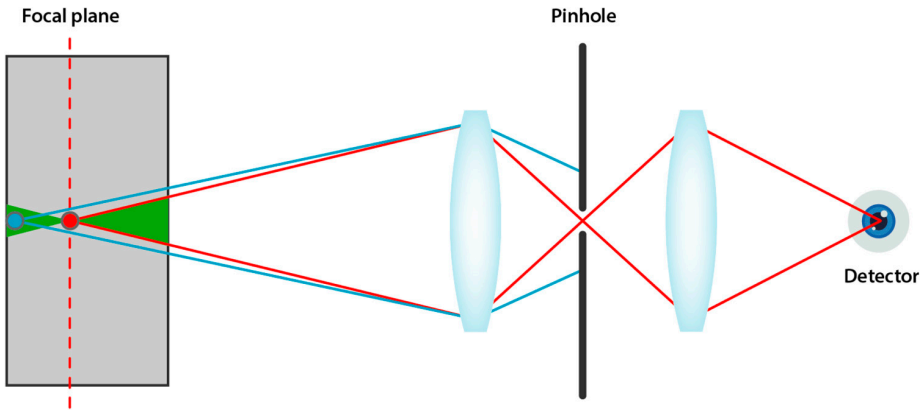

Figure 13. Light detection in confocal microscopy
Out-of-focus light (blue rays), originating from a point in the illuminated volume that is outside of the current focal plane, is blocked by the pinhole assembly whereas in-focus light (red rays) pass through the pinhole to the detector. Reproduced from Vangindertael, J et al. "An introduction to optical super-resolution microscopy for the adventurous biologist." *Methods and applications in fluorescence*vol. 6,2 022003. 16 Mar. 2018, doi:10.1088/2050-6120/aaae0c. Distributed under Creative Commons Attribution (CC BY) license (http://creativecommons.org/licenses/by/4.0/).

the individual fluorophores, and several detectors or assemblies of detector elements like spectral detectors.

While providing improved image contrast and resolution compared to widefield microscopy, LSCM also comes with some drawbacks. Due to the line-by-line scanning nature of image formation with classical LSCM, image acquisition has typically been slow and thus challenging when aiming to capture fast events in live-cells. Additionally, since a considerable share of the light emitted from the sample and collected by the objective is discarded (blocked by the pinhole), LSCM is not considered as light efficient as other techniques and the risk of sample damage (photobleaching or phototoxicity) is thus higher. Even so, LSCM have been workhorses of biological and biotechnological research for decades and will continue to have a strong position as upgraded but reliable and user-friendly systems.

An advancement of the LSCM technique has been the development of more sensitive detectors, for example gallium arsenide phosphide (GaAsP) detectors, enabling more efficient detection of light in low signal conditions, as well as array detectors for super-resolution imaging. One example of a confocal array detector is the Airyscan detector introduced by ZEISS[551], that was used in all papers included in this thesis. The Airyscan detector is a 32-channel GaAsP-PMT area detector. It collects a pinhole-plane image at every scan position. Each detector element has the role of a single, tiny pinhole. *A priori* information about the light path and the spatial arrangement of each detector

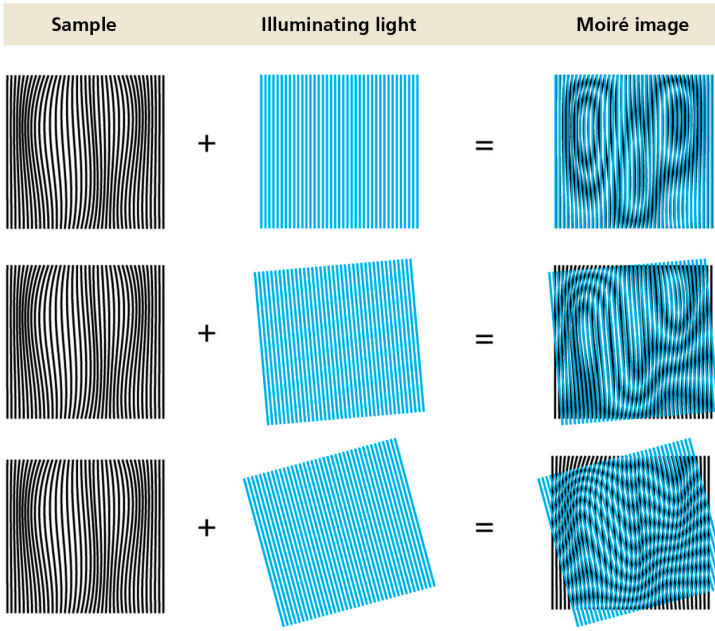

Figure 14. Structured illumination provides spatial frequency information for super-resolution imaging
Illuminating samples containing fine spatial details (high spatial frequencies) with well-defined periodic light patterns generates Moiré fringes of a lower spatial frequency. Because the illumination pattern is known, the high spatial frequency information can be mathematically recovered from the lower frequency (Moiré) patterns by computation, by using several orientations of the illumination pattern. Adapted from Vangindertael, J et al. "An introduction to optical super-resolution microscopy for the adventurous biologist." *Methods and applications in fluorescence*vol. 6,2 022003. 16 Mar. 2018, doi:10.1088/2050-6120/aaae0c. Distributed under the terms and conditions of Creative Commons Attribution (CC BY) license (http://creativecommons.org/licenses/by/4.0/).

element enables very light-efficient imaging with improved signal-to-noise ratio and also a spatial resolution beyond the diffraction limit (*i.e.* super-resolution).

Structured illumination microscopy

One of the techniques that have pioneered the field of super-resolution microscopy was invented by Mats Gustafsson[552], who died of brain cancer in 2011. Illuminating the sample with a structured (classically finely striped) light pattern produces images with fringes, called Moiré patterns. Since the illumination pattern is known, the high spatial frequency information of the sample can be mathematically recovered from the lower frequency Moiré pattern. This requires that several images are obtained, that typically have a different orientation of the illuminating pattern. The exact number of images depends on for example the illumination pattern and strategies to shift or rotate it as well as the computational reconstruction used. Structured illumination microscopy

(SIM) offers a two-fold improvement in resolution compared to conventional microscopy, that is possible to achieve with living samples and standard fluorescent molecules.

Although a widefield microscopy technique, SIM have inherent optical sectioning properties, comparable to confocal microscopy. This stems from the fact that out-of-focus light is not modulated in the same way by the illuminating pattern as light from the focal plane, making it possible to reduce the contribution of out-of-focus light to the final image during reconstruction.

In **Paper III** and **IV**, high-spatiotemporal microscopy imaging was performed with an adaptation of the SIM technique called instant SIM (iSIM)[553]. Here, a microlens array is used to generate a multifocal structured excitation pattern illuminating the sample, with a matched pinhole array to reject out-of-focus emission light. A microlens array is used to locally contract light passing each pinhole before it is scanned onto a camera used to sum and register the fluorescence.

With this approach, iSIM directly captures optically sectioned images with $\sqrt{2}$-fold improvement in spatial resolution in a single camera exposure. This circumvents the need to acquire multiple images with alternating illumination pattern. Although image post-processing (deconvolution) is used to obtain a full two-fold resolution improvement, SIM reconstruction in a classical sense is not needed. This makes iSIM a powerful and versatile microscopy imaging technique for live-cell experiments requiring both high speed and spatial resolution.

Image processing and analysis

Several customized image analysis pipelines were developed as described in the individual papers, to facilitate data handling, image restoration (*i.e.* deconvolution, channel registration and correction of chromatic aberration), endosome tracking and fluorescence quantification. This technical challenge was devoted much time and effort, but also made it possible to handle and analyze large quantities of data (likely close to 100 terabytes, equivalent to ~50,000,000 'standard' smartphone images with an individual file size of 2 MB). Indeed, for all papers included in this thesis, several thousands of endosome damage events have been evaluated and a considerable fraction have been further analyzed by tracking and fluorescence quantification.

Widefield and iSIM microscopy images were deconvolved with Huygens Professional for Windows Version 17.04 and 23.04 (Scientific Volume Imaging B.V., Hilversum, Netherlands), respectively. Image deconvolution is an iterative computational image

restoration process, that use *a priori* information about the optical system (*e.g.* the so called point spread function, that describes the distortion of light from a sub-diffraction limit light emitter), the excitation and emission wavelengths of light and the physical size of the sample captured by each pixel of the camera. Deconvolution allows out-of-focus light in the imaged volume to be computationally removed, while at the same time enhancing the signal-to-noise ratio (contrast) and spatial resolution. The many iterative calculations performed during deconvolution requires considerable computational power. Previously, this made the process slow, reducing the throughput. The development of graphical processing unit- (GPU) based processing in recent years have accelerated the computational speed, in addition to improved deconvolution algorithms. Image restoration and denoising strategies leveraging artificial intelligence (AI) have been launched in recent years. Although very powerful tools, the techniques still battle with developing reliable models for versatile biological samples, markers and microscopy modalities, as well as validating results and avoiding artifacts.

Additional methods

Other common laboratory techniques that were used include standard assays for flow cytometry, reverse-transcription quantitative polymerase chain reaction (RT-qPCR) and spectrophotometry. Details are provided in the Methods section of the individual papers.

Results and discussion

Imaging endosomal escape of RNA payload

Capturing endosomal release of cholesterol-siRNA

In **Paper I**, it was first demonstrated that selected small molecule drugs could trigger recruitment of Gal-3 to intracellular compartments. The response of several members of the galectin family to treatment with the membrane-destabilizing small molecule drug siramesine (SIR) was evaluated. Recruitment of Gal-9 was detectable fastest, and with higher signal-to-background intensity than Gal-8, -3 and -1.

Overexpression of YFP-tagged Gal-9 in cells was used to capture drug-induced damage events with potential of releasing endosomal cargo (Fig. 15, top panel). It was discovered that release of both dextran and cholesterol-conjugated siRNA (chol-siRNA) from individual vesicles could be captured with a spatiotemporal resolution high enough to quantitate the fluorescence intensity of single endosomes. The majority of captured release events were efficient, releasing >95% or ~80% of dextran or chol-siRNA payload, respectively. However, the fraction of damaged endosomes that contained siRNA payload was different when comparing the selected small molecule drugs (Fig. 16). This hit-rate was higher for chloroquine (CQ) (27%) than for SIR (11%). The amount of dextran released from endosomes to the cytosol correlated with the number of Gal-9 foci, but CQ treatment generated higher cytosolic amounts of dextran per detectable Gal-9 foci, corroborating the relevance of hit-rate differences in the efficiency of cytosolic delivery.

In **Paper IV**, Gal-9 and additional cytosolic proteins were explored as potential markers of spontaneous chol-siRNA release (*i.e.* without small molecule drug perturbation). No detectable Gal-9 response was triggered by chol-siRNA treatment at high concentration for up to 24 h. The ESCRT-III components CHMP2A and ALIX localized to a fraction of endosomes containing chol-siRNA 4–6 h after start of treatment. However, no increase in the number of $CHMP2A^+$ or $ALIX^+$ compartments was seen with chol-siRNA treatment, and no siRNA release was observed from $CHMP2A^+$ endosomes. $CHMP2A^+$ and chol-$siRNA^+$ endosomes were also often $CD63^+$, suggesting that the

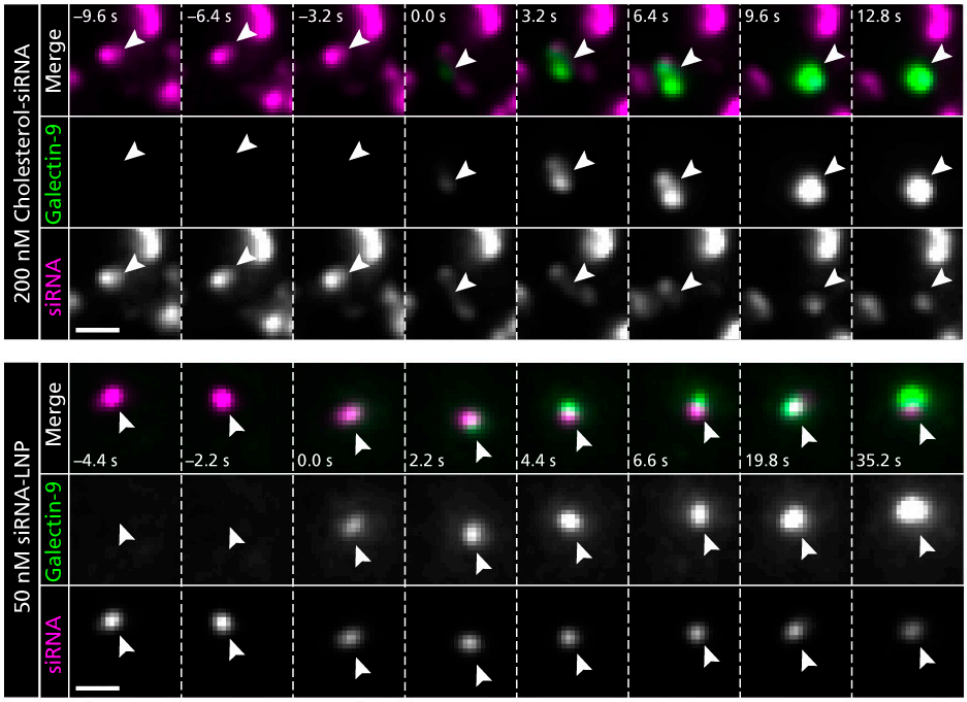

Figure 15. Capturing release of RNA payload from individual endosomes
HeLa cells expressing the cytosolic membrane damage sensor Gal-9 (YFP-tagged) was incubated with 200 nM cholesterol-conjugated (DY547-labeled) siRNA for 6 h followed by treatment with 60 μM chloroquine (top sequence, Paper I) or with 50 nM siRNA LNPs (AF647-labeled siRNA, bottom sequence, Paper III). Arrowheads indicate endosomes containing siRNA payload that display sudden Gal-9 recruitment. Scalebar: 2 μm (top) and 1 μm (bottom).

observed ESCRT-III activity may represent baseline 'house-keeping' activity, that cross roads with chol-siRNA in LEs and MVBs during endocytic trafficking. In addition to Gal-9, CHMP2A and ALIX, the activity of the cytosolic proteins PLA2G16 (a phospholipase recruited to endosomes showing release of viral RNA during infection) and G3BP1 (an RNA-binding protein involved in stress-granule formation) was also investigated during chol-siRNA treatment, without finding evidence for their involvement in damage response during chol-siRNA delivery.

Imaging release of siRNA and mRNA delivered by LNPs

Hit-rate — The key link between endosomal damage and payload release

In **Paper III**, Gal-9 was used as a sensor to evaluate endosomal damage and RNA release using LNPs. Both siRNA and mRNA LNPs triggered dose-dependent Gal-9 response. Damage induction was fastest with siRNA LNPs, that also seemed to have faster uptake than mRNA LNPs. Evaluating Gal-9 response during live-cell imaging with relatively low LNP concentrations (4–50 nM siRNA, 0.75 µg mL^{-1} mRNA) made it possible to pinpoint individual release events with a temporal resolution of 2–3 s. Surprisingly, the hit-rate differed substantially between siRNA and mRNA LNPs, with damaged endosomes having siRNA payload in 67–74% of cases, compared to only ~20% with mRNA LNPs (Fig. 16). The higher siRNA hit-rate was found also when using a different fluorophore label (Cy5 instead of AF647, the same as for mRNA) and with two concentrations of LNPs where only one quarter of siRNAs were fluorescently labeled.

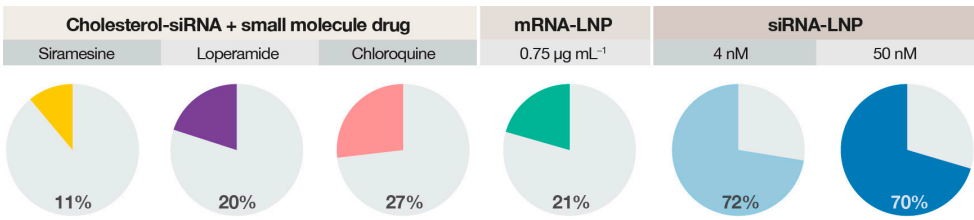

Figure 16. Hit-rate is the key link between endosomal damage and payload release
Membrane damage events can only contribute to cytosolic delivery (be productive) when the disrupted endosome contains RNA cargo. The fraction of potentially productive damage events is referred to as 'hit-rate'. The figure shows the hit-rate for three small molecule drugs during cholesterol-siRNA delivery (Paper I) and siRNA LNPs or mRNA LNPs (Paper III).

Release of RNA from damaged endosomes is inefficient and incomplete

Quantification of RNA fluorescence by endosome tracking showed that the siRNA fluorescence intensity was initially stable but decreased suddenly just as galectin recruitment was detectable. With mRNA LNPs, an initial fast signal decrease at the time of galectin recruitment was less pronounced but suggestive when evaluating the average of all events (Fig. 17).

To account for the heterogeneity of the release events, data was subgrouped with respect to events exhibiting a sharp drop in RNA fluorescence, or not, at the time of galectin recruitment. With mRNA LNPs, 26% of all vesicles showed rapid RNA release, where the RNA fluorescence decreased by 24% at ~10 s after damage, and then appeared

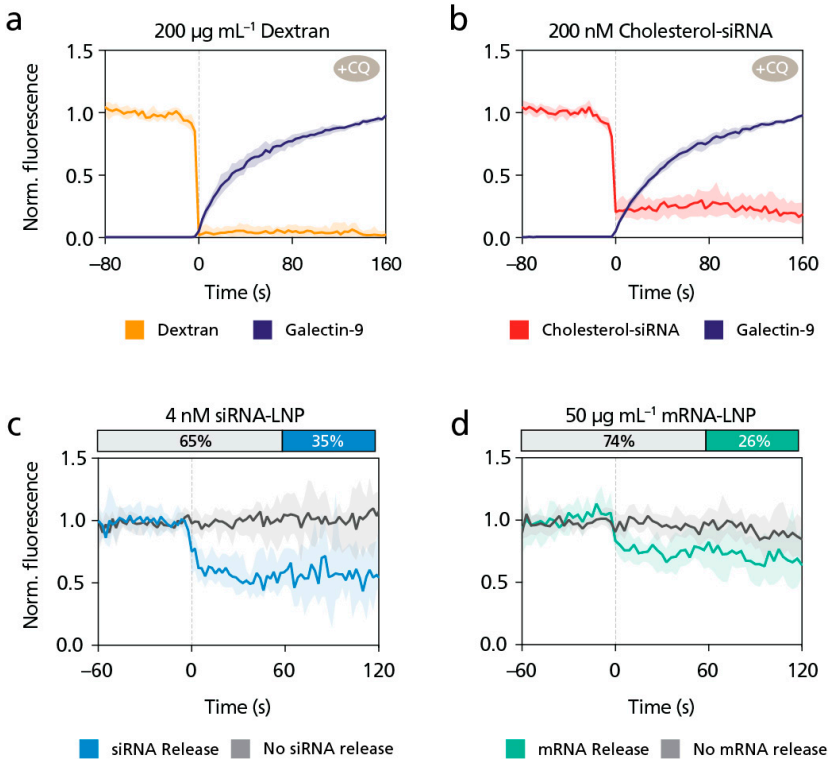

Figure 17. Measuring endosomal escape of RNA payload on a single-vesicle level
Endosomes containing **(a)** dextran, **(b)** cholesterol-siRNA, **(c)** siRNA LNP or **(d)** mRNA LNP payload that showed sudden recruitment of the damage sensor Galectin-9 were tracked in 3D over time, quantifying the fluorescence intensity from the payload. Traces were aligned in time so that $t = 0$ s is the first time with detectable Galectin-9 recruitment. **(c,d)** Traces were divided in two groups based on whether release of RNA payload could be detected upon endosome damage. The bars over the lower graphs show the fraction of damaged vesicles were RNA release was detectable. Median ± 95% confidence interval of median is shown. Cells were treated with 60 µM chloroquine in (a,b). Additional details are provided in Paper I (a,b) and Paper IV (c,d).

largely stable. With siRNA LNPs, there was a higher fraction of endosomes showing fast initial release, ranging from 35% (4 nM) to 53% (50 nM), in a dose-dependent manner. The relative magnitude of the fast release was comparable to that of mRNA, between 37% with 4 nM and 23% with 50 nM at ~10 s after start of galectin recruitment. In summary, only a fraction of damage events triggered by LNPs where Gal-9 is recruited show immediate and fast release of RNA cargo, and most of the RNA content remains in the endosome after the release.

LNPs trigger ESCRT activity that limits endosomal membrane disruption

In addition to a strong Gal-9 response, siRNA LNP treatment also triggered ESCRT-III activity as shown by increased number of CHMP2A^{+} compartments. In many cases, CHMP2 would be recruited to LNP-containing endosomes without or before Gal-9, indicating that the response preceded endosomal membrane disruption detectable by galectins. Knockdown of the three key ESCRT components — TSG101, ALIX and CHMP6 — increased the number of Gal-9 foci formed during siRNA LNP treatment, showing that ESCRT-mediated membrane repair counteracts and limits the number of possible siRNA release events.

Imaging cytosolic release of lipoplex-siRNA

In **Paper II**, release of lipoplex-formulated siRNA was visualized at a lower spatiotemporal resolution but with a high detection sensitivity and high dynamic range, by monitoring the cytosolic fluorescence intensity in long live-cell microscopy acquisitions. Sudden increases in the cytosolic fluorescence were detectable, that always coincided with Gal-9 recruitment to a lipoplex-containing endosome. An analysis pipeline was devised to automatically track cells, detect cytosolic release events and quantitate the siRNA and d1-EGFP fluorescence intensity. Shortly after release, siRNA transitioned from a homogenous cytosolic distribution to a vesicular pattern, contributing to the decay of the cytosolic siRNA signal (Fig. 18).

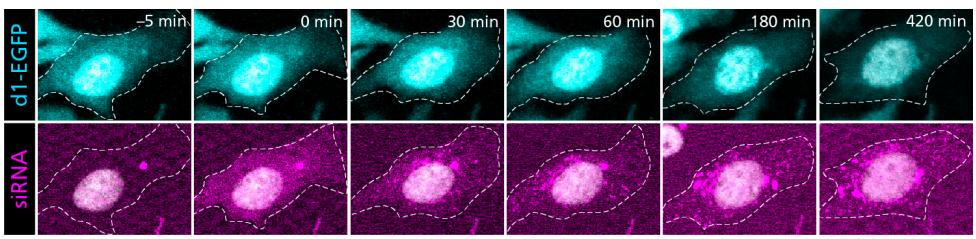

Figure 18. Cytosolic release of lipoplex-formulated siRNA
HeLa cells expressing d1-EGFP (top) were incubated with lipoplex-formulated siRNA targeting EGFP (AF647-labeled, bottom) during time-lapse confocal microscopy. A sensitive GaAsP array detector (Airyscan) was used to detect redistribution of siRNA to the cytosol (apparent at t = 0 min). Cytosolic siRNA is gradually redistributed into foci following endosomal release. Knockdown of the d1-EGFP protein (half-life ~50 min) can be monitored and quantified by measuring EGFP fluorescence over several hours following siRNA release. For details, see Paper II.

Interactions between LNPs and the endosomal membrane

In **Paper III**, the integrity of LNPs and their interaction with endosomal membranes in cells was investigated in detail using super-resolution microscopy.

LNPs disintegrate when trafficking through the endocytic pathway

The appearance of siRNA and mRNA LNPs was assessed at different stages along the endocytic pathway, by live-cell microscopy of cells expressing EEA1, Rab5 or the MVB- and LE-marker CD63. In $EEA1^+$ endosomes, the majority of fluorescently labeled siRNA and mRNA was confined to intraluminal point-like structures with a size corresponding to single LNPs visualized in dispersion on glass-slides. Endosomes containing single or multiple intact LNPs could be observed. In $CD63^+$ compartments, the appearance of siRNA inside the endosomal lumen had changed substantially, now typically filling the entire lumen with a homogenously distributed signal. In some vesicles, more commonly observed with mRNA LNPs and with siRNA in $Rab5^+$ compartments, the RNA was partly dispersed in the endosomal lumen, but a LNP remnant was still visible. Thus, direct observation and comparison of intralumenal disintegration of LNPs during endocytic trafficking in live cells was achieved.

Membrane-tethered LNPs trigger localized endosomal damage response

The appearance of Gal-9 and CHMP2A recruitment to LNP-containing endosomes was investigated during stages in the endocytic route where LNP disintegration was likely to promote endosomal damage. Visualization of Gal-9 or CHMP2A in $EEA1^+$ or $Rab5^+$ endosomes typically showed localized recruitment of the damage responder, to a membrane nanodomain in close proximity to LNPs tethered to the luminal membrane leaflet (Fig. 19c). Quantification of the distance between the intensity maximum of the damage marker and LNP confirmed a close spatial association, where both Gal-9 and CHMP2A were typically displaced ~60–80 nm toward the outside (cytosolic) side of the endosome compared to the LNP remnant.

Ionizable lipid integrates into endosomal membrane nanodomains

A modified ionizable lipid was developed to further investigate LNP disintegration and lipid–membrane interactions. The fluorescent molecule BODIPY was conjugated to DLin-MC3-DMA, and used to form dual-labeled LNPs with AF647-labeled siRNA. The new LNP showed several interesting spectral properties. The BODIPY

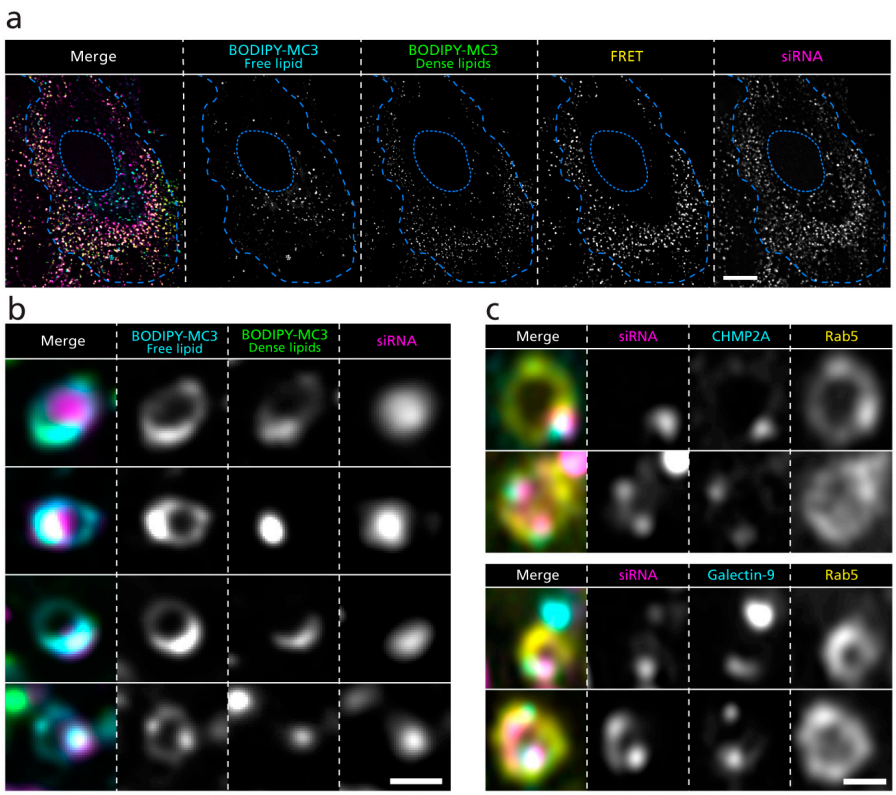

Figure 19. Super-resolution microscopy reveals LNP interaction with endosomal membrane
(a,b) A novel ionizable lipid was synthesized, where the fluorescent molecule BODIPY was covalently attached to Dlin-MC3-DMA (BODIPY-MC3), and used to formulate LNPs with AF647-labled siRNA. The emission spectrum of BODIPY-MC3 was red-shifted when lipid density was high (*e.g.* intact in LNPs), while also showing fluorescence quenching in the ordinary emission spectrum that resolved when lipid density decreased. Intact LNPs showed BODIPY-MC3–siRNA FRET (Förster resonance energy transfer), that decreased when LNPs disintegrated. **(a)** A HeLa cell with internalized siRNA BODIPY-MC3 LNPs is shown. Images were acquired with an iSIM microscope. Scalerbar: 10 µm. **(b)** Individual endosomes containing siRNA BODIPY-MC3 LNPs were imaged using a confocal microsope with a super-resolution array detector (Airyscan). Scalebar: 1 µm. **(c)** HeLa cells were transfected with Rab5-mScarlet and CHMP2A-GFP or Gal-9-YFP, and indubated with siRNA-containing LNPs (ordinary MC3). Images were acquired with a confocal microsope with an Airyscan detector. Scalebar: 1 µm. For additional details, see Paper III.

fluorescence was massively quenched in intact LNPs, that instead showed a red-shifted BODIPY emission spectrum. Intact particles also displayed significant quenching of AF647 fluorescence, and BODIPY–AF647 FRET. As LNPs disintegrated, BODIPY-MC3 and AF647-siRNA fluorescence increased, red-shifted BODIPY fluorescence and BODIPY–AF647 FRET decreased. In this way, the integrity of LNPs during disintegration could be monitored not just spatially — by evaluating the distribution of siRNA and MC3 in endosomes — but also by the spectral properties (Fig. 19a,b).

Evaluation of the dual-labeled LNPs in live cells showed that there was a gradient of intact-to-disintegrated LNPs from the periphery of cells to the perinuclear area — corresponding to the typical gradient of endosomal pH covered by transition from peripheral EEs to perinuclear lysosomes (Fig. 19a). LNPs visualized 2–4 h after internalization showed various degrees of particle disintegration, where siRNA filled the endosomal lumen with or without siRNA confined to a LNP remnant.

Intriguingly, ionizable lipid released from the LNP could be observed in the endosomal membrane, and its local concentration was highest closest to the membrane-tethered LNP remnant (Fig. 19b). The direct visualization of iL enriched in the endosomal membrane during LNP disintegration corresponded to the membrane nanodomain showing localized recruitment of Gal-9 and CHMP2A, linking the incorporation of iL in the endosomal membrane to its destabilization and disruption.

Profiling the identity of endosomal compartments releasing RNA payload to the cytosol

In **Paper I and III,** detailed investigations of the identity of compartments damaged during treatment with small molecule drugs or LNPs, respectively, were performed. Gal-9 was used as a marker to pinpoint the time of membrane disruption, and the presence of several selected organelle markers was evaluated around this timepoint. With small molecule treatment, it was found that the most prevalent markers of the damaged vesicles were markers of lysosomes and late endosomal compartment, like LAMP1, Rab7, CD63. The compartment identity profile was not identical when comparing CQ and SIR — for example, compartments targeted by CQ were more often LAMP1$^+$ (45% compared to 33% with SIR), and SIR targeted Rab9$^+$ endosomes to a greater extent (45% compared to 20% with CQ). In addition, it was observed that damages caused by CQ treatment could trigger recruitment of Rab5, that was not seen with SIR.

With LNPs, Gal-9 was recruited to endosomes with markers of early endosomal compartments. The most prevalent marker was Rab5, that was present on ~60% or 96% of compartments damaged by siRNA or mRNA LNPs, respectively. EEA1 was the second most common identity marker, followed by Rab7. Gal-9 recruitment to LAMP1$^+$ compartments was very rare. The findings highlight a clear difference in the identity of compartments that release RNA payload during LNP-mediated delivery or when escape is induced by small molecule drugs — at least with the more classical CADs investigated here.

Measuring cytosolic siRNA delivery and knockdown response

Small molecule drugs can improve cholesterol-siRNA activity by triggering endosomal escape

As the small molecule drugs that were investigated in **Paper I** caused membrane damage and cytosolic release of chol-siRNA, their effect on knockdown efficiency was evaluated subsequently. By using the d1-EGFP reporter system in HeLa cells, it was found that several drugs could enhance chol-siRNA mediated knockdown in a dose- and time-dependent manner that was in line with observations of the varying hit-rate of compartments containing payload. Although all compounds were toxic to cells at high doses, with most compounds, a substantial number of Gal-9$^+$ damage events (at least 10–20 events per cell) was still well tolerated. Interestingly, the apparent toxicity per Gal-9$^+$ endosome damage event seemed to differ between compounds, suggesting that the observed toxicity only partly is caused by endosomal damages, and that other mechanisms likely also contribute to varying extent. In addition to 2D cell cultures, experiments were also performed in 3D cancer cell spheroids, where Gal-9 response to small molecule drug treatment and an improvement in knockdown could be confirmed. In summary, it was found that Gal-9 response to small molecule treatment predicts potential chol-siRNA knockdown enhancement, but that the improvement is not necessarily equal for two compounds that trigger formation of the same number of Gal-9$^+$ foci.

Absolute quantification of cytosolic siRNA release

In **Paper II**, cytosolic release and subsequent redistribution of fluorescently labeled siRNA was readily detectable using live-cell fluorescence microscopy. To translate the siRNA fluorescence intensity measured in microscopy acquisitions to siRNA concentration, a fluorescence reference standard was generated by four-fold serial dilution of AF647-siRNA between 1 and 1,000 nM. In addition, a 1 µM siRNA calibration sample was imaged before start of all experiments and used for baseline correction during analysis. Identical microscopy settings were used for the reference standard, calibration and all experiments, to allow reliable conversion between fluorescence intensity and concentration. The cytosolic siRNA concentration could then also be converted into the corresponding number of siRNA molecules per cell, by measuring the volume of the HeLa cells used in experiments.

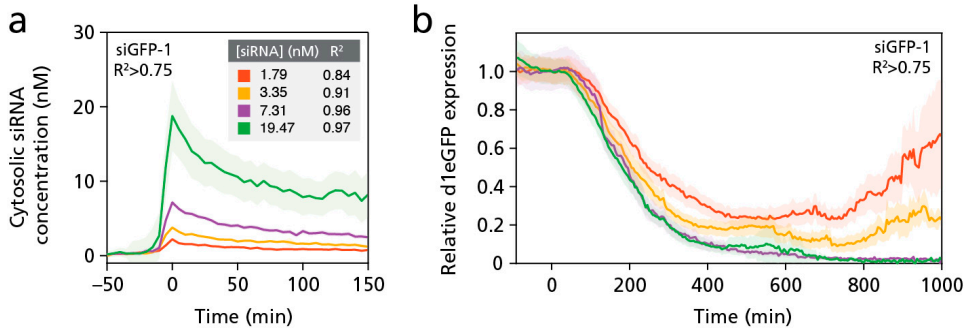

Figure 20. Quantification of cytosolic siRNA concentration and time-resolved target knockdown
HeLa cells expressing d1-EGFP were incubated with lipoplex-formulated siRNA targeting EGFP (AF647-labeled) and monitored during time-lapse confocal microscopy. A custom analysis pipeline was devised to detect and quantify cytosolic siRNA and d1-EGFP knockdown. Traces of inividual cells were aligned in time so that $t = 0$ is the first timepoint with detectable siRNA in the cytosol. A mathematical model was developed, that was fitted to individual siRNA release events. The model fit (coefficient of determination, R^2) was determined for each event. Traces were sorted and divided into quantiles based on the siRNA release magnitude. Traces with a high siRNA model fit ($R^2 > 0.75$) for the more potent siRNA sequence (siGFP-1) are shown. **(a)** The fluorescence intensity of siRNA in the cytosol was measuring using a sensitive confocal array detector (Airyscan) and converted into siRNA concentration using a known fluorescence reference standard. The median peak siRNA concentration and mean R^2 for each quantile is shown in the inserted box. Lines are mean, shaded areas are 95% confidence interval. **(b)** EGFP fluorescence was measured in cells where siRNA release to the cytosol was detected (at $t = 0$), and normalized to the mean intensity per cell before detectable siRNA release. Lines are mean, shaded areas are 80% confidence interval. For additional details, see Paper III.

Time-resolved target gene knockdown

In **Paper II**, the d1-EGFP reporter system made it possible to evaluate target knockdown after cytosolic siRNA delivery in a time-resolved manner, by measuring the EGFP fluorescence up to almost 17 h after cytosolic release. This unveiled a dose–response relationship with respect to knockdown induction, depth, and duration in the range from a few hundred to several thousand cytosolic siRNA molecules per cell (Fig. 20). The half-maximal knockdown induction and knockdown nadir was reached at a few hundred picomolar with a potent siRNA sequence — corresponding to ~1,000 cytosolic siRNA molecules. It was also observed that, in this model system, siRNA doses that were higher than necessary to reach initial knockdown saturation seemed to prolong knockdown duration. The dose-response relationship was evaluated for two siRNA sequences targeting EGFP with different potency — as previously determined from traditional experiments measuring the extracellular IC50 (the administered concentration) — highlighting the capability of this method to discriminate differences in cytosolic IC50.

In **Paper IV**, the kinetics of d1-EGFP knockdown mediated by chol-siRNA was characterized in a similar way as in Paper II. The dose-response of free chol-siRNA was

compared to the knockdown observed when chol-siRNA was delivered by lipoplex-formulation. To gain insight into the knockdown dynamics resulting from cytosolic chol-siRNA delivery, a strategy based on modeling EGFP knockdown was used.

Modeling siRNA release and EGFP knockdown

In **Paper II**, a mathematical model was devised, that could be fitted to cytosolic siRNA measurements and capture fast release and decay of the cytosolic siRNA signal over ~75 min. One of three characteristic release scenarios was used to fit the model to the data — typical high-magnitude release with exponential decay; high-noise low-magnitude release (step-function); or two separate release events occurring in quick succession. The model autonomously determined the most appropriate scenario to fit the model using Bayesian Information Criterion (BIC).

This modeling strategy enabled estimations of siRNA release amounts for both low and high-magnitude release events, where measurement of lower siRNA amounts inherently becomes noisier as the intensities approach the detection limit of the microscopy system. Additionally, the model fit — expressed as the coefficient of determination, R^2 — provided a measure of the accuracy and reliability of each individual cytosolic siRNA quantification (Fig. 20a).

A mathematical model was also developed for determining EGFP knockdown given a measured cytosolic siRNA concentration, by using expression measurements from all time points and all release events. This model allowed us to determine the absolute cytosolic IC50 with measures of statistical dispersion calculated by bootstrapping. For example, evaluating knockdown at 10 h after siRNA release, the cytosolic IC50 was estimated to be 0.36 (0.14–0.65) nM (median and 95% confidence interval) for the more potent siRNA, and 3.36 (2.15–4.87) nM for the less potent siRNA sequence.

In **Paper IV**, a simpler approach was used to fit an existing plateau–single phase decay model to d1-EGFP knockdown response measured in single cells. The model was well suited for characteristic knockdown responses measured in cells after delivery of lipoplex-formulated siRNA. It provided estimates of the time when knockdown started and the fluorescence half-life. The goodness-of-fit was evaluated by several criteria, that were used to determine if EGFP knockdown followed the proposed model or not. The majority of EGFP knockdown events with lipoplex-formulated chol-siRNA followed the kinetics proposed by the model, whereas only ~40% of knockdown responses with free chol-siRNA did so. For all chol-siRNA doses evaluated (50, 200 and 1,000 nM),

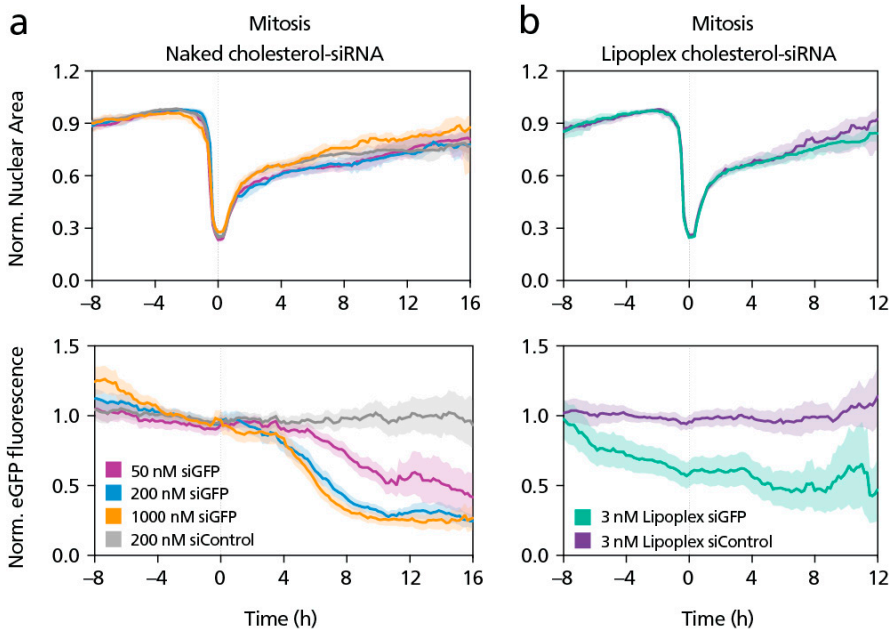

Figure 21. Cell-cycle state influences timing of cholesterol-siRNA mediated knockdown
HeLa cells expressing d1-EGFP were incubated with **(a)** naked (free) or **(b)** lipoplex-formulated cholesterol-siRNA targeting EGFP (siGFP) or a non-target control sequence (siControl) during time-lapse confocal microscopy. Cells were tracked to measure EGFP fluorescence and the size of cell nuclei. Cell traces having a nuclear size profile typical for mitosis were identified and further analyzed. Traces were aligned in time so that the smallest nuclear size (at metaphase) was at $t = 0$ h. The corresponding EGFP measurements shown in the lower graphs were normalized to the median EGFP fluorescence of cells incubated with naked or lipoplexed siControl. For all curves, lines are mean and shaded areas are 95% confidence interval. For additional details, see Paper IV.

knockdown kinetics derived from measurements with good model fits were very similar, with estimated start of EGFP knockdown ~6 h after start of chol-siRNA treatment and ~1 h EGFP half-life. This approach to modeling EGFP knockdown showed that a model describing a more bolus-like cytosolic delivery event (typical of lipoplexes) did not capture well the typical knockdown response observed during chol-siRNA treatment.

Cell-cycle state — but not ESCRT activity — influences cholesterol-siRNA mediated knockdown timing and efficiency

In **Paper IV**, since several ESCRT components were observed to localize to endosomes containing chol-siRNA payload, the possible effects on knockdown efficiency from inhibition of ESCRT activity was investigated. Relevant ESCRT activity could include

potential membrane repair response induced by chol-siRNA or other house-keeping processes taking place at these endosomes. Knockdown of the three ESCRT components TSG101, ALIX and CHMP6 — that was shown to increase the number of Gal-9$^+$ membrane damages during LNP treatment — did, however, not affect the efficiency of chol-siRNA mediated target knockdown. In summary, several points of evidence speak against a role of ESCRT during cytosolic delivery of chol-siRNA.

It was observed that, in long microscopy acquisitions monitoring EGFP knockdown during chol-siRNA treatment, EGFP fluorescence seemed to decrease more rapidly shortly after cell division. This was apparent also in quantitative data after aligning single-cell measurements in time so that mitosis occurred synchronously (Fig. 21a). Surprisingly, clear EGFP knockdown was typically not observed before mitosis had occurred. This contrasted with the knockdown observed from siRNA delivered by lipoplex-formulation, that started independently of cell division (Fig. 21b). The link between cell division and start of EGFP knockdown was further investigated by synchronizing cells to different stages in the cell cycle before starting chol-siRNA treatment. Remarkably, cells synchronized to late S-phase when starting chol-siRNA treatment showed a clearly improved EGFP knockdown response, lowering the IC50 approximately 4-fold from ~160 nM (no synchronization) to ~40 nM. This finding further supports a link between cellular events occurring close to mitosis and endosomal release of chol-siRNA.

Strengths and limitations

All experiments and results included in this thesis were produced in *in vitro* cell cultures. As such, results should be considered contextual and might not hold true for all conditions or translate into other models. Indeed, in **Paper I**, it was found that treatment effects from membrane-destabilizing small molecule drugs varied between cell lines, indicating that important functional differences likely also exists between different tissues *in vivo*. It is plausible that the small molecule drugs that enhanced chol-siRNA mediated knockdown in **Paper I** are toxic *in vivo* at concentrations that would have similar effects on the rate of vesicle disruption as was observed in the *in vitro* experiments presented here. Importantly, however, toxicity does not necessarily have to be related only to the number of damaged or leaky endosomes *per se*, but could instead have other or at least additional contributing causes.

In **Paper I and III**, measurements of the RNA fluorescence intensity of individual endosomes were performed at the time of membrane damage and potential payload release. Even though this type of quantifications can be used to make reasonable general conclusions on endosomal escape efficiency, measures of for example the fraction of payload released should not be considered exact or equal for all conditions, since the accuracy of the measurements is affected by the microscopy system used, data processing and analysis. It is also possible that different LNP formulations (*e.g.* with different ionizable lipids) could have very different endosomal escape characteristics.

In **Paper II**, it was estimated that the measurement error was <20% for the vast majority of individual release events when taking the main sources of measurement uncertainty into account (*e.g.* imprecision in reference curve calibration and photobleaching-induced variability), indicating that the measurements were indeed reliable. Using mathematical modeling, both siRNA release quantifications and the resulting knockdown response were additionally gauged. However, only the cytosolic dose-response relationship of one reporter target (d1-EGFP) was investigated, using two siRNA sequences in one cell line. It is likely that different conditions could be found where the cytosolic IC50 is lower and higher, than what was found here. Still, the presented data provides a description of this relationship in a well-known *in vitro* cell line with a well-known target, as a starting point for further exploration.

The method used here is labor intensive and requires sensitive optimization for reliable results, which limits the throughput considerably if envisioning for example screening efforts. In addition, the sensitivity of the microscope used allows detection of burst-like release of relatively large amounts of RNA molecules (or rather fluorophores) to the cytosol, but cannot detect or reliably quantify cytosolic amounts of RNA delivered with LNPs — with therapeutically relevant concentrations — or conjugated siRNAs. Further technological advancements might provide solutions to this in the future.

In **Paper III**, interaction between endosomal membrane and ionizable lipid in living cells was investigated using a novel dual-labeled LNP with fluorescently tagged Dlin-MC3-DMA. This is, to my knowledge, the first time this interaction is visualized in living cells, providing new insight into how ionizable lipid distributes in the vesicle membrane and triggers membrane disruption. However, limitations to the spatial resolution of the confocal array detector used require that endosomes are fairly large in order to make sub-endosomal characterization of LNP–membrane interactions possible. Overexpression of some markers — and likewise often regulators — of endosomal compartments might influence their phenotype (*e.g.* size or shape) and function. For example, overexpression of EEA1 might promote the formation of larger early endosomes, facilitating imaging of intraluminal LNPs. Even so, the lipid bilayer of enlarged endogenous endosomes is still a better representation of the native membrane than cell-free membrane mimics. Importantly, such models cannot easily reconstitute membrane strain from curvature or vesicle–vesicle interactions, that are possibly of importance in membrane disruption.

In **Paper IV**, the possible routes of cytosolic delivery of cholesterol-conjugated siRNA were explored. It is a critical observation that the endosomal escape of cholesterol-siRNA does not seem to trigger galectin response (as evaluated by Gal-9). It is also intriguing that — in contrast to LNP treatment — ESCRT activity was not affected by high cholesterol-siRNA concentrations, and inhibition of ESCRT activity did not affect knockdown efficiency. Still, since the number of potentially disrupted endosomes is low and cumulative — and likely also much more subtle than damage events provoked by lipoplexes or LNPs — it is difficult to exclude the possibility of very rare galectin$^+$ or ESCRT$^+$ damage events that might promote cholesterol-siRNA release. However, alternative pathways where galectin and ESCRT response is not elicited seems, at this time, more likely. The link between cell-cycle state and cholesterol-siRNA knockdown is elusive and warrants further investigations using additional cell lines and cell synchronization assays in a first step. The observation is interesting, since it could imply that highly proliferative cells might be more prone to cytosolic delivery of lipid-conjugated siRNA payload, with possible implications for targeting cancer cells and tumor.

Conclusions

From the findings presented in the papers of this thesis, I conclude that:

- Galectin-9 can be used as a sensitive marker of endosome disruption induced by small molecule drugs or lipid nanoparticles, facilitating investigation of endosomal escape of RNA payload in live cells using fluorescence microscopy.

- Cationic amphiphilic small molecule drugs can disrupt late endosomal compartments and lysosomes, to promote release of lipid-modified siRNA and enhance target gene knockdown in 2D and 3D cell cultures.

- Cytosolic release of lipoplex-formulated siRNA can be detected and quantified using sensitive live-cell confocal microscopy, to determine the absolute cytosolic siRNA concentration and cytosolic dose-response relationship.

- Endosomal release of LNP-formulated siRNA and mRNA is inefficient and incomplete, and a considerable fraction of damage events are non-productive or occur in endosomes without RNA payload.

- LNPs formulated with the ionizable lipid Dlin-MC3-DMA primarily disrupt early endosomal compartments marked by Rab5 and EEA1.

- Tethering of LNPs to the luminal leaflet of early endosomes causes localized membrane damage, marked by recruitment of Galectin-9 or components in the ESCRT machinery.

- A dual-labeled LNP with fluorescently tagged MC3 can reveal incorporation of ionizable lipid into the endosomal lipid bilayer as the LNP disintegrates, promoting membrane destabilization.

- Cytosolic delivery of cholesterol-siRNA does not trigger Galectin-9 or ESCRT response typical of endosome damage induced by small molecule drugs or LNP treatment.

Future perspectives

Therapies based on RNA and oligonucleotides now have real and life-changing impact in the clinics. This is, however, only the beginning of an area where targeted therapies based on these novel pharmacological principles will reach more and more patients in diverse clinical settings. The delivery of oligonucleotides and RNA to the liver is widely regarded as having been solved, and several more therapies that are currently under clinical or preclinical development will most likely be approved, addressing targets in the liver. For many of these diseases — often with a clearly established and rare genetic cause — there are currently no available treatments. However, focus is now shifting to much more common conditions like for example hypercholesterolemia or cardiovascular disease.

Beyond the liver, the CNS is likely to be one of the next organs where RNA therapies will be clinically approved. Indeed, ASO therapies targeting disease-causing genes in the CNS have already been approved, indicating openings for additional therapeutic modalities like siRNA. The CNS niche is also promising from a cancer therapy perspective since it offers unique ways of drug administration and local treatment of brain tumors. If clinically successful, siRNA or oligonucleotide therapies targeting genes involved in common neurodegenerative diseases (*e.g.* Alzheimer's disease) will be an incredible milestone, that could hopefully accelerate the development of RNA-based brain tumor therapies.

There is still a lot to learn about mRNA and siRNA therapies in cancer treatment. Lessons from immunotherapies like checkpoint inhibitors and CAR-T cell therapy have shown the potency of immunomodulation in the treatment of cancer. It is reasonable to believe that the first successful examples of RNA therapies in cancer treatment will act through immune-mediated pathways, for example mRNA-based cancer vaccines or RNAi-mediated immunomodulation that promote antitumoral immune response. Achieving clinically meaningful outcomes with direct targeting of cancer cells via RNAi is likely a more difficult prospect, but will hopefully be a versatile and potent treatment option for long-term disease control in the future.

The endosomal escape bottleneck is a primary concern in realizing extrahepatic RNA delivery. It will likely be partially overcome with more advanced and tailored delivery

vehicles, that more efficiently reach the target tissue and deliver a higher fraction of the administered RNA dose to the correct cells. One solution could very well be to combined delivery strategies with ways of disrupting the endosomal membrane to facilitate cytosolic release, in a non-toxic manner. This is already the case with ionizable lipids in prototypical LNPs, but the endosomal escape efficiency of RNA payload delivered with LNPs is still poor and requires further improvement. An alternative approach would be to use new, more tolerable small molecule drugs to enhance RNA release, or to interfere with key regulatory processes implicated in damage formation or repair. If such efforts are to be successful, however, additional insight into the endosomal escape process in needed, to devise rational strategies to approach the problem.

As is discussed throughout this thesis — and shown in the included papers — a lot remains to be uncovered and understood about the endosomal escape process. Pinpointing the elusive mechanisms whereby conjugated siRNA (both lipid-modified siRNA and receptor-targeted conjugates like GalNAc-siRNA) enter the cytosol is one of the most important questions in the field of RNA drug delivery. I hope that the strategies and findings presented in this thesis will contribute to understanding and eventually overcoming this barrier.

Acknowledgements

I am grateful to many amazing people and the fantastic work, help, support, and inspiration they have provided over many years related to this thesis or in other ways, without which this work would never have been possible. A special and heartfelt thank you to:

My main supervisor, **Anders Wittrup**. You are amazing, in all meanings of the word! The open, unpretentious attitude filled with never waning optimisms and patience you show in leading me and the lab toward all high-set goals have meant so much not only for the outcome of this thesis but also for my development during all these years.

My favorite co-supervisors, **Pontus Nordenfelt** and **Hakon Leffler**, that have provided invaluable advice and support along the way, and for introducing me to the world of Matlab and galectins — probably by far the most important tools to produce this thesis.

My fellow lab members and dearest of friends — **Johanna**, **Hanke**, **Myriam**, **Sten** and **Wahed** — without you by my side this work would not have been possible or worthwhile. A special thanks also to **Hanna**, whose work and spirit we treasure and miss having in the lab.

My co-authors and collaborators — **Jonas Wallin** at the Department of Mathematical Statistics at Lund University, and **Lennart Lindfors**, **Erik Oude Blenke**, **Said Haran** and **Aditya Pote** at Astra Zeneca.

My science Großvater, **Mattias Belting**, for your inspiring and intimidating approach to hardcore science. All members of the Belting lab — **Maria**, **Anna**, **Emma**, **Kelin**, **Sarah**, **Axel**, **Hugo**, **Jiaxin**, **Valeria**, **Federica**, **Emelie**, **Aadya**, **Ann-Sofie**, and many past members that have inspired and provided help along the way.

All other groups and people on the Gunnar Nilsson floor — **Helena Jernström** for invaluable advice and support. **Christopher**, **Somayeh**, **Anna**, **Edward**, **Stevanus** and past members of the GIT group, whose company and help I appreciate tremendously. **Bo Baldetorp**, for all fruitful discussions and your genuine interest and support of the

work we do. **Susanne André**, without your excellent help and assistance, little of this work would have been achieved and with much greater difficulty.

All other colleagues at the Kamprad lab, **Ann**, **Karin**, **Björn**, **Maja**, **Hedda**, **Sara**, **Alexandra**, **Sofie**, **Mohamed**, **Anders**, **Gabriel**, **Oskar, Vinay, Marie, Carina, Mattias** and many more and past colleagues.

My family — **Mamma**, for your endless support and love. **Anna** and **Sebastian**, you make me so proud. **Pappa**, for all memorable times. To all extended family members, for your care and support.

I am thankful to all funding agencies supporting our research: **Knut and Alice Wallenberg Foundation**, **John och Augusta Perssons Stiftelse**, **Swedish Research Council**, **Svenska Sällskapet för Medicinsk Forskning**, **Governmental Funding of Clinic Research within the National Health Service** (ALF), **Region Skåne** and **Gunnar Nilssons Cancerstiftelse**. A special thanks to **Fru Berta Kamprads Stiftelse**, that has provided generous funding towards the investment in two new bleeding-edge microscopy systems, ensuring that the Kamprad lab environment will remain a strong hub for microscopy-focused cancer research for years to come.

References

1. Swanton, C. *et al.* Embracing cancer complexity: Hallmarks of systemic disease. *Cell* **187**, 1589–1616 (2024).
2. Hanahan, D. Hallmarks of Cancer: New Dimensions. *Cancer Discov* **12**, 31–46 (2022).
3. Socialstyrelsen. Dataanalyser av cancer 1975–2019. *socialstyrelsen.se* (2021).
4. Cancer Research UK. Cancer survival statistics for all cancers combined. *cancerresearchuk.org* https://www.cancerresearchuk.org/health-professional/cancer-statistics/survival/all-cancers-combined#heading-Zero (2022).
5. Siegel Mph, R. L., Giaquinto, A. N., Ahmedin, |, Dvm, J. & Siegel, R. L. Cancer statistics, 2024. (2024) doi:10.3322/caac.21820.
6. Socialstyrelsen och Cancerfonden. Cancer i siffror. https://www.socialstyrelsen.se/globalassets/sharepoint-dokument/dokument-webb/statistik/cancer-i-siffror-2023.pdf (2023).
7. Sung, H., Siegel, R. L., Rosenberg, P. S. & Jemal, A. Emerging cancer trends among young adults in the USA: analysis of a population-based cancer registry. *Lancet Public Health* **4**, e137–e147 (2019).
8. Sung, H. *et al.* Global Cancer Statistics 2020: GLOBOCAN Estimates of Incidence and Mortality Worldwide for 36 Cancers in 185 Countries. *CA Cancer J Clin* **71**, 209–249 (2021).
9. Ugai, T. *et al.* Is early-onset cancer an emerging global epidemic? Current evidence and future implications. *Nat Rev Clin Oncol* **19**, 656–673 (2022).
10. Zhao, J. *et al.* Global trends in incidence, death, burden and risk factors of early-onset cancer from 1990 to 2019. *BMJ Oncology* **2**, e000049 (2023).
11. Akimoto, N. *et al.* Rising incidence of early-onset colorectal cancer — a call to action. *Nat Rev Clin Oncol* **18**, 230–243 (2021).
12. Chelmow, D. *et al.* Executive Summary of the Early-Onset Breast Cancer Evidence Review Conference. *Obstetrics and Gynecology* **135**, 1457–1478 (2020).
13. Anders, C. K. *et al.* Young Age at Diagnosis Correlates With Worse Prognosis and Defines a Subset of Breast Cancers With Shared Patterns of Gene Expression. *Journal of Clinical Oncology* **26**, 3324–3330 (2008).

14. Yantiss, R. K. *et al.* Clinical, Pathologic, and Molecular Features of Early-onset Colorectal Carcinoma. *American Journal of Surgical Pathology* **33**, 572–582 (2009).

15. Ansari, D., Althini, C., Ohlsson, H. & Andersson, R. Early-onset pancreatic cancer: a population-based study using the SEER registry. *Langenbecks Arch Surg* **404**, 565–571 (2019).

16. Popkin, B. M., Adair, L. S. & Ng, S. W. Global nutrition transition and the pandemic of obesity in developing countries. *Nutr Rev* **70**, 3–21 (2012).

17. Hofseth, L. J. *et al.* Early-onset colorectal cancer: initial clues and current views. *Nat Rev Gastroenterol Hepatol* **17**, 352–364 (2020).

18. Rudolph, A., Chang-Claude, J. & Schmidt, M. K. Gene–environment interaction and risk of breast cancer. *Br J Cancer* **114**, 125–133 (2016).

19. Collaborative Group on Hormonal Factors in Breast Cancer. Breast cancer and breastfeeding: collaborative reanalysis of individual data from 47 epidemiological studies in 30 countries, including 50 302 women with breast cancer and 96 973 women without the disease. *The Lancet* **360**, 187–195 (2002).

20. Collaborative Group on Hormonal Factors in Breast Cancer. Menarche, menopause, and breast cancer risk: individual participant meta-analysis, including 118 964 women with breast cancer from 117 epidemiological studies. *Lancet Oncol* **13**, 1141–1151 (2012).

21. Hamilton, A. C. & Coleman, H. G. Shifting tides: the rising tide of early-onset cancers demands attention. *BMJ Oncology* **2**, 106 (2023).

22. World Health Organization. Ageing and health. *who.int* https://www.who.int/news-room/fact-sheets/detail/ageing-and-health (2022).

23. Laconi, E., Marongiu, F. & DeGregori, J. Cancer as a disease of old age: changing mutational and microenvironmental landscapes. *Br J Cancer* **122**, 943–952 (2020).

24. National Cancer Institute Surveillance Research Program. SEER Incidence Rates by Age at Diagnosis 2016-2020, November 2022 Submission (1975-2020), SEER 22 registries. *SEER*Explorer: An interactive website for SEER cancer statistics [Internet]* https://seer.cancer.gov/statistics-network/explorer/application.html?site=1&data_type=1&graph_type=3&compareBy=sex&chk_sex_1=1&rate_type=2&race=1&advopt_precision=1&advopt_show_ci=on&hdn_view=0#resultsRegion0 (2023).

25. Cancer Research UK. Cancer incidence by age. *cancerresearchuk.org* https://www.cancerresearchuk.org/health-professional/cancer-statistics/incidence/age#heading-Zero (2021).

26. Siegel, R. L., Miller, K. D. & Jemal, A. Cancer statistics, 2020. *CA Cancer J Clin* **70**, 7–30 (2020).

27. World Health Organization. Global cancer burden growing, amidst mounting need for services. *who.int* https://www.who.int/news/item/01-02-2024-global-cancer-burden-growing--amidst-mounting-need-for-services (2024).

28. Marosi, C. & Köller, M. Challenge of cancer in the elderly. *ESMO Open* **1**, e000020 (2016).

29. Maggiore, R. J. *et al.* Toxicity and survival outcomes in older adults receiving concurrent or sequential chemoradiation for stage III non-small cell lung cancer in Alliance trials (Alliance A151812). *J Geriatr Oncol* **12**, 563–571 (2021).

30. Mohile, S. G. *et al.* Practical assessment and management of vulnerabilities in older patients receiving chemotherapy: Asco guideline for geriatric oncology. *Journal of Clinical Oncology* **36**, 2326–2347 (2018).

31. Hurria, A. *et al.* Validation of a Prediction Tool for Chemotherapy Toxicity in Older Adults With Cancer. *Journal of Clinical Oncology* **34**, 2366–2371 (2016).

32. Ganesh, K. & Massagué, J. Targeting metastatic cancer. *Nat Med* **27**, 34–44 (2021).

33. Flannery, M. A. *et al.* Understanding Treatment Tolerability in Older Adults With Cancer. *Journal of Clinical Oncology* **39**, 2150–2163 (2021).

34. Weinstein, I. B. Addiction to Oncogenes—the Achilles Heal of Cancer. *Science (1979)* **297**, 63–64 (2002).

35. Haslam, A., Kim, M. S. & Prasad, V. Updated estimates of eligibility for and response to genome-targeted oncology drugs among US cancer patients, 2006-2020. *Annals of Oncology* **32**, 926–932 (2021).

36. Bollag, G. *et al.* Vemurafenib: the first drug approved for BRAF-mutant cancer. *Nature Publishing Group* (2012) doi:10.1038/nrd3847.

37. Kopetz, S. *et al.* Phase II Pilot Study of Vemurafenib in Patients With Metastatic BRAF-Mutated Colorectal Cancer. *J Clin Oncol* (2015) doi:10.1200/JCO.2015.63.2497.

38. Kobayashi, S. *et al.* EGFR Mutation and Resistance of Non–Small-Cell Lung Cancer to Gefitinib. *New England Journal of Medicine* **352**, 786–792 (2005).

39. Gorre, M. E. *et al.* Clinical Resistance to STI-571 Cancer Therapy Caused by BCR-ABL Gene Mutation or Amplification. *Science (1979)* **293**, 876–880 (2001).

40. Montagut, C. *et al.* Identification of a mutation in the extracellular domain of the Epidermal Growth Factor Receptor conferring cetuximab resistance in colorectal cancer. *Nat Med* **18**, 221–223 (2012).

41. Van Allen, E. M. *et al.* The Genetic Landscape of Clinical Resistance to RAF Inhibition in Metastatic Melanoma. *Cancer Discov* **4**, 94–109 (2014).

42. Jin, H., Wang, L. & Bernards, R. Rational combinations of targeted cancer therapies: background, advances and challenges. *Nat Rev Drug Discov* **22**, 213–234 (2023).

43. Elbashir, S. M. *et al.* Duplexes of 21-nucleotide RNAs mediate RNA interference in cultured mammalian cells. *Nature* **411**, 494–498 (2001).

44. Fire, A. *et al.* Potent and specific genetic interference by double-stranded RNA in Caenorhabditis elegans. *Nature* **391**, 806–811 (1998).

45. Lee, R. C., Feinbaum, R. L. & Ambrost, V. The C. elegans Heterochronic Gene lin-4 Encodes Small RNAs with Antisense Complementarity to &II-14. *Cell* **75**, 843–854 (1993).

46. Wightman, B., Ha, I. & Ruvkun, G. Posttranscriptional regulation of the heterochronic gene lin-14 by lin-4 mediates temporal pattern formation in C. elegans. *Cell* **75**, 855–862 (1993).

47. Borchert, G. M., Lanier, W. & Davidson, B. L. RNA polymerase III transcribes human microRNAs. *Nat Struct Mol Biol* **13**, 1097–1101 (2006).

48. Monteys, A. M. *et al.* Structure and activity of putative intronic miRNA promoters. *RNA* **16**, 495–505 (2010).

49. Ozsolak, F. *et al.* Chromatin structure analyses identify miRNA promoters. *Genes Dev* **22**, 3172–3183 (2008).

50. Zeng, Y., Yi, R. & Cullen, B. R. Recognition and cleavage of primary microRNA precursors by the nuclear processing enzyme Drosha. *EMBO Journal* **24**, 138–148 (2005).

51. Gregory, R. I. *et al.* The Microprocessor complex mediates the genesis of microRNAs. *Nature* **432**, 235–240 (2004).

52. Lee, Y. *et al.* The nuclear RNase III Drosha initiates microRNA processing. *Nature* **425**, 415–419 (2003).

53. Winter, J., Jung, S., Keller, S., Gregory, R. I. & Diederichs, S. Many roads to maturity: microRNA biogenesis pathways and their regulation. *Nat Cell Biol* **11**, 228–234 (2009).

54. Ruby, J. G., Jan, C. H. & Bartel, D. P. Intronic microRNA precursors that bypass Drosha processing. *Nature* **448**, 83–86 (2007).

55. Yi, R., Qin, Y., Macara, I. G. & Cullen, B. R. Exportin-5 mediates the nuclear export of pre-microRNAs and short hairpin RNAs. *Genes Dev* **17**, 3011–3016 (2003).

56. Lund, E., Güttinger, S., Calado, A., Dahlberg, J. E. & Kutay, U. Nuclear Export of MicroRNA Precursors. *Science (1979)* **303**, 95–98 (2004).

57. Saito, K., Ishizuka, A., Siomi, H. & Siomi, M. C. Processing of Pre-microRNAs by the Dicer-1–Loquacious Complex in Drosophila Cells. *PLoS Biol* **3**, e235 (2005).

58. Förstemann, K. *et al.* Normal microRNA Maturation and Germ-Line Stem Cell Maintenance Requires Loquacious, a Double-Stranded RNA-Binding Domain Protein. *PLoS Biol* **3**, e236 (2005).

59. Provost, P. *et al.* Ribonuclease activity and RNA binding of recombinant human Dicer. *EMBO Journal* **21**, 5864–5874 (2002).

60. Filipowicz, W. Minireview RNAi: The Nuts and Bolts of the RISC Machine. *Cell* **122**, 17–20 (2005).

61. Siomi, H. & Siomi, M. C. On the road to reading the RNA-interference code. *Nature* **457**, 396–404 (2009).

62. Shin, C. *et al.* Expanding the MicroRNA Targeting Code: Functional Sites with Centered Pairing. *Mol Cell* **38**, 789–802 (2010).

63. Kiriakidou, M. *et al.* An mRNA m7G Cap Binding-like Motif within Human Ago2 Represses Translation. *Cell* **129**, 1141–1151 (2007).

64. Chendrimada, T. P. *et al.* MicroRNA silencing through RISC recruitment of eIF6. *Nature* **447**, 823–828 (2007).

65. Eulalio, A., Behm-Ansmant, I. & Izaurralde, E. P bodies: at the crossroads of post-transcriptional pathways. *Nat Rev Mol Cell Biol* **8**, 9–22 (2007).

66. Iwakawa, H.-O. & Tomari, Y. Life of RISC: Formation, action, and degradation of RNA-induced silencing complex. *Mol Cell* **82**, 30–43 (2022).

67. Pratt, A. J. & MacRae, I. J. The RNA-induced Silencing Complex: A Versatile Gene-silencing Machine. *Journal of Biological Chemistry* **284**, 17897–17901 (2009).

68. Lim, L. P. *et al.* Microarray analysis shows that some microRNAs downregulate large numbers of target mRNAs. *Nature* **433**, 769–773 (2005).

69. Rupaimoole, R. & Slack, F. J. MicroRNA therapeutics: towards a new era for the management of cancer and other diseases. *Nature Publishing Group* (2017) doi:10.1038/nrd.2016.246.

70. Bautista-Sánchez, D. *et al.* The Promising Role of miR-21 as a Cancer Biomarker and Its Importance in RNA-Based Therapeutics. *Mol Ther Nucleic Acids* **20**, 409–420 (2020).

71. Pharmacodynamics Study of MRX34, MicroRNA Liposomal Injection in Melanoma Patients With Biopsy Accessible Lesions (MRX34-102). *ClinicalTrials.gov* https://www.clinicaltrials.gov/study/NCT02862145 (2016) NCT02862145.

72. MesomiR 1: A Phase I Study of TargomiRs as 2nd or 3rd Line Treatment for Patients With Recurrent MPM and NSCLC. *ClinicalTrials.gov* https://www.clinicaltrials.gov/study/NCT02369198 (2017) NCT02369198.

73. SOLAR: Efficacy and Safety of Cobomarsen (MRG-106) vs. Active Comparator in Subjects With Mycosis Fungoides (SOLAR). *ClinicalTrials.gov* https://www.clinicaltrials.gov/study/NCT03713320 (2022) NCT03713320.

74. Bernstein, E., Caudy, A. A., Hammond, S. M. & Hannon, G. J. Role for a bidentate ribonuclease in the initiation step of RNA interference. *Nature* **409**, 363–366 (2001).

75. Elbashir, S. M., Lendeckel, W. & Tuschl, T. RNA interference is mediated by 21-and 22-nucleotide RNAs. (2001) doi:10.1101/gad.862301.

76. Nykänen, A., Haley, B. & Zamore, P. D. ATP Requirements and Small Interfering RNA Structure in the RNA Interference Pathway. *Cell* **107**, 309–321 (2001).

77. Zamore, P. D., Tuschl, T., Sharp, P. A. & Bartel, D. P. RNAi: double-stranded RNA directs the ATP-dependent cleavage of mRNA at 21 to 23 nucleotide intervals. *Cell* **101**, 25–33 (2000).

78. Khvorova, A., Reynolds, A. & Jayasena, S. D. Functional siRNAs and miRNAs Exhibit Strand Bias. *Cell* **115**, 209–216 (2003).

79. Schwarz, D. S. *et al.* Asymmetry in the Assembly of the RNAi Enzyme Complex. *Cell* **115**, 199–208 (2003).

80. Sakurai, K. *et al.* A role for human Dicer in pre-RISC loading of siRNAs. *Nucleic Acids Res* **39**, 1510–1525 (2011).

81. Brown, C. R. *et al.* Investigating the pharmacodynamic durability of GalNAc–siRNA conjugates. *Nucleic Acids Res* **48**, 11827–11844 (2020).

82. Haley, B. & Zamore, P. D. Kinetic analysis of the RNAi enzyme complex. *Nat Struct Mol Biol* **11**, 599–606 (2004).

83. Davidson, B. L. & McCray, P. B. Current prospects for RNA interference-based therapies. *Nat Rev Genet* **12**, 329–340 (2011).

84. Siolas, D. *et al.* Synthetic shRNAs as potent RNAi triggers. *Nat Biotechnol* **23**, 227–231 (2005).

85. Kim, D.-H. *et al.* Synthetic dsRNA Dicer substrates enhance RNAi potency and efficacy. *Nat Biotechnol* **23**, 222–226 (2005).

86. Jadhav, V., Vaishnaw, A., Fitzgerald, K. & Maier, M. A. RNA interference in the era of nucleic acid therapeutics. *Nat Biotechnol* **42**, 394–405 (2024).

87. Kanasty, R., Robert Dorkin, J., Vegas, A. & Anderson, D. Delivery materials for siRNA therapeutics. *Nature Publishing Group* (2013) doi:10.1038/NMAT3765.

88. Larsson, E., Sander, C. & Marks, D. mRNA turnover rate limits siRNA and microRNA efficacy. *Mol Syst Biol* **6**, 433 (2010).

89. Ferguson, C. M., Echeverria, D., Hassler, M., Ly, S. & Khvorova, A. Cell Type Impacts Accessibility of mRNA to Silencing by RNA Interference. *Mol Ther Nucleic Acids* **21**, 384–393 (2020).

90. Birmingham, A. *et al.* 3′ UTR seed matches, but not overall identity, are associated with RNAi off-targets. *Nat Methods* **3**, 199–204 (2006).

91. Jackson, A. L. *et al.* Expression profiling reveals off-target gene regulation by RNAi. *Nat Biotechnol* **21**, 635–637 (2003).

92. Jackson, A. L. *et al.* Position-specific chemical modification of siRNAs reduces "off-target" transcript silencing. *RNA* **12**, 1197–1205 (2006).

93. Cohen, J. C., Boerwinkle, E., Mosley, T. H. & Hobbs, H. H. Sequence Variations in *PCSK9,* Low LDL, and Protection against Coronary Heart Disease. *New England Journal of Medicine* **354**, 1264–1272 (2006).

94. Kim, D. H. & Rossi, J. J. Strategies for silencing human disease using RNA interference. *Nat Rev Genet* **8**, 173–184 (2007).

95. Judge, A. D. *et al.* Sequence-dependent stimulation of the mammalian innate immune response by synthetic siRNA. *Nat Biotechnol* **23**, 457–462 (2005).

96. Hornung, V. *et al.* Sequence-specific potent induction of IFN-α by short interfering RNA in plasmacytoid dendritic cells through TLR7. *Nat Med* **11**, 263–270 (2005).

97. Heil, F. *et al.* Species-Specific Recognition of Single-Stranded RNA via Toll-like Receptor 7 and 8. *Science (1979)* **303**, 1526–1529 (2004).

98. Karikó, K., Bhuyan, P., Capodici, J. & Weissman, D. *Small Interfering RNAs Mediate Sequence-Independent Gene Suppression and Induce Immune Activation by Signaling through Toll-Like Receptor 3 1. The Journal of Immunology* vol. 172 http://journals.aai.org/jimmunol/article-pdf/172/11/6545/1183902/6545.pdf (2004).

99. Robbins, M., Judge, A. & MacLachlan, I. siRNA and Innate Immunity. *Oligonucleotides* **19**, 89–102 (2009).

100. Hornung, V. *et al.* 5'-Triphosphate RNA Is the Ligand for RIG-I. *Science (1979)* **314**, 994–997 (2006).

101. Kim, D.-H. *et al.* Interferon induction by siRNAs and ssRNAs synthesized by phage polymerase. *Nat Biotechnol* **22**, 321–325 (2004).

102. Marques, J. T. *et al.* A structural basis for discriminating between self and nonself double-stranded RNAs in mammalian cells. *Nat Biotechnol* **24**, 559–565 (2006).

103. Rettig, G. R. & Behlke, M. A. Progress toward in vivo use of siRNAs-II. *Molecular Therapy* vol. 20 483–512 Preprint at https://doi.org/10.1038/mt.2011.263 (2012).

104. Boccaletto, P. *et al.* MODOMICS: A database of RNA modification pathways. 2021 update. *Nucleic Acids Res* **50**, D231–D235 (2022).

105. Judge, A. D., Bola, G., Lee, A. C. H. & MacLachlan, I. Design of Noninflammatory Synthetic siRNA Mediating Potent Gene Silencing in Vivo. *Molecular Therapy* **13**, 494–505 (2006).

106. Egli, M. & Manoharan, M. Critical Reviews and Perspectives Chemistry, structure and function of approved oligonucleotide therapeutics. *Nucleic Acids Res* **51**, 2529–2573 (2023).

107. Allerson, C. R. *et al.* Fully 2'-Modified Oligonucleotide Duplexes with Improved in Vitro Potency and Stability Compared to Unmodified Small Interfering RNA. *J Med Chem* **48**, 901–904 (2005).

108. Dowdy, S. F. Overcoming cellular barriers for RNA therapeutics. *Nature Biotechnology* vol. 35 222–229 Preprint at https://doi.org/10.1038/nbt.3802 (2017).

109. Ryter, J. M. & Schultz, S. C. Molecular basis of double-stranded RNA-protein interactions: structure of a dsRNA-binding domain complexed with dsRNA. *EMBO J* **17**, 7505–7513 (1998).

110. Il Chang, C. *et al.* Asymmetric Shorter-duplex siRNA Structures Trigger Efficient Gene Silencing With Reduced Nonspecific Effects. *Molecular Therapy* **17**, 725–732 (2009).

111. Sun, X., Rogoff, H. A. & Li, C. J. Asymmetric RNA duplexes mediate RNA interference in mammalian cells. *Nat Biotechnol* **26**, 1379–1382 (2008).

112. Nair, J. K. *et al.* Multivalent N -acetylgalactosamine-conjugated siRNA localizes in hepatocytes and elicits robust RNAi-mediated gene silencing. *J Am Chem Soc* **136**, 16958–16961 (2014).

113. Brown, K. M. *et al.* Expanding RNAi therapeutics to extrahepatic tissues with lipophilic conjugates. *Nat Biotechnol* **40**, 1500–1508 (2022).

114. Adams, D. *et al.* Patisiran, an RNAi Therapeutic, for Hereditary Transthyretin Amyloidosis. *New England Journal of Medicine* **379**, 11–21 (2018).

115. Akinc, A. *et al.* Targeted delivery of RNAi therapeutics with endogenous and exogenous ligand-based mechanisms. *Molecular Therapy* **18**, 1357–1364 (2010).

116. Balwani, M. *et al.* Phase 3 Trial of RNAi Therapeutic Givosiran for Acute Intermittent Porphyria. *New England Journal of Medicine* **382**, 2289–2301 (2020).

117. Fitzgerald, K. *et al.* A Highly Durable RNAi Therapeutic Inhibitor of PCSK9. *New England Journal of Medicine* **376**, 41–51 (2017).

118. Ray, K. K. *et al.* Two Phase 3 Trials of Inclisiran in Patients with Elevated LDL Cholesterol. *New England Journal of Medicine* **382**, 1507–1519 (2020).

119. Garrelfs, S. F. *et al.* Lumasiran, an RNAi Therapeutic for Primary Hyperoxaluria Type 1. *New England Journal of Medicine* **384**, 1216–1226 (2021).

120. Baum, M. A. *et al.* PHYOX2: a pivotal randomized study of nedosiran in primary hyperoxaluria type 1 or 2. *Kidney Int* **103**, 207–217 (2023).

121. Adams, D. *et al.* Efficacy and safety of vutrisiran for patients with hereditary transthyretin-mediated amyloidosis with polyneuropathy: a randomized clinical trial. *Amyloid* **30**, 18–26 (2023).

122. Barratt, J. *et al.* Phase 2 Trial of Cemdisiran in Adult Patients with IgA Nephropathy: A Randomized Controlled Trial. *Clinical Journal of the American Society of Nephrology* **19**, 452–462 (2024).

123. Young, G. *et al.* Efficacy and safety of fitusiran prophylaxis in people with haemophilia A or haemophilia B with inhibitors (ATLAS-INH): a multicentre, open-label, randomised phase 3 trial. *The Lancet* **401**, 1427–1437 (2023).

124. Friedrich, M. & Aigner, A. Therapeutic siRNA: State-of-the-Art and Future Perspectives. *BioDrugs* **36**, 549–571 (2022).

125. Tabernero, J. *et al.* First-in-humans trial of an RNA interference therapeutic targeting VEGF and KSP in cancer patients with liver involvement. *Cancer Discov* **3**, 406–417 (2013).

126. Garber, K. Worth the RISC? *Nat Biotechnol* **35**, 198–202 (2017).

127. Maraganore, J. Reflections on Alnylam. *Nat Biotechnol* **40**, 641–650 (2022).

128. EphA2 siRNA in Treating Patients With Advanced or Recurrent Solid Tumors. *ClinicalTrials.gov* https://clinicaltrials.gov/study/NCT01591356 (2024) NCT01591356.

129. iExosomes in Treating Participants With Metastatic Pancreas Cancer With KrasG12D Mutation. *ClinicalTrials.gov* https://clinicaltrials.gov/study/NCT03608631 (2023) NCT03608631.

130. A Phase 2 Study of siG12D LODER in Combination With Chemotherapy in Patients With Locally Advanced Pancreatic Cancer (PROTACT). *ClinicalTrials.gov* https://clinicaltrials.gov/study/NCT01676259 (2021) NCT01676259.

131. Study of ARO-HIF2 in Patients With Advanced Clear Cell Renal Cell Carcinoma. *ClinicalTrials.gov* https://clinicaltrials.gov/study/NCT04169711 (2022) NCT04169711.

132. Ookh, W. *et al.* Codelivery of TGF β and Cox2 siRNA inhibits HCC by promoting T-cell penetration into the tumor and improves response to Immune Checkpoint Inhibitors. *NAR Cancer* **6**, 1–11 (2024).

133. Ph. 1, Evaluation of Safety, Tolerability, PK, Anti-tumor Activity of STP707 IV in Subjects With Solid Tumors. *ClinicalTrials.gov* https://clinicaltrials.gov/study/NCT05037149 (2024) NCT05037149.

134. Wolff, J. A. *et al.* Direct Gene Transfer into Mouse Muscle in Vivo. *New Series* **247**, 1465–1468 (1990).

135. Dolgin, E. The tangled history of mRNA vaccines. *Nature* **597**, 318–324 (2021).

136. A Phase I, Open Label Dose Escalation Study to Evaluate Safety of iHIVARNA-01 in Chronically HIV-infected Patients Under Stable Combined Antiretroviral Therapy. *ClinicalTrials.gov* https://clinicaltrials.gov/study/NCT02413645 (2017) NCT02413645.

137. Safety, Tolerability, and Immunogenicity of VAL-506440 in Healthy Adult Subjects. *ClinicalTrials.gov* https://www.clinicaltrials.gov/study/NCT03076385 (2022) NCT03076385.

138. Safety, Tolerability, and Immunogenicity of mRNA-1325 in Healthy Adult Subjects. *ClinicalTrials.gov* https://www.clinicaltrials.gov/study/NCT03014089 (2019) NCT03014089.

139. Huang, X. *et al.* Nanotechnology-based strategies against SARS-CoV-2 variants. *Nat Nanotechnol* **17**, 1027–1037 (2022).

140. Kong, N. *et al.* Synthetic mRNA nanoparticle-mediated restoration of p53 tumor suppressor sensitizes p53-deficient cancers to mTOR inhibition. *Sci Transl Med* **11**, 1565 (2019).

141. Hewitt, S. L. *et al.* Durable anticancer immunity from intratumoral administration of IL-23, IL-36γ, and OX40L mRNAs. *Sci Transl Med* **11**, 9143 (2019).

142. Parayath, N. N., Stephan, S. B., Koehne, A. L., Nelson, P. S. & Stephan, M. T. In vitro-transcribed antigen receptor mRNA nanocarriers for transient expression in circulating T cells in vivo. *Nat Commun* **11**, 6080 (2020).

143. Choi, B. D. *et al.* Intraventricular CARv3-TEAM-E T Cells in Recurrent Glioblastoma. *New England Journal of Medicine* (2024) doi:10.1056/NEJMoa2314390.

144. Liu, C. *et al.* mRNA-based cancer therapeutics. *Nat Rev Cancer* **23**, 526–543 (2023).

145. Jemielity, J., Kowalska, J., Rydzik, A. M. & Darzynkiewicz, E. Synthetic mRNA cap analogs with a modified triphosphate bridge – synthesis, applications and prospects. *New Journal of Chemistry* **34**, 829 (2010).

146. Zarghampoor, F., Azarpira, N., Khatami, S. R., Behzad-Behbahani, A. & Foroughmand, A. M. Improved translation efficiency of therapeutic mRNA. *Gene* **707**, 231–238 (2019).

147. Alexaki, A. *et al.* Effects of codon optimization on coagulation factor IX translation and structure: Implications for protein and gene therapies. *Sci Rep* **9**, 15449 (2019).

148. Chaudhary, N., Weissman, D. & Whitehead, K. A. mRNA vaccines for infectious diseases: principles, delivery and clinical translation. *Nat Rev Drug Discov* **20**, 817–838 (2021).

149. Karikó, K., Buckstein, M. & Ni, H. Suppression of RNA Recognition by Toll-like Receptors: The Impact of Nucleoside Modification and the Evolutionary Origin of RNA. *Immunity* **23**, 165–175 (2005).

150. Linares-Fernández, S., Lacroix, C., Exposito, J.-Y. & Verrier, B. Tailoring mRNA Vaccine to Balance Innate/Adaptive Immune Response. *Trends Mol Med* **26**, 311–323 (2020).

151. Chen, H. *et al.* Branched chemically modified poly(A) tails enhance the translation capacity of mRNA. *Nat Biotechnol* (2024) doi:10.1038/s41587-024-02174-7.

152. Karikó, K., Muramatsu, H., Ludwig, J. & Weissman, D. Generating the optimal mRNA for therapy: HPLC purification eliminates immune activation and improves translation of nucleoside-modified, protein-encoding mRNA. *Nucleic Acids Res* **39**, e142–e142 (2011).

153. Mohamad-Gabriel Alameh, A. *et al.* Lipid nanoparticles enhance the efficacy of mRNA and protein subunit vaccines by inducing robust T follicular helper cell and humoral responses. *Immunity* **54**, (2021).

154. Pastor, F. *et al.* An RNA toolbox for cancer immunotherapy. *Nature Publishing Group* **17**, (2018).

155. Lang, F., Schrörs, B., Löwer, M., Türeci, Ö. & Sahin, U. Identification of neoantigens for individualized therapeutic cancer vaccines. *Nat Rev Drug Discov* **21**, 261–282 (2022).

156. Andtbacka, R. H. I. *et al.* Talimogene Laherparepvec Improves Durable Response Rate in Patients With Advanced Melanoma. *Journal of Clinical Oncology* **33**, 2780–2788 (2015).

157. Ferrucci, P. F., Pala, L., Conforti, F. & Cocorocchio, E. Talimogene Laherparepvec (T-VEC): An Intralesional Cancer Immunotherapy for Advanced Melanoma. *Cancers (Basel)* **13**, 1383 (2021).

158. Moderna, I. Moderna and Merck Announce mRNA-4157/V940, an Investigational Personalized mRNA Cancer Vaccine, in Combination With KEYTRUDA(R) (pembrolizumab), was Granted Breakthrough Therapy Designation by the FDA for Adjuvant Treatment of Patients With High-Risk Melanoma Following Complete Resection. *2023* https://investors.modernatx.com/news/news-details/2023/Moderna-and-Merck-Announce-mRNA-4157V940-an-Investigational-Personalized-mRNA-Cancer-Vaccine-in-Combination-With-KEYTRUDAR-pembrolizumab-was-Granted-Breakthrough-Therapy-Designation-by-the-FDA-for-Adjuvant-Treatment-of-Patients-With-High-Risk-Melanom/default.aspx.

159. Weber, J. S. *et al.* Individualised neoantigen therapy mRNA-4157 (V940) plus pembrolizumab versus pembrolizumab monotherapy in resected melanoma (KEYNOTE-942): a randomised, phase 2b study. *The Lancet* **403**, 632–644 (2024).

160. Carvalho, T. Personalized anti-cancer vaccine combining mRNA and immunotherapy tested in melanoma trial. *Nat Med* **29**, 2379–2380 (2023).

161. Briukhovetska, D. *et al.* Interleukins in cancer: from biology to therapy. *Nat Rev Cancer* **21**, 481–499 (2021).

162. Thayer, A. Interleukin-2 wins FDA market clearance. *Chemical & Engineering News Archive* **70**, 5 (1992).

163. Kirkwood, J. M. *et al.* Interferon alfa-2b adjuvant therapy of high-risk resected cutaneous melanoma: the Eastern Cooperative Oncology Group Trial EST 1684. *Journal of Clinical Oncology* **14**, 7–17 (1996).

164. Hewitt, S. L. *et al.* Durable anticancer immunity from intratumoral administration of IL-23, IL-36γ, and OX40L mRNAs. *Sci Transl Med* **11**, 9143 (2019).

165. Thi, T. T. H. *et al.* Lipid-Based Nanoparticles in the Clinic and Clinical Trials: From Cancer Nanomedicine to COVID-19 Vaccines. *Vaccines (Basel)* **9**, 359 (2021).

166. Olson, D. *et al.* 767 Safety and preliminary efficacy of mRNA-2752, a lipid nanoparticle encapsulating mRNAs encoding human OX40L/IL-23/IL-36γ for intratumoral (ITu) injection, and durvalumab (IV) in TNBC, HNSCC, and melanoma. in *Regular and Young Investigator Award Abstracts* vol. 10 A797–A797 (BMJ Publishing Group Ltd, 2022).

167. Dose Escalation and Efficacy Study of mRNA-2416 for Intratumoral Injection Alone and in Combination With Durvalumab for Participants With Advanced Malignancies. *ClinicalTrials.gov* https://www.clinicaltrials.gov/study/NCT03323398 (2022) NCT03323398.

168. Weinberg, R. A. Tumor Suppressor Genes. *New Series* **22**, 1138–1146 (1991).

169. Kong, N. *et al.* Synthetic mRNA nanoparticle-mediated restoration of p53 tumor suppressor sensitizes p53-deficient cancers to mTOR inhibition. *Sci Transl Med* **11**, 1565 (2019).

170. Islam, M. A. *et al.* Restoration of tumour-growth suppression in vivo via systemic nanoparticle-mediated delivery of PTEN mRNA. *Nat Biomed Eng* **2**, 850–864 (2018).

171. Lin, Y. X. *et al.* Reactivation of the tumor suppressor PTEN by mRNA nanoparticles enhances antitumor immunity in preclinical models. *Sci Transl Med* **13**, 9772 (2021).

172. Pirollo, K. F. *et al.* Safety and efficacy in advanced solid tumors of a targeted nanocomplex carrying the p53 gene used in combination with docetaxel: A phase 1b study. *Molecular Therapy* **24**, 1697–1706 (2016).

173. Munir, M. U. Nanomedicine Penetration to Tumor: Challenges, and Advanced Strategies to Tackle This Issue. (2022) doi:10.3390/cancers14122904.

174. Li, S. *et al.* Payload distribution and capacity of mRNA lipid nanoparticles. *Nat Commun* **13**, 5561 (2022).

175. Carrasco, M. J. *et al.* Ionization and structural properties of mRNA lipid nanoparticles influence expression in intramuscular and intravascular administration. *Commun Biol* **4**, 956 (2021).

176. Arteta, M. Y. *et al.* Successful reprogramming of cellular protein production through mRNA delivered by functionalized lipid nanoparticles. *Proc Natl Acad Sci U S A* **115**, E3351–E3360 (2018).

177. Stephenson, M. L. & Zamecnik, P. C. Inhibition of Rous sarcoma viral RNA translation by a specific oligodeoxyribonucleotide. *Proceedings of the National Academy of Sciences* **75**, 285–288 (1978).

178. Zamecnik, P. C. & Stephenson, M. L. Inhibition of Rous sarcoma virus replication and cell transformation by a specific oligodeoxynucleotide. *Proc Natl Acad Sci U S A* **75**, 280–284 (1978).

179. Rinaldi, C. & A Wood, M. J. Antisense oligonucleotides: the next frontier for treatment of neurological disorders. *Nature Publishing Group* (2017) doi:10.1038/nrneurol.2017.148.

180. Baker, B. F. *et al.* 2′-O-(2-Methoxy)ethyl-modified Anti-intercellular Adhesion Molecule 1 (ICAM-1) Oligonucleotides Selectively Increase the ICAM-1 mRNA Level and Inhibit Formation of the ICAM-1 Translation Initiation Complex in Human Umbilical Vein Endothelial Cells. *Journal of Biological Chemistry* **272**, 11994–12000 (1997).

181. Lauffer, M. C., van Roon-Mom, W. & Aartsma-Rus, A. Possibilities and limitations of antisense oligonucleotide therapies for the treatment of monogenic disorders. *Communications Medicine* **4**, 6 (2024).

182. Wu, H. *et al.* Determination of the Role of the Human RNase H1 in the Pharmacology of DNA-like Antisense Drugs. *Journal of Biological Chemistry* **279**, 17181–17189 (2004).

183. Dominski, Z. & Kole, R. *Restoration of Correct Splicing in Thalassemic Pre-MRNA by Antisense Oligonucleotides*. *Proc. Natl.' Acad. Sci. USA* vol. 90 https://www.pnas.org (1993).

184. Sud, R., Geller, E. T. & Schellenberg, G. D. Antisense-mediated exon skipping decreases Tau protein expression: A potential therapy for tauopathies. *Mol Ther Nucleic Acids* **3**, (2014).

185. Geary, R. S. Antisense oligonucleotide pharmacokinetics and metabolism. *Expert Opin Drug Metab Toxicol* **5**, 381–391 (2009).

186. Yu, R. Z., Grundy, J. S. & Geary, R. S. Clinical pharmacokinetics of second generation antisense oligonucleotides. *Expert Opin Drug Metab Toxicol* **9**, 169–182 (2013).

187. AMANTANA, A. & IVERSEN, P. Pharmacokinetics and biodistribution of phosphorodiamidate morpholino antisense oligomers. *Curr Opin Pharmacol* **5**, 550–555 (2005).

188. Hung, G. *et al.* Characterization of Target mRNA Reduction Through *In Situ* RNA Hybridization in Multiple Organ Systems Following Systemic Antisense Treatment in Animals. *Nucleic Acid Ther* **23**, 369–378 (2013).

189. Yu, R. Z. *et al.* Cross-species comparison of in vivo PK/PD relationships for second-generation antisense oligonucleotides targeting apolipoprotein B-100. *Biochem Pharmacol* 77, 910–919 (2009).

190. Zhang, H. *et al.* Reduction of liver Fas expression by an antisense oligonucleotide protects mice from fulminant hepatitis. *Nat Biotechnol* **18**, 862–867 (2000).

191. Phillips, J. A. *et al.* Pharmacokinetics, Metabolism, and Elimination of a 20-mer Phosphorothioate Oligodeoxynucleotide (CGP 69846A) after Intravenous and Subcutaneous Administration. *Biochem Pharmacol* **54**, 657–668 (1997).

192. Smith, R. A. *et al.* Antisense oligonucleotide therapy for neurodegenerative disease. *J Clin Invest* **116**, (2006).

193. Kordasiewicz, H. B. *et al.* Sustained Therapeutic Reversal of Huntington's Disease by Transient Repression of Huntingtin Synthesis. *Neuron* **74**, 1031–1044 (2012).

194. Butler, M., Stecker, K. & Bennett, C. F. Cellular distribution of phosphorothioate oligodeoxynucleotides in normal rodent tissues. *Lab Invest* 77, 379–88 (1997).

195. Benimetskaya, L. *et al.* Mac-1 (CD11b/CD18) is an oligodeoxynucleotide-binding protein. *Nat Med* **3**, 414–420 (1997).

196. Lorenz, P., Misteli, T., Baker, B. F., Bennett, C. F. & Spector, D. L. *Nucleocytoplasmic Shuttling: A Novel in Vivo Property of Antisense Phosphorothioate Oligodeoxynucleotides. Nucleic Acids Research* vol. 28 (2000).

197. de Smet, M. D., Meenken, C. & van den Horn, G. J. Fomivirsen – a phosphorothioate oligonucleotide for the treatment of CMV retinitis. *Ocul Immunol Inflamm* 7, 189–198 (1999).

198. Kulkarni, J. A. *et al.* The current landscape of nucleic acid therapeutics. *Nat Nanotechnol* **16**, 630–643 (2021).

199. van Roon-Mom, W., Ferguson, C. & Aartsma-Rus, A. From Failure to Meet the Clinical Endpoint to U.S. Food and Drug Administration Approval: 15th Antisense Oligonucleotide Therapy Approved Qalsody (Tofersen) for Treatment of SOD1 Mutated Amyotrophic Lateral Sclerosis. *Nucleic Acid Ther* **33**, 234–237 (2023).

200. European Medicines Agency. Refusal of the marketing authorisation for Exondys (eteplirsen). https://www.ema.europa.eu/en/documents/smop-initial/questions-and-answers-refusal-marketing-authorisation-exondys-eteplirsen-outcome-re-examination_en.pdf (2018).

201. European Medicines Agency. Public summary of opinion on orphan designation: Viltolarsen for the treatment of Duchenne muscular dystrophy. https://www.ema.europa.eu/en/documents/orphan-designation/eu3202282-public-summary-opinion-orphan-designation-viltolarsen-treatment-duchenne-muscular-dystrophy_en.pdf (2020).

202. Study to Assess the Safety, Tolerability, and Efficacy of Viltolarsen in Ambulant and Non-Ambulant Boys With DMD (Galactic53). *ClinicalTrials.gov* https://www.clinicaltrials.gov/study/NCT04956289 (2023) NCT04956289.

203. Study to Assess the Safety and Efficacy of Viltolarsen in Ambulant Boys With DMD (RACER53-X). *ClinicalTrials.gov* https://www.clinicaltrials.gov/study/NCT04768062 (2024) NCT04768062.

204. AstraZeneca PLC. Wainua (eplontersen) granted first-ever regulatory approval in the US for the treatment of adults with polyneuropathy of hereditary transthyretin-mediated amyloidosis. https://www.astrazeneca.com/media-centre/press-releases/2023/wainua-eplontersen-granted-first-ever-regulatory-approval-us-treatment-of-adults-with-polyneuropathy-hereditary-transthyretin-mediated-amyloidosis.html (2023).

205. Miller, T. M. *et al.* Trial of Antisense Oligonucleotide Tofersen for SOD1 ALS. *New England Journal of Medicine* **387**, 1099–1110 (2022).

206. Kim, J. *et al.* Patient-Customized Oligonucleotide Therapy for a Rare Genetic Disease. *New England Journal of Medicine* **381**, 1644–1652 (2019).

207. Aartsma-Rus, A. *et al.* Development of tailored splice-switching oligonucleotides for progressive brain disorders in Europe: development, regulation, and implementation considerations. (2023) doi:10.1261/rna.

208. Jinek, M. *et al.* A programmable dual-RNA-guided DNA endonuclease in adaptive bacterial immunity. *Science (1979)* **337**, 816–821 (2012).

209. Mali, P. *et al.* RNA-guided human genome engineering via Cas9. *Science (1979)* **339**, 823–826 (2013).

210. Cong, L. *et al.* Multiplex Genome Engineering Using CRISPR/Cas Systems. *Science (1979)* **339**, 819–823 (2013).

211. Adli, M. The CRISPR tool kit for genome editing and beyond. *Nat Commun* **9**, 1911 (2018).

212. Shalem, O., Sanjana, N. E. & Zhang, F. High-throughput functional genomics using CRISPR–Cas9. *Nature Publishing Group* (2015) doi:10.1038/nrg3899.

213. Dominguez, A. A., Lim, W. A. & Qi, L. S. Beyond editing: repurposing CRISPR-Cas9 for precision genome regulation and interrogation. *Nature Publishing Group* **17**, (2015).

214. Pickar-Oliver, A. & Gersbach, C. A. The next generation of CRISPR–Cas technologies and applications. *Nat Rev Mol Cell Biol* doi:10.1038/s41580-019-0131-5.

215. Makarova, K. S. *et al.* Evolutionary classification of CRISPR–Cas systems: a burst of class 2 and derived variants. *Nat Rev Microbiol* doi:10.1038/s41579-019-0299-x.

216. Hille, F. *et al.* The Biology of CRISPR-Cas: Backward and Forward. *Cell* **172**, 1239–1259 (2018).

217. Jiang, F. & Doudna, J. A. CRISPR-Cas9 Structures and Mechanisms. *Annu Rev Biophys* **46**, 505–529 (2017).

218. Sternberg, S. H., LaFrance, B., Kaplan, M. & Doudna, J. A. Conformational control of DNA target cleavage by CRISPR–Cas9. *Nature* **527**, 110–113 (2015).

219. Yeh, C. D., Richardson, C. D. & Corn, J. E. Advances in genome editing through control of DNA repair pathways. *Nat Cell Biol* **21**, 1468–1478 (2019).

220. Lieber, M. R. The Mechanism of Double-Strand DNA Break Repair by the Nonhomologous DNA End-Joining Pathway. *Annu Rev Biochem* **79**, 181–211 (2010).

221. Heyer, W.-D., Ehmsen, K. T. & Liu, J. Regulation of homologous recombination in eukaryotes. *Annu Rev Genet* **44**, 113–139 (2010).

222. Jasin, M. & Rothstein, R. Repair of Strand Breaks by Homologous Recombination. *Cold Spring Harb Perspect Biol* **5**, a012740–a012740 (2013).

223. Komor, A. C., Kim, B., Packer, M. S., Zuris, J. A. & Liu, D. R. Programmable editing of a target base in genomic DNA without double-stranded DNA cleavage. *Nature* **533**, (2016).

224. Gaudelli, N. M. *et al.* Programmable base editing of A•T to G•C in genomic DNA without DNA cleavage. *Nature* **551**, 464–471 (2017).

225. Anzalone, A. V *et al.* Search-and-replace genome editing without double-strand breaks or donor DNA. *Nature* **576**, 149 (2019).

226. Anzalone, A. V., Koblan, L. W. & Liu, D. R. Genome editing with CRISPR–Cas nucleases, base editors, transposases and prime editors. *Nat Biotechnol* **38**, 824–844 (2020).

227. Klompe, S. E., Vo, P. L. H., Halpin-Healy, T. S. & Sternberg, S. H. Transposon-encoded CRISPR–Cas systems direct RNA-guided DNA integration. *Nature* **571**, 219–225 (2019).

228. Lampe, G. D. *et al.* Targeted DNA integration in human cells without double-strand breaks using CRISPR-associated transposases. *Nat Biotechnol* **42**, 87–98 (2024).

229. Chaikind, B., Bessen, J. L., Thompson, D. B., Hu, J. H. & Liu, D. R. A programmable Cas9-serine recombinase fusion protein that operates on DNA sequences in mammalian cells. *Nucleic Acids Res* **44**, 9758–9770 (2016).

230. U.S. Food & Drug Administration. FDA Approves First Gene Therapies to Treat Patients with Sickle Cell Disease. https://www.fda.gov/news-events/press-announcements/fda-approves-first-gene-therapies-treat-patients-sickle-cell-disease (2023).

231. Liu, N. *et al.* Direct Promoter Repression by BCL11A Controls the Fetal to Adult Hemoglobin Switch. *Cell* **173**, 430-442.e17 (2018).

232. Sheridan, C. The world's first CRISPR therapy is approved: who will receive it? *Nature Biotechnology* vol. 42 3–4 Preprint at https://doi.org/10.1038/d41587-023-00016-6 (2024).

233. Chiesa, R. *et al.* Base-Edited CAR7 T Cells for Relapsed T-Cell Acute Lymphoblastic Leukemia. *New England Journal of Medicine* **389**, 899–910 (2023).

234. Ka, T., Horie, H. & Ono, K. VERVE-101: a promising CRISPR-based gene editing t hera py t hat reduces LDL-C a nd PCSK9 levels in HeFH patients. *European Heart Journal-Cardiovascular Pharmacotherapy* **10**, 89–90 (2024).

235. Verve Therapeutics, I. Verve Therapeutics Announces Interim Data for VERVE-101 Demonstrating First Human Proof-of-Concept for In Vivo Base Editing with Dose-Dependent Reductions in LDL-C and Blood PCSK9 Protein in Patients with Heterozygous Familial Hypercholesterolemia. https://vervetx.gcs-web.com/news-releases/news-release-details/verve-therapeutics-announces-interim-data-verve-101/ (2023).

236. Katti, A., Diaz, B. J., Caragine, C. M., Sanjana, N. E. & Dow, L. E. CRISPR in cancer biology and therapy. *Nat Rev Cancer* **22**, 259–279 (2022).

237. Parfrey, L. W., Lahr, D. J. G., Knoll, A. H. & Katz, L. A. Estimating the timing of early eukaryotic diversification with multigene molecular clocks. *Proc Natl Acad Sci U S A* **108**, 13624–13629 (2011).

238. Koumandou, V. L. *et al.* Molecular paleontology and complexity in the last eukaryotic common ancestor. *Crit Rev Biochem Mol Biol* **48**, 373–396 (2013).

239. Gould, S. B., Garg, S. G. & Martin, W. F. Bacterial Vesicle Secretion and the Evolutionary Origin of the Eukaryotic Endomembrane System. *Trends Microbiol* **24**, (2016).

240. Alberts, B. *et al.* The Compartmentalization of Cells. in *Molecular Biology of the Cell* (Garland Science, New York, 2002).

241. Alberts, B. *et al.* The Lipid Bilayer. in *Molecular Biology of the Cell* (Garland Science, New York, 2002).

242. Harayama, T. & Riezman, H. Understanding the diversity of membrane lipid composition. *Nat Rev Mol Cell Biol* **19**, 281–296 (2018).

243. Huotari, J. & Helenius, A. Endosome maturation. *EMBO Journal* **30**, 3481–3500 (2011).

244. Steinman, R. M., Mellman, I. S., Muller, W. A. & Cohn, Z. A. Endocytosis and the recycling of plasma membrane. *J Cell Biol* **96**, 1–27 (1983).

245. Bitsikas, V., Corrêa, I. R. & Nichols, B. J. Clathrin-independent pathways do not contribute significantly to endocytic flux. *Elife* **2014**, 1–26 (2014).

246. Traub, L. M. Regarding the Amazing Choreography of Clathrin Coats. *PLoS Biol* **9**, e1001037 (2011).

247. Traub, L. M. Tickets to ride: selecting cargo for clathrin-regulated internalization. *Nat Rev Mol Cell Biol* **10**, 583–596 (2009).

248. Banushi, B., Joseph, S. R., Lum, B., Lee, J. J. & Simpson, F. Endocytosis in cancer and cancer therapy. *Nat Rev Cancer* **23**, 450–473 (2023).

249. Traub, L. M. & Bonifacino, J. S. Cargo Recognition in Clathrin-Mediated Endocytosis. *Cold Spring Harb Perspect Biol* **5**, a016790–a016790 (2013).

250. Kaksonen, M. & Roux, A. Mechanisms of clathrin-mediated endocytosis. *Nature Publishing Group* **19**, (2018).

251. Ferreira, A. P. A. & Boucrot, E. Mechanisms of Carrier Formation during Clathrin-Independent Endocytosis. *Trends Cell Biol* **28**, 188–200 (2018).

252. Parton, R. G. & Simons, K. The multiple faces of caveolae. *Nat Rev Mol Cell Biol* **8**, 185–194 (2007).

253. Lamaze, C. *et al.* Interleukin 2 Receptors and Detergent-Resistant Membrane Domains Define a Clathrin-Independent Endocytic Pathway. *Mol Cell* **7**, 661–671 (2001).

254. Boucrot, E. *et al.* Endophilin marks and controls a clathrin-independent endocytic pathway. *Nature* (2014) doi:10.1038/nature14067.

255. Mayor, S. & Pagano, R. E. Pathways of clathrin-independent endocytosis. *Nat Rev Mol Cell Biol* **8**, 603–612 (2007).

256. Sabharanjak, S., Sharma, P., Parton, R. G. & Mayor, S. GPI-Anchored Proteins Are Delivered to Recycling Endosomes via a Distinct cdc42-Regulated, Clathrin-Independent Pinocytic Pathway. *Dev Cell* **2**, 411–423 (2002).

257. Johannes, L., Wunder, C. & Shafaq-Zadah, M. Glycolipids and Lectins in Endocytic Uptake Processes. *J Mol Biol* **428**, 4792–4818 (2016).

258. Lakshminarayan, R. *et al.* Galectin-3 drives glycosphingolipid-dependent biogenesis of clathrin-independent carriers. *Nat Cell Biol* **16**, 592–603 (2014).

259. Meister, M. & Tikkanen, R. Endocytic trafficking of membrane-bound cargo: A flotillin point of view. *Membranes (Basel)* **4**, 356–371 (2014).

260. Torgersen, M. L., Skretting, G., van Deurs, B. & Sandvig, K. Internalization of cholera toxin by different endocytic mechanisms. *J Cell Sci* **114**, 3737–3747 (2001).

261. Mercer, J. & Helenius, A. Gulping rather than sipping: macropinocytosis as a way of virus entry. *Curr Opin Microbiol* **15**, 490–499 (2012).

262. Maxfield, F. R. & McGraw, T. E. Endocytic recycling. *Nat Rev Mol Cell Biol* **5**, 121–132 (2004).

263. Zerial, M. & McBride, H. Rab proteins as membrane organizers. *Nat Rev Mol Cell Biol* **2**, 107–117 (2001).

264. Grant, B. D. & Donaldson, J. G. Pathways and mechanisms of endocytic recycling. *Nat Rev Mol Cell Biol* **10**, 597–608 (2009).

265. Hurley, J. H. & Emr, S. D. THE ESCRT COMPLEXES: Structure and Mechanism of a Membrane-Trafficking Network. *Annu Rev Biophys Biomol Struct* **35**, 277–298 (2006).

266. Bonifacino, J. S. & Hurley, J. H. Retromer. *Curr Opin Cell Biol* **20**, 427–436 (2008).

267. Rink, J., Ghigo, E., Kalaidzidis, Y. & Zerial, M. Rab Conversion as a Mechanism of Progression from Early to Late Endosomes. *Cell* **122**, 735–749 (2005).

268. Gruenberg, J. & Stenmark, H. The biogenesis of multivesicular endosomes. *Nat Rev Mol Cell Biol* **5**, 317–323 (2004).

269. Bucci, C., Thomsen, P., Nicoziani, P., McCarthy, J. & van Deurs, B. *Rab7: A Key to Lysosome Biogenesis V. Molecular Biology of the Cell* vol. 11 www.molbiolcell.org. (2000).

270. Luzio, J. P., Pryor, P. R. & Bright, N. A. Lysosomes: fusion and function. *Nat Rev Mol Cell Biol* **8**, 622–632 (2007).

271. Saftig, P. & Klumperman, J. Lysosome biogenesis and lysosomal membrane proteins: trafficking meets function. *Nat Rev Mol Cell Biol* **10**, 623–635 (2009).

272. Hawkins, H. K., Ericsson, J. L., Biberfeld, P. & Trump, B. F. Lysosome and phagosome stability in lethal cell injury. Morphologic tracer studies in cell injury due to inhibition of energy metabolism, immune cytolysis and photosensitization. *Am J Pathol* **68**, 255–8 (1972).

273. Stoka, V., Turk, V. & Turk, B. Lysosomal cathepsins and their regulation in aging and neurodegeneration. *Ageing Res Rev* **32**, 22–37 (2016).

274. Wang, F., Gómez-Sintes, R. & Boya, P. Lysosomal membrane permeabilization and cell death. (2018) doi:10.1111/tra.12613.

275. Al-Hashimi, A. *et al.* Significance of nuclear cathepsin V in normal thyroid epithelial and carcinoma cells ☆. (2020) doi:10.1016/j.bbamcr.2020.118846.

276. Goulet, B. *et al.* Increased Expression and Activity of Nuclear Cathepsin L in Cancer Cells Suggests a Novel Mechanism of Cell Transformation. *Mol Cancer Res* **5**, 899–907 (2007).

277. Reinheckel, T. & Tholen, M. Low-level lysosomal membrane permeabilization for limited release and sublethal functions of cathepsin proteases in the cytosol and nucleus. *FEBS Open Bio* **12**, 694–707 (2022).

278. Hämälistö, S. *et al.* Spatially and temporally defined lysosomal leakage facilitates mitotic chromosome segregation. *Nat Commun* **11**, 229 (2020).

279. Maxson, M. E. & Grinstein, S. The vacuolar-type H+-ATPase at a glance – more than a proton pump. *J Cell Sci* **127**, 4987–4993 (2014).

280. Scheel, O., Zdebik, A. A., Lourdel, S. & Jentsch, T. J. Voltage-dependent electrogenic chloride/proton exchange by endosomal CLC proteins. *Nature* **436**, 424–427 (2005).

281. Scott, C. C. & Gruenberg, J. Ion flux and the function of endosomes and lysosomes: pH is just the start. *BioEssays* **33**, 103–110 (2011).

282. Maxfield, F. R. & Yamashiro, D. J. Endosome Acidification and the Pathways of Receptor-Mediated Endocytosis. in *Advances in experimental medicine and biology* vol. 225 189–198 (1987).

283. Hu, Y. B., Dammer, E. B., Ren, R. J. & Wang, G. The endosomal-lysosomal system: From acidification and cargo sorting to neurodegeneration. *Transl Neurodegener* **4**, 1–10 (2015).

284. Schwartz, S. L., Cao, C., Pylypenko, O., Rak, A. & Wandinger-Ness, A. Rab GTPases at a glance. *J Cell Sci* **121**, 246 (2008).

285. Stenmark, H. Rab GTPases as coordinators of vesicle traffic. *Nat Rev Mol Cell Biol* **10**, 513–525 (2009).

286. van der Beek, J., Jonker, C., van der Welle, R., Liv, N. & Klumperman, J. CORVET, CHEVI and HOPS – Multisubunit tethers of the endo-lysosomal system in health and disease. *Journal of Cell Science* vol. 132 Preprint at https://doi.org/10.1242/jcs.189134 (2019).

287. Vicinanza, M., D'Angelo, G., Di Campli, A. & De Matteis, M. A. Function and dysfunction of the PI system in membrane trafficking. *EMBO Journal* **27**, 2457–2470 (2008).

288. Christoforidis, S. *et al.* Phosphatidylinositol-3-OH kinases are Rab5 effectors. *Nat Cell Biol* **1**, 249–252 (1999).

289. Ikonomov, O. C., Sbrissa, D. & Shisheva, A. Mammalian Cell Morphology and Endocytic Membrane Homeostasis Require Enzymatically Active Phosphoinositide 5-Kinase PIKfyve. *Journal of Biological Chemistry* **276**, 26141–26147 (2001).

290. Murray, J. W., Bananis, E. & Wolkoff, A. W. Reconstitution of ATP-dependent Movement of Endocytic Vesicles Along Microtubules In Vitro: An Oscillatory Bidirectional Process. *Mol Biol Cell* **11**, 419–433 (2000).

291. Soppina, V., Rai, A. K., Ramaiya, A. J., Barak, P. & Mallik, R. Tug-of-war between dissimilar teams of microtubule motors regulates transport and fission of endosomes. *Proceedings of the National Academy of Sciences* **106**, 19381–19386 (2009).

292. Reddy, A., Caler, E. V & Andrews, N. W. Plasma Membrane Repair Is Mediated by Ca 2-Regulated Exocytosis of Lysosomes ation efficiently deliver macromolecules into the cytosol of cells through reversible plasma membrane disrup-tions (McNeil et al. *Cell* **106**, 157–169 (2001).

293. Idone, V. *et al.* Repair of injured plasma membrane by rapid Ca2+-dependent endocytosis. *J Cell Biol* **180**, 905–914 (2008).

294. Taguchi, T. Emerging roles of recycling endosomes. *J Biochem* **153**, 505–510 (2013).

295. Medina, D. L. *et al.* Transcriptional Activation of Lysosomal Exocytosis Promotes Cellular Clearance. *Dev Cell* **21**, 421–430 (2011).

296. Kalluri, R. & LeBleu, V. S. The biology, function, and biomedical applications of exosomes. *Science (1979)* **367**, (2020).

297. Lim, K.-H. & Staudt, L. M. Toll-Like Receptor Signaling. *Cold Spring Harb Perspect Biol* **5**, a011247–a011247 (2013).

298. Gruenberg, J. & van der Goot, F. G. Mechanisms of pathogen entry through the endosomal compartments. *Nat Rev Mol Cell Biol* **7**, 495–504 (2006).

299. Inpanathan, S. & Botelho, R. J. The Lysosome Signaling Platform: Adapting With the Times. *Front Cell Dev Biol* **7**, (2019).

300. Liu, G. Y. & Sabatini, D. M. mTOR at the nexus of nutrition, growth, ageing and disease. *Nat Rev Mol Cell Biol* **21**, 183–203 (2020).

301. Sarett, S. M. *et al.* Lipophilic siRNA targets albumin in situ and promotes bioavailability, tumor penetration, and carrier-free gene silencing. *Proc Natl Acad Sci U S A* **114**, E6490–E6497 (2017).

302. Hou, X., Zaks, T., Langer, R. & Dong, Y. Lipid nanoparticles for mRNA delivery. *Nat Rev Mater* **6**, 1078–1094 (2021).

303. Zhang, Y.-N., Poon, W., Tavares, A. J., McGilvray, I. D. & Chan, W. C. W. Nanoparticle–liver interactions: Cellular uptake and hepatobiliary elimination. *Journal of Controlled Release* **240**, 332–348 (2016).

304. Kim, J., Eygeris, Y., Ryals, R. C., Jozić, A. & Sahay, G. Strategies for non-viral vectors targeting organs beyond the liver. *Nat Nanotechnol* (2023) doi:10.1038/s41565-023-01563-4.

305. Wu, D. *et al.* The blood-brain barrier: structure, regulation, and drug delivery. doi:10.1038/s41392-023-01481-w.

306. Hansen, A. E. *et al.* Positron Emission Tomography Based Elucidation of the Enhanced Permeability and Retention Effect in Dogs with Cancer Using Copper-64 Liposomes. *ACS Nano* **9**, 6985–6995 (2015).

307. Wilhelm, S. *et al.* Analysis of nanoparticle delivery to tumours. *Nat Rev Mater* **1**, 16014 (2016).

308. Goula, D. *et al. Polyethylenimine-Based Intravenous Delivery of Transgenes to Mouse Lung. Gene Therapy* vol. 5 http://www.stockton-press.co.uk/gt (1998).

309. Zhong, R. *et al.* Hydrogels for RNA delivery. *Nat Mater* **22**, 818–831 (2023).

310. Patel, A. K. *et al.* Inhaled Nanoformulated mRNA Polyplexes for Protein Production in Lung Epithelium. *Advanced Materials* **31**, (2019).

311. Katrin Herrmann, I., John Andrew Wood, M. & Fuhrmann, G. Extracellular vesicles as a next-generation drug delivery platform. doi:10.1038/s41565-021-00931-2.

312. Banskota, S. *et al.* Engineered virus-like particles for efficient in vivo delivery of therapeutic proteins. *Cell* **185**, 250-265.e16 (2022).

313. Kowalski, P. S., Rudra, A., Miao, L. & Anderson, D. G. Delivering the Messenger: Advances in Technologies for Therapeutic mRNA Delivery. *Molecular Therapy* **27**, 710–728 (2019).

314. Kormann, M. S. D. *et al.* Expression of therapeutic proteins after delivery of chemically modified mRNA in mice. *Nat Biotechnol* **29**, 154–157 (2011).

315. Heyes, J., Palmer, L., Bremner, K. & MacLachlan, I. Cationic lipid saturation influences intracellular delivery of encapsulated nucleic acids. *Journal of Controlled Release* **107**, 276–287 (2005).

316. Semple, S. C. *et al.* Rational design of cationic lipids for siRNA delivery. *Nat Biotechnol* **28**, 172–176 (2010).

317. Jayaraman, M. *et al.* Maximizing the potency of siRNA lipid nanoparticles for hepatic gene silencing in vivo. *Angewandte Chemie - International Edition* **51**, 8529–8533 (2012).

318. Akinc, A. *et al.* The Onpattro story and the clinical translation of nanomedicines containing nucleic acid-based drugs. *Nat Nanotechnol* **14**, 1084–1087 (2019).

319. Hassett, K. J. *et al.* Optimization of Lipid Nanoparticles for Intramuscular Administration of mRNA Vaccines. *Mol Ther Nucleic Acids* **15**, 1–11 (2019).

320. Steven M. Ansell & Xinyao Du. Lipids and lipid nanoparticle formulations for delivery of nucleic acids. (2019).

321. Kim, J., Eygeris, Y., Gupta, M. & Sahay, G. Self-assembled mRNA vaccines. *Adv Drug Deliv Rev* **170**, 83–112 (2021).

322. Koltover, I., Salditt, T., Rädler, J. O. & Safinya, C. R. An Inverted Hexagonal Phase of Cationic Liposome-DNA Complexes Related to DNA Release and Delivery. *Science (1979)* **281**, 78–81 (1998).

323. Patel, S. *et al.* Naturally-occurring cholesterol analogues in lipid nanoparticles induce polymorphic shape and enhance intracellular delivery of mRNA. *Nat Commun* **11**, 983 (2020).

324. Eygeris, Y., Patel, S., Jozic, A., Sahay, G. & Sahay, G. Deconvoluting Lipid Nanoparticle Structure for Messenger RNA Delivery. *Nano Lett* **20**, 4543–4549 (2020).

325. Klibanov, A. L., Maruyama, K., Torchilin, V. P. & Huang, L. Amphipathic polyethyleneglycols effectively prolong the circulation time of liposomes. *FEBS Lett* **268**, 235–237 (1990).

326. Knop, K., Hoogenboom, R., Fischer, D. & Schubert, U. S. Poly(ethylene glycol) in Drug Delivery: Pros and Cons as Well as Potential Alternatives. *Angewandte Chemie International Edition* **49**, 6288–6308 (2010).

327. Schober, G. B., Story, S. & Arya, D. P. A careful look at lipid nanoparticle characterization: analysis of benchmark formulations for encapsulation of RNA cargo size gradient. (123AD) doi:10.1038/s41598-024-52685-1.

328. Hassett, K. J. *et al.* Impact of lipid nanoparticle size on mRNA vaccine immunogenicity. *Journal of Controlled Release* **335**, 237–246 (2021).

329. Cheng, Q. *et al.* Selective organ targeting (SORT) nanoparticles for tissue-specific mRNA delivery and CRISPR–Cas gene editing. *Nature Nanotechnology 2020 15:4* **15**, 313–320 (2020).

330. Dobrowolski, C. *et al.* Nanoparticle single-cell multiomic readouts reveal that cell heterogeneity influences lipid nanoparticle-mediated messenger RNA delivery. *Nat Nanotechnol* **17**, 871–879 (2022).

331. Witten, J., Hu, Y., Langer, R. & Anderson, D. G. Recent advances in nanoparticulate RNA delivery systems. *Proc Natl Acad Sci U S A* **121**, (2024).

332. Sahay, G. *et al.* Efficiency of siRNA delivery by lipid nanoparticles is limited by endocytic recycling. *Nat Biotechnol* **31**, 653–658 (2013).

333. Gilleron, J. *et al.* Image-based analysis of lipid nanoparticle-mediated siRNA delivery, intracellular trafficking and endosomal escape. *Nat Biotechnol* **31**, 638–646 (2013).

334. Wittrup, A. *et al.* Visualizing lipid-formulated siRNA release from endosomes and target gene knockdown. *Nat Biotechnol* **33**, 870–876 (2015).

335. Paramasivam, P. *et al.* Endosomal escape of delivered mRNA from endosomal recycling tubules visualized at the nanoscale. *Journal of Cell Biology* **221**, (2022).

336. Aliakbarinodehi, N. *et al.* Interaction Kinetics of Individual mRNA-Containing Lipid Nanoparticles with an Endosomal Membrane Mimic: Dependence on pH, Protein Corona Formation, and Lipoprotein Depletion. *ACS Nano* **16**, 20163–20173 (2022).

337. Hafez, I. M., Maurer, N. & Cullis, P. R. On the mechanism whereby cationic lipids promote intracellular delivery of polynucleic acids. *Gene Ther* **8**, 1188–1196 (2001).

338. Maugeri, M. *et al.* Linkage between endosomal escape of LNP-mRNA and loading into EVs for transport to other cells. *Nat Commun* **10**, (2019).

339. Maier, M. A. *et al.* Biodegradable Lipids Enabling Rapidly Eliminated Lipid Nanoparticles for Systemic Delivery of RNAi Therapeutics. *Molecular Therapy* **21**, 1570–1578 (2013).

340. Sabnis, S. *et al.* A Novel Amino Lipid Series for mRNA Delivery: Improved Endosomal Escape and Sustained Pharmacology and Safety in Non-human Primates. *Molecular Therapy* **26**, 1509–1519 (2018).

341. Whitehead, K. A. *et al.* Degradable lipid nanoparticles with predictable in vivo siRNA delivery activity. *Nat Commun* **5**, 4277 (2014).

342. Miao, L. *et al.* Synergistic lipid compositions for albumin receptor mediated delivery of mRNA to the liver. *Nat Commun* **11**, 2424 (2020).

343. Hajj, K. A. *et al.* Branched-Tail Lipid Nanoparticles Potently Deliver mRNA In Vivo due to Enhanced Ionization at Endosomal pH. *Small* **15**, (2019).

344. Liu, S. *et al.* Membrane-destabilizing ionizable phospholipids for organ-selective mRNA delivery and CRISPR–Cas gene editing. *Nat Mater* **20**, 701–710 (2021).

345. Lee, S. M. *et al.* A Systematic Study of Unsaturation in Lipid Nanoparticles Leads to Improved mRNA Transfection In Vivo. *Angewandte Chemie International Edition* **60**, 5848–5853 (2021).

346. Kauffman, K. J. *et al.* Optimization of Lipid Nanoparticle Formulations for mRNA Delivery in Vivo with Fractional Factorial and Definitive Screening Designs. *Nano Lett* **15**, 7300–7306 (2015).

347. Li, B. *et al.* An Orthogonal Array Optimization of Lipid-like Nanoparticles for mRNA Delivery in Vivo. *Nano Lett* **15**, 8099–8107 (2015).

348. Hou, X. *et al.* Vitamin lipid nanoparticles enable adoptive macrophage transfer for the treatment of multidrug-resistant bacterial sepsis. *Nat Nanotechnol* **15**, 41–46 (2020).

349. Patel, P., Ibrahim, N. M. & Cheng, K. The Importance of Apparent pKa in the Development of Nanoparticles Encapsulating siRNA and mRNA. *Trends Pharmacol Sci* **42**, 448–460 (2021).

350. Tesei, G. *et al.* Lipid shape and packing are key for optimal design of pH-sensitive mRNA lipid nanoparticles. *Proc Natl Acad Sci U S A* **121**, (2024).

351. Philipp, J. *et al.* pH-dependent structural transitions in cationic ionizable lipid mesophases are critical for lipid nanoparticle function. *Proc Natl Acad Sci U S A* **120**, (2023).

352. Zheng, L., Bandara, S. R., Tan, Z. & Leal, C. Lipid nanoparticle topology regulates endosomal escape and delivery of RNA to the cytoplasm. *Proceedings of the National Academy of Sciences* **120**, (2023).

353. Bilalov, A., Olsson, U. & Lindman, B. Complexation between DNA and surfactants and lipids: Phase behavior and molecular organization. *Soft Matter* vol. 8 11022–11033 Preprint at https://doi.org/10.1039/c2sm26553b (2012).

354. Marrink, S.-J. & Mark, A. E. Molecular View of Hexagonal Phase Formation in Phospholipid Membranes. *Biophys J* **87**, 3894–3900 (2004).

355. Jouhet, J. Importance of the hexagonal lipid phase in biological membrane organization. *Front Plant Sci* **4**, (2013).

356. Perutková, Š. *et al.* Chapter 9 Stability of the Inverted Hexagonal Phase. in *Advances in Planar Lipid Bilayers and Liposomes* vol. 9 237–278 (2009).

357. Cullis, P. R., Hope, M. J. & Tilcock, C. P. S. Lipid polymorphism and the roles of lipids in membranes. *Chem Phys Lipids* **40**, 127–144 (1986).

358. Langmuir, /, Zhang, J., Fan, H., Levorse, D. A. & Crocker, L. S. Ionization Behavior of Amino Lipids for siRNA Delivery: Determination of Ionization Constants, SAR, and the Impact of Lipid pK a on Cationic Lipid-Biomembrane Interactions. *Langmuir* **27**, 1907–1914 (2011).

359. Spadea, A. *et al.* Nucleic Acid-Loaded Lipid Nanoparticle Interactions with Model Endosomal Membranes. *ACS Appl Mater Interfaces* **14**, 30371–30384 (2022).

360. Aliakbarinodehi, N. *et al.* Time Resolved Inspection of Ionizable-Lipid Facilitated Lipid Nanoparticle Disintegration and Cargo Release at an Endosomal Membrane Mimic. *bioRxiv* 2024.02.22.580934 (2024) doi:10.1101/2024.02.22.580934.

361. Thomas, M. *et al.* Ligand-targeted delivery of small interfering RNAs to malignant cells and tissues. in *Annals of the New York Academy of Sciences* vol. 1175 32–39 (Blackwell Publishing Inc., 2009).

362. Lorenz, C., Hadwiger, P., John, M., Vornlocher, H.-P. & Unverzagt, C. Steroid and lipid conjugates of siRNAs to enhance cellular uptake and gene silencing in liver cells. *Bioorg Med Chem Lett* **14**, 4975–4977 (2004).

363. Cesarone, G., Edupuganti, O. P., Chen, C. P. & Wickstrom, E. Insulin receptor substrate 1 knockdown in human MCF7 ER+ breast cancer cells by nuclease-resistant IRS1 siRNA conjugated to a disulfide-bridged D-peptide analogue of insulin-like growth factor 1. *Bioconjug Chem* **18**, 1831–1840 (2007).

364. McNamara, J. O. *et al.* Cell type-specific delivery of siRNAs with aptamer-siRNA chimeras. *Nat Biotechnol* **24**, 1005–1015 (2006).

365. Song, E. *et al.* Antibody mediated in vivo delivery of small interfering RNAs via cell-surface receptors. *Nat Biotechnol* **23**, 709–717 (2005).

366. Coelho, T. *et al.* Eplontersen for Hereditary Transthyretin Amyloidosis With Polyneuropathy. *JAMA* **330**, 1448–1458 (2023).

367. Spiess, M. The asialoglycoprotein receptor: a model for endocytic transport receptors. *Biochemistry* **29**, 10009–10018 (1990).

368. Cummings, R. D. & McEver, R. P. *Essentials of Glycobiology*. vol. Chapter 31 (Cold Spring Harbor Laboratory Press, Cold Spring Harbor (NY), 2009).

369. Brown, C. R. *et al.* Investigating the pharmacodynamic durability of GalNAc–siRNA conjugates. *Nucleic Acids Res* **48**, 11827–11844 (2020).

370. Juliano, R. L. The delivery of therapeutic oligonucleotides. *Nucleic Acids Res* **44**, 6518–6548 (2016).

371. Letsinger, R. L., Zhang, G., Sun, D. K., Ikeuchi, T. & Sarin, P. S. Cholesteryl-conjugated oligonucleotides: Synthesis, properties, and activity as inhibitors of replication of human immunodeficiency virus in cell culture. *Proc Natl Acad Sci U S A* **86**, 6553–6556 (1989).

372. van Meer, G. & de Kroon, A. I. P. M. Lipid map of the mammalian cell. *J Cell Sci* **124**, 5–8 (2011).

373. Razin, S. *Cholesterol Incorporation into Bacterial Membranes*. *JOURNAL OF BACTERIOLOGY* https://journals.asm.org/journal/jb (1975).

374. Ly, S. *et al.* Visualization of self-delivering hydrophobically modified siRNA cellular internalization. *Nucleic Acids Res* **45**, 15–25 (2016).

375. Wolfrum, C. *et al.* Mechanisms and optimization of in vivo delivery of lipophilic siRNAs. *Nat Biotechnol* **25**, 1149–1157 (2007).

376. Goldstein, J. L., Brown, M. S., Anderson, R. G. W., Russell, D. W. & Schneider, W. J. Receptor-Mediated Endocytosis: Concepts Emerging from the LDL Receptor System. *Annu Rev Cell Biol* **1**, 1–39 (1985).

377. Gaibelet, G. *et al.* Specific Cellular Incorporation of a Pyrene-Labelled Cholesterol: Lipoprotein-Mediated Delivery toward Ordered Intracellular Membranes. *Ordered Intracellular Membranes. PLoS ONE* **10**, 121563 (2015).

378. Chernikov, I. V., Vlassov, V. V. & Chernolovskaya, E. L. Current Development of siRNA Bioconjugates: From Research to the Clinic. *Front Pharmacol* **10**, 444 (2019).

379. Gilleron, J. *et al.* Identification of siRNA delivery enhancers by a chemical library screen. *Nucleic Acids Res* **43**, 7984–8001 (2015).

380. Merrill, N. J. *et al.* Human cerebrospinal fluid contains diverse lipoprotein subspecies enriched in proteins implicated in central nervous system health. *Sci Adv* **9**, (2023).

381. Yoon, J. H. *et al.* Brain lipidomics: From functional landscape to clinical significance. *Sci Adv* **8**, 9317 (2022).

382. Byrne, M. *et al.* Novel hydrophobically modified asymmetric RNAi compounds (sd-rxRNA) demonstrate robust efficacy in the eye. *Journal of Ocular Pharmacology and Therapeutics* **29**, 855–864 (2013).

383. Hickerson, R. P. *et al.* Gene silencing in skin after deposition of self-delivery siRNA with a motorized microneedle array device. *Mol Ther Nucleic Acids* **2**, e129 (2013).

384. DiFiglia, M. *et al.* Therapeutic silencing of mutant huntingtin with siRNA attenuates striatal and cortical neuropathology and behavioral deficits. *Proc Natl Acad Sci U S A* **104**, 17204–17209 (2007).

385. Soutschek, J. *et al.* Therapeutic silencing of an endogenous gene by systemic administration of modified siRNAs. *Nature* **432**, 173–178 (2004).

386. Biscans, A. *et al.* Diverse lipid conjugates for functional extra-hepatic siRNA delivery in vivo. *Nucleic Acids Res* **47**, 1082–1096 (2019).

387. Osborn, M. F. & Khvorova, A. Improving siRNA Delivery in Vivo Through Lipid Conjugation. *Nucleic Acid Ther* **28**, 128–136 (2018).

388. Biscans, A., Ly, S., McHugh, N., Cooper, D. A. & Khvorova, A. Engineered ionizable lipid siRNA conjugates enhance endosomal escape but induce toxicity in vivo. *Journal of Controlled Release* **349**, 831–843 (2022).

389. Godinho, B. M. D. C. *et al.* Transvascular Delivery of Hydrophobically Modified siRNAs: Gene Silencing in the Rat Brain upon Disruption of the Blood-Brain Barrier. *Molecular Therapy* **26**, 2580–2591 (2018).

390. Nikan, M. *et al.* Docosahexaenoic Acid Conjugation Enhances Distribution and Safety of siRNA upon Local Administration in Mouse Brain. *Mol Ther Nucleic Acids* **5**, e344 (2016).

391. Davis, S. M. *et al.* Chemical optimization of siRNA for safe and efficient silencing of placental sFLT1. *Mol Ther Nucleic Acids* **29**, 135–149 (2022).

392. Nikan, M. *et al.* Synthesis and Evaluation of Parenchymal Retention and Efficacy of a Metabolically Stable O-Phosphocholine-N-docosahexaenoyl- l -serine siRNA Conjugate in Mouse Brain. *Bioconjug Chem* **28**, 1758–1766 (2017).

393. Biscans, A. *et al.* Diverse lipid conjugates for functional extra-hepatic siRNA delivery in vivo. *Nucleic Acids Res* **47**, 1082–1096 (2019).

394. Study of CBP-4888 in Healthy, Non-Pregnant Female Subjects. *ClinicalTrials.gov* https://classic.clinicaltrials.gov/ct2/show/NCT05881993 (2024) NCT05881993.

395. Tang, Q. & Khvorova, A. RNAi-based drug design: considerations and future directions. *Nat Rev Drug Discov* (2024) doi:10.1038/s41573-024-00912-9.

396. Alnylam Pharmaceuticals Inc. Alnylam Reports Additional Positive Interim Phase 1 Results for ALN-APP, in Development for Alzheimer's Disease and Cerebral Amyloid Angiopathy. https://investors.alnylam.com/press-release?id=27761 (2023).

397. Alterman, J. F. *et al.* A divalent siRNA chemical scaffold for potent and sustained modulation of gene expression throughout the central nervous system. *Nat Biotechnol* **37**, 884–894 (2019).

398. Ferguson, C. M. *et al.* Silencing *Apoe* with divalent-siRNAs improves amyloid burden and activates immune response pathways in Alzheimer's disease. *Alzheimer's & Dementia* **20**, 2632–2652 (2024).

399. Chernikov, I. V. *et al.* Cholesterol-Containing Nuclease-Resistant siRNA Accumulates in Tumors in a Carrier-free Mode and Silences MDR1 Gene. *Mol Ther Nucleic Acids* **6**, 209–220 (2017).

400. Tang, T. *et al.* Local administration of siRNA through Microneedle: Optimization, Biodistribution, Tumor Suppression and Toxicity. *Sci Rep* **6**, 30430 (2016).

401. Sarli, S. L. *et al.* Quantifying the activity profile of ASO and siRNA conjugates in glioblastoma xenograft tumors *in vivo*. *Nucleic Acids Res* **2024**, 1–19 (2024).

402. Osborn, M. F. *et al.* Efficient gene silencing in brain tumors with hydrophobically modified siRNAs. *Mol Cancer Ther* **17**, 1251–1258 (2018).

403. Kuzu, O. F., Noory, M. A. & Robertson, G. P. The Role of Cholesterol in Cancer. (2016) doi:10.1158/0008-5472.CAN-15-2613.

404. Cheng, C., Geng, F., Cheng, X. & Guo, D. Lipid metabolism reprogramming and its potential targets in cancer. *Cancer Commun* **38**, 27 (2018).

405. Bovenga, F., Sabbà, C. & Moschetta, A. Cell Metabolism Perspective Uncoupling Nuclear Receptor LXR and Cholesterol Metabolism in Cancer. (2015) doi:10.1016/j.cmet.2015.03.002.

406. Han, M. *et al.* Therapeutic implications of altered cholesterol homeostasis mediated by loss of CYP46A1 in human glioblastoma. *EMBO Mol Med* **12**, (2020).

407. Broadfield, L. A., Pane, A. A., Talebi, A., Swinnen, J. V. & Fendt, S.-M. Lipid metabolism in cancer: New perspectives and emerging mechanisms. *Dev Cell* **56**, 1363–1393 (2021).

408. Komin, A., Russell, L. M., Hristova, K. A. & Searson, P. C. Peptide-based strategies for enhanced cell uptake, transcellular transport, and circulation: Mechanisms and challenges. *Adv Drug Deliv Rev* **110–111**, 52–64 (2017).

409. Falato, L., Gestin, M. & Langel, Ü. Cell-penetrating peptides delivering siRNAs: An overview. *Methods in Molecular Biology* **2282**, 329–352 (2021).

410. Varkouhi, A. K., Scholte, M., Storm, G. & Haisma, H. J. Endosomal escape pathways for delivery of biologicals. *Journal of Controlled Release* **151**, 220–228 (2011).

411. Salim, L., Islam, G. & Desaulniers, J. P. Targeted delivery and enhanced gene-silencing activity of centrally modified folic acid–siRNA conjugates. *Nucleic Acids Res* **48**, 75–85 (2020).

412. Klein, D. *et al.* Centyrin ligands for extrahepatic delivery of siRNA. *Molecular Therapy* **29**, 2053–2066 (2021).

413. Cao, W. *et al.* Antibody–siRNA conjugates (ARC): Emerging siRNA drug formulation. *Med Drug Discov* **15**, 100128 (2022).

414. Zavoiura, O. *et al.* Nanobody–siRNA Conjugates for Targeted Delivery of siRNA to Cancer Cells. *Cite This: Mol. Pharmaceutics* **18**, (2021).

415. Kruspe, S. & Giangrande, P. Aptamer-siRNA Chimeras: Discovery, Progress, and Future Prospects. *Biomedicines* **5**, 45 (2017).

416. Dassie, J. P. *et al.* Systemic administration of optimized aptamer-siRNA chimeras promotes regression of PSMA-expressing tumors. *Nat Biotechnol* **27**, 839–846 (2009).

417. Gilboa-Geffen, A. *et al.* Gene Knockdown by EpCAM Aptamer–siRNA Chimeras Suppresses Epithelial Breast Cancers and Their Tumor-Initiating Cells. *Mol Cancer Ther* **14**, 2279–2291 (2015).

418. Su, S., Chhabra, G., Singh, C. K., Ndiaye, M. A. & Ahmad, N. PLK1 inhibition-based combination therapies for cancer management. *Transl Oncol* **16**, 101332 (2022).

419. Dowdy, S. F. Endosomal escape of RNA therapeutics: How do we solve this rate-limiting problem? *RNA* **29**, 396–401 (2023).

420. Lu, J. *et al.* RAB18 is a key regulator of GalNAc-conjugated siRNA-induced silencing in Hep3B cells. (2022) doi:10.1016/j.omtn.2022.04.003.

421. Juliano, R. L. Chemical Manipulation of the Endosome Trafficking Machinery: Implications for Oligonucleotide Delivery. *Biomedicines* **9**, 512 (2021).

422. Meng, Y., Heybrock, S., Neculai, D. & Saftig, P. Cholesterol Handling in Lysosomes and Beyond. *Trends in Cell Biology* vol. 30 452–466 Preprint at https://doi.org/10.1016/j.tcb.2020.02.007 (2020).

423. Eltoukhy, A. A., Sahay, G., Cunningham, J. M. & Anderson, D. G. Niemann-Pick C1 Affects the Gene Delivery Efficacy of Degradable Polymeric Nanoparticles. *ACS Nano* **8**, 7905–7913 (2014).

424. Méndez-Acevedo, K. M., Valdes, V. J., Asanov, A. & Vaca, L. A novel family of mammalian transmembrane proteins involved in cholesterol transport OPEN. doi:10.1038/s41598-017-07077-z.

425. Nguyen, T. A. *et al.* SIDT2 Transports Extracellular dsRNA into the Cytoplasm for Innate Immune Recognition. *Immunity* **47**, 498-509.e6 (2017).

426. Feinberg, E. H. & Hunter, C. P. Transport of dsRNA into cells by the transmembrane protein SID-1. *Science (1979)* **301**, 1545–1547 (2003).

427. Shih, J. D. & Hunter, C. P. SID-1 is a dsRNA-selective dsRNA-gated channel. doi:10.1261/rna.2596511.

428. Shih, J. D., Fitzgerald, M. C., Sutherlin, M. & Hunter, C. P. The SID-1 double-stranded RNA transporter is not selective for dsRNA length. *RNA* **15**, 384–390 (2009).

429. Duxbury, M. S., Ashley, S. W. & Whang, E. E. RNA interference: A mammalian SID-1 homologue enhances siRNA uptake and gene silencing efficacy in human cells. *Biochem Biophys Res Commun* **331**, 459–463 (2005).

430. Nguyen, T. A. *et al.* SIDT1 Localizes to Endolysosomes and Mediates Double-Stranded RNA Transport into the Cytoplasm. *The Journal of Immunology* **202**, 3483–3492 (2019).

431. Fortier, M. E. *et al.* The viral mimic, polyinosinic:polycytidylic acid, induces fever in rats via an interleukin-1-dependent mechanism. *Am J Physiol Regul Integr Comp Physiol* **287**, 759–766 (2004).

432. Zhao, J. C., Saleh, A. & Crooke, S. T. SIDT2 Inhibits Phosphorothioate Antisense Oligonucleotide Activity by Regulating Cellular Localization of Lysosomes. *https://home.liebertpub.com/nat* **33**, 108–116 (2023).

433. Deprey, K., Batistatou, N. & Kritzer, J. A. A critical analysis of methods used to investigate the cellular uptake and subcellular localization of RNA therapeutics. *Nucleic Acids Res* **48**, 7623–7639 (2020).

434. Chatterjee, S., Kon, E., Sharma, P. & Peer, D. Endosomal escape: A bottleneck for LNP-mediated therapeutics. *PNAS* **121**, (2024).

435. Overhoff, M. Quantitative detection of siRNA and single-stranded oligonucleotides: relationship between uptake and biological activity of siRNA. *Nucleic Acids Res* **32**, e170–e170 (2004).

436. Liu, D. V., Yang, N. J. & Wittrup, K. D. A nonpolycationic fully proteinaceous multiagent system for potent targeted delivery of siRNA. *Mol Ther Nucleic Acids* **3**, e162 (2014).

437. Stalder, L. *et al.* The rough endoplasmatic reticulum is a central nucleation site of siRNA-mediated RNA silencing. *EMBO J* **32**, 1115–1127 (2013).

438. Rehman, Z. U., Hoekstra, D. & Zuhorn, I. S. Mechanism of polyplex- and lipoplex-mediated delivery of nucleic acids: Real-time visualization of transient membrane destabilization without endosomal lysis. *ACS Nano* **7**, 3767–3777 (2013).

439. Tamura, A., Oishi, M. & Nagasaki, Y. Enhanced Cytoplasmic Delivery of siRNA Using a Stabilized Polyion Complex Based on PEGylated Nanogels with a Cross-Linked Polyamine Structure. *Biomacromolecules* **10**, 1818–1827 (2009).

440. Akita, H. *et al.* Nanoparticles for ex vivo siRNA delivery to dendritic cells for cancer vaccines: Programmed endosomal escape and dissociation. *Journal of Controlled Release* **143**, 311–317 (2010).

441. Sakurai, Y. *et al.* Endosomal escape and the knockdown efficiency of liposomal-siRNA by the fusogenic peptide shGALA. *Biomaterials* **32**, 5733–5742 (2011).

442. Basha, G. *et al.* Influence of cationic lipid composition on gene silencing properties of lipid nanoparticle formulations of siRNA in antigen-presenting cells. *Molecular Therapy* **19**, 2186–2200 (2011).

443. He, C. *et al.* High-resolution visualization and quantification of nucleic acid–based therapeutics in cells and tissues using Nanoscale secondary ion mass spectrometry (NanoSIMS). *Nucleic Acids Res* **49**, 1–14 (2021).

444. Van Der Bent, M. L. *et al.* The nuclear concentration required for antisense oligonucleotide activity in myotonic dystrophy cells. *The FASEB Journal* **33**, 11314–11325 (2019).

445. Buntz, A. *et al.* Quantitative fluorescence imaging determines the absolute number of locked nucleic acid oligonucleotides needed for suppression of target gene expression. *Nucleic Acids Res* **47**, 953–969 (2019).

446. Ohrt, T. *et al.* Fluorescence correlation spectroscopy and fluorescence cross-correlation spectroscopy reveal the cytoplasmic origination of loaded nuclear RISC in vivo in human cells. *Nucleic Acids Res* **36**, 6439–6449 (2008).

447. Bidère, N. *et al.* Cathepsin D Triggers Bax Activation, Resulting in Selective Apoptosis-inducing Factor (AIF) Relocation in T Lymphocytes Entering the Early Commitment Phase to Apoptosis. *Journal of Biological Chemistry* **278**, 31401–31411 (2003).

448. Aits, S., Jäättelä, M. & Nylandsted, J. Methods for the quantification of lysosomal membrane permeabilization: A hallmark of lysosomal cell death. *Methods Cell Biol* **126**, 261–285 (2015).

449. Boya, P. *et al.* Lysosomal Membrane Permeabilization Induces Cell Death in a Mitochondrion-dependent Fashion. *The Journal of Experimental Medicine J. Exp. Med. The* **197**, 1323–1334 (2003).

450. Asokan, A. & Cho, M. J. Cytosolic delivery of macromolecules. *Biochimica et Biophysica Acta (BBA) - Biomembranes* **1611**, 151–160 (2003).

451. Cabantous, S., Terwilliger, T. C. & Waldo, G. S. Protein tagging and detection with engineered self-assembling fragments of green fluorescent protein. *Nat Biotechnol* **23**, 102–107 (2005).

452. Kilchrist, K. V., Tierney, J. W. & Duvall, C. L. Genetically Encoded Split-Luciferase Biosensors to Measure Endosome Disruption Rapidly in Live Cells. *ACS Sens* **5**, 1929–1936 (2020).

453. Lönn, P. *et al.* Enhancing Endosomal Escape for Intracellular Delivery of Macromolecular Biologic Therapeutics. *Sci Rep* **6**, (2016).

454. Verdurmen, W. P. R., Luginbühl, M., Honegger, A. & Plückthun, A. Efficient cell-specific uptake of binding proteins into the cytoplasm through engineered modular transport systems. *Journal of Controlled Release* **200**, 13–22 (2015).

455. Yu, P., Liu, B. & Kodadek, T. A high-throughput assay for assessing the cell permeability of combinatorial libraries. *Nat Biotechnol* **23**, 746–751 (2005).

456. Holub, J. M., LaRochelle, J. R., Appelbaum, J. S. & Schepartz, A. Improved Assays for Determining the Cytosolic Access of Peptides, Proteins, and Their Mimetics. *Biochemistry* **52**, 9036–9046 (2013).

457. Chyan, W. & Raines, R. T. Enzyme-Activated Fluorogenic Probes for Live-Cell and in Vivo Imaging. *ACS Chem Biol* **13**, 1810–1823 (2018).

458. Deprey, K. *et al.* Quantitative Measurement of Cytosolic and Nuclear Penetration of Oligonucleotide Therapeutics. *ACS Chem Biol* **17**, 348–360 (2022).

459. Jiang, Y. *et al.* Quantitating Endosomal Escape of a Library of Polymers for mRNA Delivery. *Nano Lett* **20**, 1117–1123 (2020).

460. Teo, S. L. Y. *et al.* Unravelling cytosolic delivery of cell penetrating peptides with a quantitative endosomal escape assay. *Nat Commun* **12**, 3721 (2021).

461. Munson, M. J. *et al.* A high-throughput Galectin-9 imaging assay for quantifying nanoparticle uptake, endosomal escape and functional RNA delivery. *Commun Biol* **4**, 211 (2021).

462. Bost, J. P. *et al.* Novel endosomolytic compounds enable highly potent delivery of antisense oligonucleotides. *Commun Biol* **5**, 185 (2022).

463. Kilchrist, K. V. *et al.* Gal8 Visualization of Endosome Disruption Predicts Carrier-Mediated Biologic Drug Intracellular Bioavailability. *ACS Nano* **13**, 1136–1152 (2019).

464. Herrera, M., Kim, J., Eygeris, Y., Jozic, A. & Sahay, G. Illuminating endosomal escape of polymorphic lipid nanoparticles that boost mRNA delivery. *Biomater Sci* **9**, 4289–4300 (2021).

465. Zhang, F., Lin, Y., Höhn, M. & Wagner, E. Chemical-electron-transfer-based lipopolyplexes for enhanced siRNA delivery. *Cell Rep Phys Sci* **4**, 101444 (2023).

466. Váňová, J. *et al.* VirPorters: Insights into the action of cationic and histidine-rich cell-penetrating peptides. *Int J Pharm* **611**, 121308 (2022).

467. Kondow-McConaghy, H. M. *et al.* Impact of the Endosomal Escape Activity of Cell-Penetrating Peptides on the Endocytic Pathway. *ACS Chem Biol* **15**, 2355–2363 (2020).

468. Wang, Y. *et al.* Endosomolytic and Tumor-Penetrating Mesoporous Silica Nanoparticles for siRNA/miRNA Combination Cancer Therapy. *ACS Appl Mater Interfaces* **12**, 4308–4322 (2020).

469. Rui, Y. *et al.* High-throughput and high-content bioassay enables tuning of polyester nanoparticles for cellular uptake, endosomal escape, and systemic in vivo delivery of mRNA. *Sci Adv* **8**, 2855 (2022).

470. Kilchrist, K. V., Evans, B. C., Brophy, C. M. & Duvall, C. L. Mechanism of Enhanced Cellular Uptake and Cytosolic Retention of MK2 Inhibitory Peptide Nano-polyplexes. *Cell Mol Bioeng* **9**, 368–381 (2016).

471. Kelly, I. B., Fletcher, R. B., McBride, J. R., Weiss, S. M. & Duvall, C. L. Tuning Composition of Polymer and Porous Silicon Composite Nanoparticles for Early Endosome Escape of Anti-microRNA Peptide Nucleic Acids. *ACS Appl Mater Interfaces* **12**, 39602–39611 (2020).

472. Skowyra, M. L., Schlesinger, P. H., Naismith, T. V. & Hanson, P. I. Triggered recruitment of ESCRT machinery promotes endolysosomal repair. *Science (1979)* **360**, (2018).

473. Sayers, E. J. *et al.* Endocytic Profiling of Cancer Cell Models Reveals Critical Factors Influencing LNP-Mediated mRNA Delivery and Protein Expression. *Molecular Therapy* **27**, 1950–1962 (2019).

474. Barondes, S. H. *et al.* Galectins: A family of animal β-galactoside-binding lectins. *Cell* **76**, 597–598 (1994).

475. Johannes, L., Jacob, R. & Leffler, H. Galectins at a glance. *J Cell Sci* **131**, (2018).

476. Houzelstein, D. *et al.* Phylogenetic Analysis of the Vertebrate Galectin Family. *Mol Biol Evol* **21**, 1177–1187 (2004).

477. Hirabayashi, J. *et al.* Oligosaccharide specificity of galectins: a search by frontal affinity chromatography. *Biochimica et Biophysica Acta (BBA) - General Subjects* **1572**, 232–254 (2002).

478. Lepur, A., Salomonsson, E., Nilsson, U. J. & Leffler, H. Ligand Induced Galectin-3 Protein Self-association. *Journal of Biological Chemistry* **287**, 21751–21756 (2012).

479. Salomonsson, E. *et al.* Monovalent interactions of galectin-1. *Biochemistry* **49**, 9518–9532 (2010).

480. Kamili, N. A. *et al.* Key regulators of galectin-glycan interactions. *Proteomics* **16**, 3111–3125 (2016).

481. Paz, I. *et al.* Galectin-3, a marker for vacuole lysis by invasive pathogens. *Cell Microbiol* **12**, 530–544 (2010).

482. Thurston, T. L. M., Wandel, M. P., Von Muhlinen, N., Foeglein, Á. & Randow, F. Galectin 8 targets damaged vesicles for autophagy to defend cells against bacterial invasion. *Nature* **482**, 414–418 (2012).

483. Maier, O., Marvin, S. A., Wodrich, H., Campbell, E. M. & Wiethoff, C. M. Spatiotemporal Dynamics of Adenovirus Membrane Rupture and Endosomal Escape. *J Virol* **86**, 10821–10828 (2012).

484. Flavin, W. P. *et al.* Endocytic vesicle rupture is a conserved mechanism of cellular invasion by amyloid proteins. *Acta Neuropathol* **134**, 629–653 (2017).

485. Aits, S. *et al.* Sensitive detection of lysosomal membrane permeabilization by lysosomal galectin puncta assay. *Autophagy* **11**, 1408–1424 (2015).

486. Sudhakar, J. N. *et al.* Lumenal Galectin-9-Lamp2 interaction regulates lysosome and autophagy to prevent pathogenesis in the intestine and pancreas. *Nat Commun* **11**, 4286 (2020).

487. Troncoso, M. F. *et al.* The universe of galectin-binding partners and their functions in health and disease. *J. Biol. Chem* 105400–105401 (2023) doi:10.1016/j.jbc.2023.105400.

488. Boyle, K. B. & Randow, F. The role of 'eat-me' signals and autophagy cargo receptors in innate immunity. *Curr Opin Microbiol* **16**, 339–348 (2013).

489. Chauhan, S. *et al.* TRIMs and Galectins Globally Cooperate and TRIM16 and Galectin-3 Co-direct Autophagy in Endomembrane Damage Homeostasis. *Dev Cell* **39**, 13–27 (2016).

490. Pandey, E. & Harris, E. N. Chloroquine and cytosolic galectins affect endosomal escape of antisense oligonucleotides after Stabilin-mediated endocytosis. *Mol Ther Nucleic Acids* **33**, 430–443 (2023).

491. Vietri, M., Radulovic, M. & Stenmark, H. The many functions of ESCRTs. *Nature Reviews Molecular Cell Biology* vol. 21 25–42 Preprint at https://doi.org/10.1038/s41580-019-0177-4 (2020).

492. Radulovic, M. *et al.* ESCRT-mediated lysosome repair precedes lysophagy and promotes cell survival. *EMBO J* **37**, (2018).

493. Shukla, S. *et al.* Mechanism and cellular function of direct membrane binding by the ESCRT and ERES-associated Ca2+-sensor ALG-2. *Proceedings of the National Academy of Sciences* **121**, (2024).

494. López-Jiménez, A. T. *et al.* The ESCRT and autophagy machineries cooperate to repair ESX-1-dependent damage at the Mycobacterium-containing vacuole but have opposite impact on containing the infection. *PLoS Pathog* **14**, e1007501 (2018).

495. Jeong, E., Willett, R., Rissone, A., La Spina, M. & Puertollano, R. TMEM55B links autophagy flux, lysosomal repair, and TFE3 activation in response to oxidative stress. *Nat Commun* **15**, 93 (2024).

496. Herbst, S. *et al.* LRRK 2 activation controls the repair of damaged endomembranes in macrophages . *EMBO J* **39**, (2020).

497. Jia, J. *et al.* Galectin-3 Coordinates a Cellular System for Lysosomal Repair and Removal. *Dev Cell* **52**, 69-87.e8 (2020).

498. Mercier, V. *et al.* Endosomal membrane tension regulates ESCRT-III-dependent intra-lumenal vesicle formation. *Nat Cell Biol* **22**, 947–959 (2020).

499. Zhen, Y., Radulovic, M., Vietri, M. & Stenmark, H. Sealing holes in cellular membranes. *EMBO J* **40**, (2021).

500. Mizushima, N., Levine, B., Cuervo, A. M. & Klionsky, D. J. Autophagy fights disease through cellular self-digestion. *Nature* **451**, 1069–1075 (2008).

501. Stolz, A., Ernst, A. & Dikic, I. Cargo recognition and trafficking in selective autophagy. *Nat Cell Biol* **16**, 495–501 (2014).

502. Hung, Y.-H., Chen, L. M.-W., Yang, J.-Y. & Yuan Yang, W. Spatiotemporally controlled induction of autophagy-mediated lysosome turnover. *Nat Commun* **4**, 2111 (2013).

503. Maejima, I. *et al.* Autophagy sequesters damaged lysosomes to control lysosomal biogenesis and kidney injury. *EMBO Journal* **32**, 2336–2347 (2013).

504. Chen, X. *et al.* Autophagy Induced by Calcium Phosphate Precipitates Targets Damaged Endosomes. *Journal of Biological Chemistry* **289**, 11162–11174 (2014).

505. Roberts, R. *et al.* Autophagy and formation of tubulovesicular autophagosomes provide a barrier against nonviral gene delivery. *Autophagy* **9**, 667–682 (2013).

506. Kaur, N. *et al.* TECPR1 is activated by damage-induced sphingomyelin exposure to mediate noncanonical autophagy . *EMBO J* **42**, (2023).

507. Mauthe, M. *et al.* Chloroquine inhibits autophagic flux by decreasing autophagosome-lysosome fusion. *Autophagy* **14**, 1435–1455 (2018).

508. Bussi, C. *et al.* Stress granules plug and stabilize damaged endolysosomal membranes. *1062 | Nature |* **623**, (2023).

509. Jia, J. *et al.* Stress granules and mTOR are regulated by membrane atg8ylation during lysosomal damage. *Journal of Cell Biology* **221**, (2022).

510. Sanders, D. W. *et al.* Competing Protein-RNA Interaction Networks Control Multiphase Intracellular Organization. *Cell* **181**, 306-324.e28 (2020).

511. Yang, P. *et al.* G3BP1 Is a Tunable Switch that Triggers Phase Separation to Assemble Stress Granules. *Cell* **181**, 325-345.e28 (2020).

512. Guillé N-Boixet, J. *et al.* RNA-Induced Conformational Switching and Clustering of G3BP Drive Stress Granule Assembly by Condensation Article RNA-Induced Conformational Switching and Clustering of G3BP Drive Stress Granule Assembly by Condensation. *Cell* **181**, 346–361 (2020).

513. Duran, J. *et al.* A mechanism that transduces lysosomal damage signals to stress granule formation for cell survival. *bioRxiv* (2024) doi:10.1101/2024.03.29.587368.

514. Niekamp, P. *et al.* Ca2+-activated sphingomyelin scrambling and turnover mediate ESCRT-independent lysosomal repair. *Nat Commun* **13**, 1875 (2022).

515. Radulovic, M. *et al.* Cholesterol transfer via endoplasmic reticulum contacts mediates lysosome damage repair. *EMBO J* **41**, (2022).

516. Ebstrup, M. L. *et al.* Annexin A7 mediates lysosome repair independently of ESCRT-III. *Front Cell Dev Biol* **11**, (2023).

517. Yim, W. W., Yamamoto, H. & Mizushima, N. Annexins A1 and A2 are recruited to larger lysosomal injuries independently of ESCRTs to promote repair. *FEBS Lett* **596**, 991–1003 (2022).

518. Ohkuma, S. & Poole, B. *Fluorescence Probe Measurement of the Intralysosomal PH in Living Cells and the Perturbation of PH by Various Agents (Lysosomes/Proton Pump/Ionophores). Cell Biology* vol. 75 https://www.pnas.org (1978).

519. Maxfield, F. R. Weak bases and ionophores rapidly and reversibly raise the pH of endocytic vesicles in cultured mouse fibroblasts. *J Cell Biol* **95**, 676–681 (1982).

520. Luthman, H. & Magnusson, G. *High Efficiency Polyoma DNA Transfection of Chloroquine Treated Cells*. *Nucleic Acids Research* vol. 11 https://academic.oup.com/nar/article/11/5/1295/1116689 (1983).

521. Kornhuber, J. *et al.* Functional Inhibitors of Acid Sphingomyelinase (FIASMAs): A Novel Pharmacological Group of Drugs with Broad Clinical Applications. *Cellular Physiology and Biochemistry* **26**, 9–20 (2010).

522. Trapp, S., Rosania, G. R., Horobin, R. W. & Kornhuber, J. Quantitative modeling of selective lysosomal targeting for drug design. *European Biophysics Journal* **37**, 1317–1328 (2008).

523. Kirkegaard, T. *et al.* Hsp70 stabilizes lysosomes and reverts Niemann–Pick disease-associated lysosomal pathology. *Nature 2010 463:7280* **463**, 549–553 (2010).

524. Petersen, N. H. T. *et al.* Transformation-Associated Changes in Sphingolipid Metabolism Sensitize Cells to Lysosomal Cell Death Induced by Inhibitors of Acid Sphingomyelinase. *Cancer Cell* **24**, 379–393 (2013).

525. Gulbins, E. & Kolesnick, R. N. It Takes a CAD to Kill a Tumor Cell with a LMP. *Cancer Cell* **24**, 279–281 (2013).

526. Thiele, D. L. & Lipsky, P. E. Mechanism of L-leucyl-L-leucine methyl ester-mediated killing of cytotoxic lymphocytes: dependence on a lysosomal thiol protease, dipeptidyl peptidase I, that is enriched in these cells. *Proceedings of the National Academy of Sciences* **87**, 83–87 (1990).

527. Repnik, U. *et al.* L-leucyl-L-leucine methyl ester does not release cysteine cathepsins to the cytosol but inactivates them in transiently permeabilized lysosomes. *J Cell Sci* **130**, 3124–3140 (2017).

528. Fuchs, H. *et al.* Glycosylated Triterpenoids as Endosomal Escape Enhancers in Targeted Tumor Therapies. *Biomedicines* **5**, 14 (2017).

529. Kurz, T., Terman, A., Gustafsson, B. & Brunk, U. T. Lysosomes and oxidative stress in aging and apoptosis. *Biochimica et Biophysica Acta (BBA) - General Subjects* **1780**, 1291–1303 (2008).

530. Boya, P. & Kroemer, G. Lysosomal membrane permeabilization in cell death. *Oncogene* **27**, 6434–6451 (2008).

531. Alphandéry, E. Iron oxide nanoparticles for therapeutic applications. *Drug Discov Today* **25**, (2020).

532. Liu, J., Jia, B., Li, Z. & Li, W. Reactive oxygen species-responsive polymer drug delivery systems. *Front Bioeng Biotechnol* **11**, (2023).

533. De Duve, C. *et al.* Lysosomotropic agents. *Biochem Pharmacol* **23**, 2495–2531 (1974).

534. Akinc, A., Thomas, M., Klibanov, A. M. & Langer, R. Exploring polyethylenimine-mediated DNA transfection and the proton sponge hypothesis. *Journal of Gene Medicine* **7**, 657–663 (2005).

535. Behr, J.-P. The Proton Sponge: a Trick to Enter Cells the Viruses Did Not Exploit. *Chimia (Aarau)* **51**, 34 (1997).

536. Vermeulen, L. M. P., De Smedt, S. C., Remaut, K. & Braeckmans, K. The proton sponge hypothesis: Fable or fact? (2018) doi:10.1016/j.ejpb.2018.05.034.

537. Yang, B. *et al.* High-throughput screening identifies small molecules that enhance the pharmacological effects of oligonucleotides. *Nucleic Acids Res* **43**, (2015).

538. Joris, F. *et al.* Repurposing cationic amphiphilic drugs as adjuvants to induce lysosomal siRNA escape in nanogel transfected cells. *Journal of Controlled Release* **269**, 266–276 (2018).

539. Osborn, M. F. *et al.* Guanabenz (Wytensin™) selectively enhances uptake and efficacy of hydrophobically modified siRNAs. *Nucleic Acids Res* **43**, 8664–8672 (2015).

540. Pagliero, R. J. *et al.* Discovery of Small Molecules That Induce Lysosomal Cell Death in Cancer Cell Lines Using an Image-Based Screening Platform. *Assay Drug Dev Technol* **14**, 489–510 (2016).

541. Ellegaard, A. M. *et al.* Repurposing Cationic Amphiphilic Antihistamines for Cancer Treatment. *EBioMedicine* **9**, 130–139 (2016).

542. Sapreme Presents Promising New Preclinical Data at 17th Annual Meeting of Oligonucleotide Therapeutics Society. *businesswire.com* https://www.businesswire.com/news/home/20210927005043/en/Sapreme-Presents-Promising-New-Preclinical-Data-at-17th-Annual-Meeting-of-Oligonucleotide-Therapeutics-Society (2021).

543. Wooddell, C. I. *et al.* Hepatocyte-targeted RNAi therapeutics for the treatment of chronic hepatitis B virus infection. in *Molecular Therapy* vol. 21 973–985 (Nature Publishing Group, 2013).

544. Weissmann, G., Hirschhorn, R. & Krakauer, K. Effect of melittin upon cellular and lysosomal membranes. *Biochem Pharmacol* **18**, 1771–1774 (1969).

545. Arrowhead Pharmaceuticals Focuses Resources on Subcutaneous and Extra-Hepatic RNAi Therapeutics. *businesswire.com* https://www.businesswire.com/news/home/20161129006166/en/Arrowhead-Pharmaceuticals-Focuses-Resources-on-Subcutaneous-and-Extra-Hepatic-RNAi-Therapeutics (2016).

546. Lönn, P. & Dowdy, S. F. Cationic PTD/CPP-mediated macromolecular delivery: Charging into the cell. *Expert Opinion on Drug Delivery* vol. 12 1627–1636 Preprint at https://doi.org/10.1517/17425247.2015.1046431 (2015).

547. Liou, J.-S. *et al.* Protein transduction in human cells is enhanced by cell-penetrating peptides fused with an endosomolytic HA2 sequence. *Peptides (N.Y.)* **37**, 273–284 (2012).

548. Samec, T. *et al.* Fusogenic peptide delivery of bioactive siRNAs targeting CSNK2A1 for treatment of ovarian cancer. *Mol Ther Nucleic Acids* **30**, 95–111 (2022).

549. Agrawal, P. *et al.* CPPsite 2.0: a repository of experimentally validated cell-penetrating peptides. *Nucleic Acids Res* **44**, (2016).

550. Li, X. *et al.* Generation of Destabilized Green Fluorescent Protein as a Transcription Reporter*. (1998).

551. Huff, J. The Airyscan detector from ZEISS: confocal imaging with improved signal-to-noise ratio and super-resolution. *Nat Methods* **12**, i–ii (2015).

552. Gustafsson, M. G. L. *et al.* Three-Dimensional Resolution Doubling in Wide-Field Fluorescence Microscopy by Structured Illumination. doi:10.1529/biophysj.107.120345.

553. York, A. G. *et al.* Instant super-resolution imaging in live cells and embryos via analog image processing. *Nat Methods* **10**, 1122–1130 (2013).

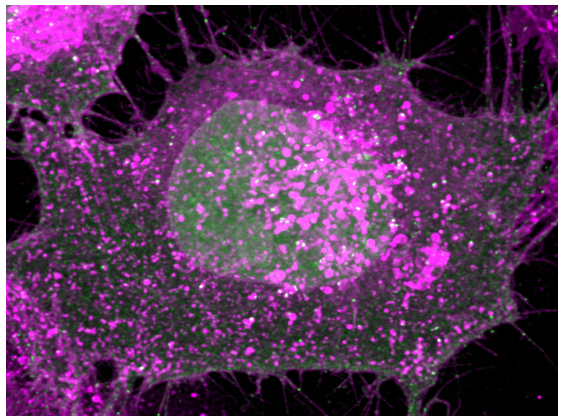

A cancer cell expressing CHMP2A (green), a protein involved in membrane damage repair response, has internalized cholesterol-modified small interfering RNA (magenta), residing in intracellular vesicles.

Endosomal escape of RNA therapeutics

Medicines based on RNA are a new class of targeted therapies that have recently entered clinical use in diverse settings. One of the main challenges in the development of new RNA medicines is the delivery of macromolecular therapeutic molecules to target tissues and cells. A fundamental barrier in the delivery process is the entrapment of therapeutic RNA in intracellular vesicles following uptake into cells. The release of RNA payload into the cytosol — a process known as endosomal escape — is very inefficient and hampers the potency of candidate RNA medicines. This thesis presents work on understanding and potentially overcoming the rate-limiting inefficiency of endosomal escape of therapeutic RNA molecules, with a focus on microscopy-based research techniques and quantitative analysis of RNA delivery.

Photo by Tove Smeds

Originally from the forest lands in Småland, southern Sweden, **Hampus Du Rietz** studied Medicine at Lund University, graduating in 2020. He joined the research lab of Anders Wittrup during his undergraduate studies, focusing on RNA therapeutics and drug delivery. This book is his doctoral thesis. It was produced at the Oncology Kamprad Lab at the Department of Clinical Sciences, Faculty of Medicine, Lund University.

Printed by Media-Tryck, Lund 2024 NORDIC SWAN ECOLABEL 3041 0903

LUND UNIVERSITY

FACULTY OF MEDICINE

Department of Clinical Sciences, Lund

Lund University, Faculty of Medicine
Doctoral Dissertation Series 2024:88
ISBN 978-91-8021-583-1
ISSN 1652-8220